UNIVERSIDADE DA BEIRA INTERIOR
Faculdade de Engenharia

# Optimization of FPSO Glen Lyon Mooring Lines

**Paulo Alexandre Rodrigues de Vasconcelos Figueiredo**

Tese para obtenção do Grau de Doutor em
**Engenharia Mecânica**
(3º ciclo de estudos)

Orientador: Professor Doutor Francisco Miguel Ribeiro Proença Brójo

**Covilhã, Junho, 2019**

# Dedication

I would like to dedicate my thesis to the most important person for me, my son. He was born with twenty four weeks and with six hundred grams and lived for four weeks. He was the best fighter ever, he fought for his life like nothing I have ever seen before. We will meet again in heaven baby, daddy Loves you. You're the best thing that has ever happen to me. Thank you for letting me be a dad for a month, thank you very much my son.

The thesis is also dedicated to my better half Vera Joaquim as well as to my family and friends.

Thank you all for the support.

# Acknowledgments

I would like to take this opportunity to express my sincere gratitude to Professor Francisco Miguel Ribeiro Proença Brójo for his dedication, encouragement, knowledge, availability and help. I would like to express my gratitude during the time as a student of Aeronautical Engineering Bachelor and Masters degree, during all the time of the PhD, as well as letting me perform the first steps in lecturing at the University the disciplines of Thermal engines, High flight Velocity and Aircraft Propulsion II.

I would like to thank to my present and past colleges of work at CEIIA, specially to Tiago Rebelo and Francisco Cunha.

I want to thank Orcina Team for loan me the software needed for my PhD, specially to Yvonne Morgan and Dave Thomas. Thank you for your support.

Last by not least I would like to thank Mr. Karl C. Strømsem for all the support regarding the development of the PhD. Your help was priceless. Thank you very much.

The current study was funded in part by Fundação para a Ciência e Tecnologia (FCT), under project UID/EMS/00151/2013 C-MAST, with reference POCI-01-0145-FEDER-007718.


# Resumo

Durante as operações de prospeção e extração de petróleo e gas em águas profundas e ultra profundas, o fundeamento de navios é um importante fator para o desenvolvimento do campo petrolífero. Para estas profundidades, infra-estruturas convencionais e.g. plataformas petrolíferas não são aplicáveis devido ao ambiente violento colinear e não colinear do local (localização, ondas, correntes subaquáticas e de superfície, marés, etc.). Para conjuntos de poços subaquáticos, é comum o uso de Platformas de produção, armazenamento e descarga (FPSO) como plataforma de superficie para periodos de exploração longos.

Os custos subaquaticos referem-se ao custo do projeto marinho e normalmente incluem os custos de capital *capex* e custos operacionais *opex*. Na produção de hidrocarbonetos os *capex* e os *opex* aumentam exponencialmente com o aumento da profundidade, resultando na necessidade do desenvolvimento da fase de projeto detalhado necessário para análises de componentes para verificar a resistência dos mesmos, dutilidade e fadiga, quer na rigidez, instabilidade, corrosão, etc.

O projeto de campos petrolíferos são na maioria das vezes sobreestimados (de forma bastante conservativa) devido a imensos requisitos e modelos complexos de avaliação de custos. Após projeto e instalação de todas as infraestruturas e componentes, assim como durante o longo periodo útil de extração de hidrocarbonetos, toda a ancoragem deve suportar as cargas ambientais de forma a não comprometer a operação.

Cada campo petrolífero possui um desenvolvimento singular, uma vez que os fenómenos ambientais são únicos em cada localização do globo terrestre. Este trabalho refere a optimização de um sistema de amarração para águas profundas para o campo de Schiehallion, ou por outras palavras, todo o desenvolvimento de ancoragem de um navio FPSO, desde o posicionamento no local com as forças ambientais e as caracteristicas do navio (Orcaflex), posterior otimização do sistema de ancoragem por um sistema equivalente (Matlab), desenho mecânico do sistema de ancoragem (CATIA), cálculo estrutural detalhado (Altair e Nastran) e análise de vida à fadiga.

De forma a reproduzir o processo de ancoragem, é efetuada uma comparação inicial do FPSO inicial (Schiehallion FPSO) que esteve em operação no local desde 1993 até à sua substituição pelo novo navio (Glen Lyon FPSO), através da implementação e gestão do campo petrolífero de acordo com os poços antigos como os poços descobertos recentemente. A posterior otimização de todo o sistema de fixação foi verificada assim como a análise estrutural final detalhada dos componentes específicos em localizações especificas com grande probabilidade de falha.

Através deste trabalho, todo o processo que leva à otimização das linhas de amarração do Glen Lyon é completamente detalhado desde a análise do navio ao detalhamento do desenho mecânico, os constrangimentos e requisitos que foram aplicados, estudos e opções efetuadas durante a fase de desenvolvimento crítico são apresentados e discutidos.

# Palavras-chave

Sistema de amarração em catenária, sistemas de fundeamento, ancoradouro offshore, corrente com e sem elo central, otimização de amarras.

# Abstract

During oil and gas inspection and extraction operations both in deep and ultra-deep water, vessel mooring is a very important factor for the development of oil fields. For these depths, standard stand-alone surface facilities e.g. jack up rigs or offshore fixed platforms are not suitable due to the harsh collinear and non-collinear environment in-situ (location, waves, surface and underwater current, sea tides, ice, etc.). For deep sea wells clusters, it is usual to use floating production storage offloading (FPSO) as surface platforms for long time exploitation periods.

Subsea expenditure, refers the cost of the subsea project and generally includes the capital expenditures (*capex*) and operational expenditures (*opex*). In the production of hydrocarbons *capex* and *opex* exponentially increases with increasing depth, resulting in a need for precise detailed design phase for analysis of systems to verify components strength, ductility and fatigue, stiffness, instabilities, corrosion etc.

The design of oilfields is most of the times overrated (in a very conservative way) due to several requirements and complex models of costs evaluation. After detailed phase and installation of all facilities and components, as well as due to the expected life design for hydrocarbons exploitation all anchoring system shall withstand the environmental loads in order to not compromise the operation.

Each oilfield has a unique development, since environmental phenomena are unique in each earth location. This work refers to the optimization process of an anchoring system for deep waters in the Schiehallion Field, or in other words, the complete development of the mooring system for a FPSO, from the positioning in-situ with environmental conditions and vessel characteristics (Orcaflex), further optimization of the mooring system for an equivalent system (Matlab), mechanical design of the mooring system (CATIA), structural detailed analysis (Altair and Nastran) as fatigue life analysis.

In order to reproduce all the mooring process, it is performed and initial comparison of the former FPSO (Schiehallion FPSO) that has been working in-situ since 1993 till its replacement for the new vessel (Glen Lyon FPSO). Due to the latest discoveries in the oilfield, the project has to be redesigned alongside with former wells and having in consideration recent discovered wells. Further optimization of the complete fixation system was verified as well as finally detailed structural analysis of specific components in key locations with higher margin of failure.

Within this work, all the methodology which led to the optimization of Glen Lyon mooring lines was fully detailed from vessel analysis to detailed mooring mechanical design, constraints and requirements were applied, trade-offs and assumptions made during this critical development phase are presented and discussed.

# Keywords

Catenary mooring system, mooring lines, offshore anchoring, studlink and studless chain, mooring lines optimization.

# Contents

# List of Figures

# List of Tables

# List of Acronyms

| | |
|---|---|
| ALS | Accidental Load state |
| API | American Petroleum Institute |
| ASME | American Society of Mechanical Engineers |
| ASV | Autonomous surface vehicle |
| AUV | Autonomous underwater vehicle |
| BBLS | Barrels |
| BOP | Blow Out Preventer |
| BTU | British Thermal Units |
| CAD | Computer aided desing |
| CAE | Computer aided engineering |
| CAM | Computer aided manufacturing |
| CAPEX | Capital Expenditures |
| CFRP | Carbon Fiber Reinforced Polymer |
| DNV-GL | Det Norske Veritas (Norway) and Germanischer Lloyd (Germany) |
| DP | Dynamic Positioning |
| ISO | International Organization for Standardization |
| FEM | Finite element method |
| FLS | Fatigue limit states |
| FPSO | Floating Production Storage Offloading |
| FPU | Floating Production Unit |
| MBL | Minimum breaking load |
| mmboe | Million Barrels of Oil Equivalent |
| MSL | Mean Sea Level |
| NPD | Norwegian Petroleum Dictorate |
| OPEX | Operational Expenditures |
| rms | Root Mean Square |
| ROV | Remote operated vehicle |
| SLS | Serviceability limit states |
| TLP | Tension Leg Platforms |
| ULS | Ultimate Load state |
| WEC | Wave Energy Converters |
| WSW | West Soutwest |

# Nomenclature

| | |
|---|---|
| a | Area |
| D | Diameter |
| m | mass |
| E | *Young's* modulus |
| Hs | Wave height |
| Tp | Wave period |
| H | Horizontal component of cable tension |
| ds | Infinitesimal element of the cable |
| D | (chapter 3) - Hydrodynamic mean normal force |
| F | Hydrodynamic mean tangential force |
| A | (chapter 3) - Cross sectional area of cable line |
| w | Weight per unit length of the line of water |
| T | Line tension |
| $l_s$ | Minimum length of the chain |
| $l_{min}$ | Minimum length of the cable line |
| X | (chapter 3) - Total horizontal distance |
| x | (chapter 3) - Suspended horizontal distance |
| $l_s$ | Suspended catenary cable length |
| M | Total displacement of the FPSO |
| $A_{ii}$ or $A_{jj}$ | Added Mass |
| $B_{jj}$ | Damping at natural frequency |
| $k_{ii}$ | Stiffness |
| $I_{44}$ | Moments of inertia of roll |
| $I_{55}$ | Moments of inertia of pitch |
| $I_{66}$ | Moments of inertia of yaw |
| $\rho$ | Density of water |
| g | Acceleration of gravity |
| $A_w$ | Waterplane area |
| $GM_T$ | Transverse metacentre heights |
| $GM_M$ | Logitudinal metacentre heights |
| $C_l$ | Horizontal stiffness |
| $\theta_l$ | Angle of infinitesimal mooring line |
| $\overline{F}_j^W$ | Steady wind force |
| $\overline{F}_j^C$ | Current force |
| $\overline{F}_j^(2)$ | Mean second order force |
| $\hat{\xi}_j^{(1)}$ | Most probable maximum value of the first order |
| $\hat{\xi}_{j1/3}^{(1)}$ | Most probable significant value of the first order |
| $\hat{\xi}_j^{(2)}$ | Most probable maximum value of the second order |
| $\hat{\xi}_{j1/3}^{(2)}$ | Most probable significant value of the second order |
| $m_0$ | Moment of Area |
| $m_2$ | Second moment of area of first order motion response spectrum |
| $S(\omega)$ | Wave spectral density |
| $\beta$ | Heading angle |
| $\nabla$ | Divergence |

| | |
|---|---|
| $\phi$ | Potential velocity |
| $\zeta$ | Wave elevation |
| U | Wind Speed |
| ET | Effective tension |

# Chapter 1

# Introduction

The present thesis considers the development of an optimized method of mooring lines for large oil and gas extraction marine vessels, moored to the seabed. This system is connected to an internal forward turret allowing the vessel to freely rotate. As in any oilfield development, it is necessary to understand the redevelopment of the wells, the harsh environmental conditions, depth and fundamental loads and the sequence of events. It is important to verify the mooring system both in macro (system analysis) and micro scale (detailed component analysis).

This chapter presents the main reason behind the choice of this topic, the motivation beneath it, the importance of understanding the complete sequence of requirements and assumptions from first development to its redevelopment, choices, steps and further analysis, as well as the contribution to the scientific community, engineer development centers and private offshore companies and suppliers. This chapter also presents the established objectives of the work.

This doctoral project has given rise to 2 publications in international conferences throughout the course of the study. In the last section a general outline of this chapter is summarized for a better understanding.

## 1.1 Motivation

In the context of deep sea oil and gas exploration, floating marine structures have an important role in the development of an oilfield. For deep waters (the depth of deep water subsea field ranges between 200m and 1500m [1]) there are a lot of challenges in the hydrocarbons inspection, research, production and extraction.

Floating structures are frequently used by the oil and gas industry for drilling, well interventions, production and storage at sea. These structures are maintained on station by a variety of mooring line types and systems. Simple anchoring systems are being used for several centuries, however in the past decades the mooring systems have been updated mainly for the oil and gas industry due to the need of increasing profit in the commercialization of hydrocarbons by lowering *CAPEX*.

Nowadays, the available mooring systems play a major role in the development of any oilfield due to the challenges of harsh environmental operational conditions and effective costs. Each oilfield has to be designed individually without any possibility of using the same layout for different oilfields.

In order to be exploitable, the oilfield shall have reliable systems adapted for long term mooring with the possibility of being updated through innovative designs and cheaper materials as well as new methodologies in an iterative process during all service life. Usually the mooring systems are designed in the conceptual phase, remaining the same in both preliminary and detailed design

and with few modifications until the decommissioning phase. In this context it is possible to update the existent oilfield through improved methodologies, new materials, new technology and in-situ testing acquired data during the exploitation phase.

Under this context, several questions arise through the mooring design, from the vessel positioning, environmental conditions, materials selection, mooring layout, type of catenary used and segment lengths. Finally it is necessary to perform strength and fatigue analysis of the most probable elements to fail.

Therefore, it is important to improve the design process adopted in computational methods in order to replicate more accurately experimental results in a wider range of environmental conditions.

The scope of this work is to improve an existing mooring system for Glen Lyon FPSO at the same time as being a cost-effective alternative as well as reducing the environmental footprint left by the oil and gas industry.

## 1.2 Purpose and Contribution

According to European Commission, sea dependent economic activities (the so called blue economy) are estimated to represent 5.4 millions jobs with a revenue value just under 500 billions euros per year. In Europe 37% of internal trades and 75% of external trades are seaborne [2].

It is known that both Sea and Coasts are the drivers of the blue growth. If ten years ago the ports and coastal communities were the centers of ideas and innovation, nowadays three new factors are becoming the new drivers. The new factors are the rapid technological progress (ROV's, AUV's, etc.) for offshore in deep waters, the global awareness of finite resources of the land and freshwater and finally the need to reduce the greenhouse gas emissions (either from new developments of offshore renewable energy and environmental protection).

Blue growth has opened new opportunities for new investments, improvements and maritime research. These opportunities are created due to significant growth potential, either economically through job creation or as a steering wheel helping Europe out of economic crisis through new product development, clean energy or sustainable food. It represents a major role of 2020 strategy. In figure 1.1 both employment and economic size of marine and maritime economic activities can be verified. Blue economy has individual factors depending on each others using the sea sustainably [3].

After several requirements, the European Commission has decided that the new opportunities with job-creation potential from research and development to deliver sustainable technology improvements and innovation are divided in five major value chains, blue energy, aquaculture, marine coastal and cruise tourism, marine mineral resources and blue biotechnology.

In the context of this dissertation it is important to analyze with deeper understanding the value chain of marine mineral resources. The prices for energy and non-energy raw materials is having increments of about 15% for non direct energy entities, and variables values for raw energy

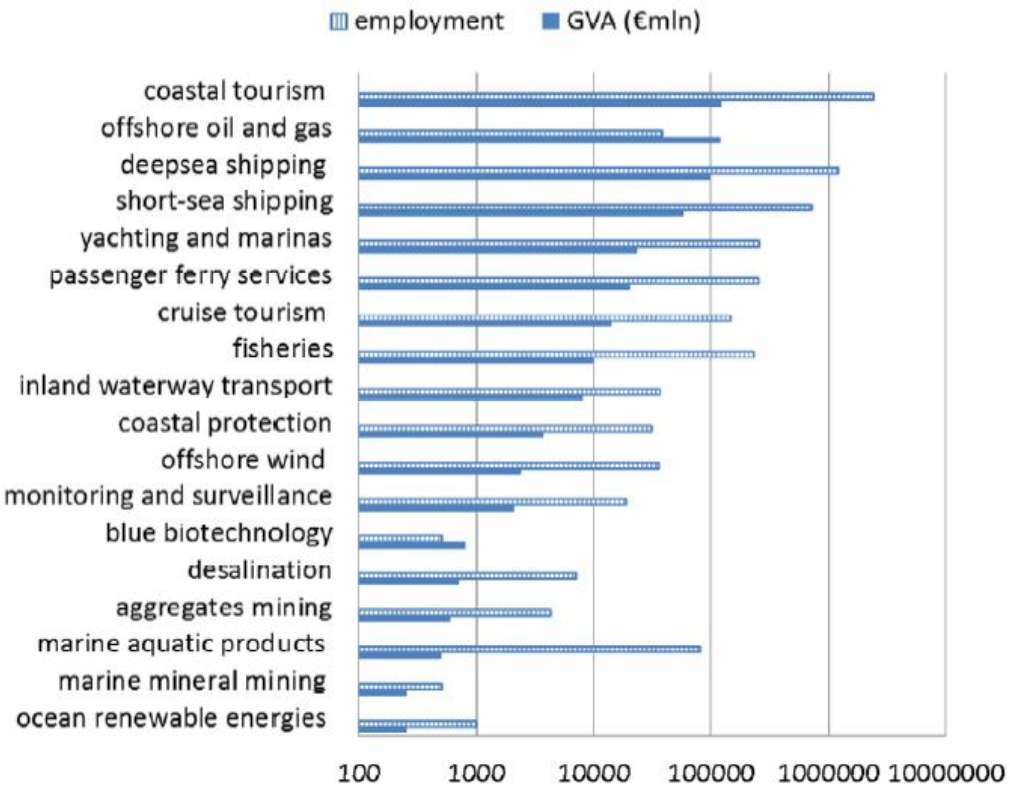


Figure 1.1: Employment and economic size of marine and maritime economic activities, logarithmic scale (image from ref. [2])

components (e.g. crude oil). These increments are a result of the new emerging economies and consumer demanding countries like China, Brazil or Europe as a whole. Besides crude oil, the exploitation and mining of minerals including cobalt, copper and zinc are expected to be 5% extracted from the seabed by 2020. This value is expected to rise again up to 10% by 2030. The mineral mining is expected to growth from 0 to €5 billion by 2020 to €10 billion by 2030.

Boron and lithium are expected to be economically feasible to be extracted from seawater. There are very promising deposits in metallic sulphides which emerge from hydrothermal ore deposits in volcanically active zones. Due to high pressures and high temperature in this regions, the impact of the disturbance of marine biodiversity should be protected since they are performed within areas under national jurisdiction (exclusive economic zones and continental shelf) and due to the fact that is easier to transport from sea to land.

Assuming that mineral extraction from seafloor does indeed take place, European marine companies and research centers with specialization in ships and underwater activities/products and services will play a major role in the development of the Blue Economy. Product suppliers and I&D research centers will have to be updated with latest technology, less expensive systems shall adopt less environmental aggressive practices in the development of those systems and components, such as mechanical parts (risers, mooring lines, jack up rigs, anchors, etc.) and technological products (ROV's, AUV's, gliders, ASV, etc.). Their experience, continuous competitiveness and dependance of financial means will allow the possibility of obtaining licenses in international waters since they are less likely to harm unique ecosystems. The experience of the oil and gas industry will be beneficial to the marine minerals extraction sector. Neverthe-

less, the industry of oil and gas will likely continue their robust evolution and it will be required new robust analysis methods and components to fulfill blue growth requirements.

## 1.3 Research objectives

Schiehallion and Loyal fields are located 130km West Shetland and 35km from Faroe Islands (UK) at quadrants 204/205. Schiehallion field was discovered in 1993 and Loyal field was discovered in 1994. They have been in production since 1998 with a total production to date over 30 mmboe of oil and associated gas though the Schiehallion FPSO [4].

The fields are exploited through FPSOs and they have produced approximately 61 million cubic meters of oil crude and 4.6 billions of cubic meters of gas from 1998 to 2009[4]. Recent studies have confirmed that a significant oil potential still remain to be exploited from these reservoirs and new nearby discoveries have confirmed the need to be developed by subsea tie-backs to Schiehallion infrastructure and FPSO [4].

Schiehallion FPSO was designed for 25 years and new discoveries will require an operational FPSO available until 2045. Current Schiehallion FPSO has been deteriorated over the years which makes the vessel infeasible to fulfill future requirements. In this context a new FPSO was developed. The fields were redeveloped with some existent facilities being reused as part of the project known as "QUAD 204". In this context a new mooring system was developed.

Since the short transition time from Schiehallion FPSO to QUAD 204 FPSO, same principles were applied. Although the environmental impact assessment has some major considerations [4] regarding the environmental sensitivities of leaking products, the mooring system is always over designed placing tonnes of stainless steel underwater without regarding the best optimized design. With a new optimized design it would be possible to minimize even more the environmental impact of the mooring lines in the seabed benthic communities, fisheries, birds and marine mammals but also reducing the *CAPEX* for BP Exploration Operating Company Limited (BP).

The main objective of this work is to develop a optimized mooring line system for the new FPSO Glen Lyon at Schiehallion Field. The process of this optimization must be continuous and efficient from environmental conditions to capital expenditures. In the end of this thesis an optimized mooring line system is presented and compared with the existent one.

Through the development of this optimization model, it will be possible to apply the same principles to other focus areas described in the Blue Growth document from European Commission [2]. It will be possible to apply both in Blue Energy (in terms of offshore renewable energy technologies such as wave power devices, ocean thermal energy conversion and offshore wind turbines), Aquaculture area, in terms of mooring the cages in the Atlantic Ocean and in Maritime, Coastal and Cruise Tourism for anchoring tourism vessels.

In the development of this thesis the standard methodology of product development cycle will be used, from conceptual design to detailed design. Each oilfield has a unique development, since environmental phenomena are unique in each earth location. Furthermore this work refers

the optimization of an anchoring system for deep water in the Schiehallion Field, or in other words, the whole development of the mooring system for a specific FPSO.

In an early phase it will be performed hydrodynamic analysis (interaction fluid-structure) in order to place the FPSO in the correct location, as well as to have the ability to weathervane in the turret due the collinear an non-collinear applied forces (environmental conditions). This analysis will provide the base line to vessel positioning and it will be compared with the mooring line described in the references in order to validate the model.

After this step, an optimization of the model will be performed in Matlab through an iteration process to demonstrate the best optimized mooring system for the Glen Lyon FPSO. With this information, several CAD models were designed in CATIA V5 with the critical locations and then a strength and fatigue analysis is performed. Margins of safety are taken and discussed.

The mooring sequence will be developed as well as the methodology of the optimization. With this thesis it will be possible to develop new fields of study in the context of blue growth strategy of mooring vessels since one of the objectives of European Commission is the sea transportation. This thesis will allow the development of mooring systems for Portuguese companies not only for oil and gas fields, but also for new fields of activity, e.g., renewable offshore energy, aquaculture, marine and coastal tourism, offshore mining etc. In terms of research and development it will be possible to increase the funding opportunities in the universities and centers of engineering due to new fields of expertise.

This new strategy alongside with new developments, research innovation and new mooring system methodologies will allow small and medium size companies with deep water activities to place their products in the market. Entities like CEiiA, OceanScan, Abissal OS, Institute of Systems and Robotics, etc. This strategy will allow also micro companies and state entities such as Forum Oceano, Observatório da Madeira, WaveEC, Compta, Sparos, Moínho de Ilhéus, FindFresh, Aquazor, Alga plus, Iberagar or OceanPrime the possibility to start Offshore Aquaculture in Portuguese Coasts as well as mining operations from the complex mooring system point of view.

## 1.4 Thesis Outline

The present document is organized in 6 chapters. The present one, provides the motivation, purpose and contribution, main research objectives and the thesis outline. In this chapter it was verified the need for research in the maritime field as well as existent investments. The European case was analyzed with special focus on the Portuguese case.

In the second chapter a brief explanation of the oil industry is performed as well as the detailed upstream process. After understanding the oil and gas development process, the layout of the northern sea oilfield is detailed. The Schiehallion field was analyzed according to the expansion process and according to recent discoveries in near oil wells. A comparison between former and new FPSO was performed as well.

After understanding both extraction processes, components and the specific oilfield layout were verified as well as the environmental conditions of the oilfield. Predominant wind, waves and currents were analyzed as well as main direction of the external loads. Since the offshore industry is heavily actuated by European/world oil and gas standards, the main standards will be analyzed regarding the mooring systems. Chapter two also includes the latest state of the art of anchoring systems.

In the third chapter, mooring line conditions were presented, as well as the need for segmentation of the mooring equipment. Segmented mooring lines were analyzed and results are compared with the former mooring system. Orcaflex from Orcina Ltd will was used for quasi-static and dynamic analysis, both for frequency and time domain. FEM elements were analyzed, mesh convergence was performed and the global mooring layout was given.

After the comparison of the FPSO's mooring system Glen Lyon in the Schiehallion field in chapter 4 an optimization was performed using Matlab (Genetic Algorithms). Results will be compared from first mooring system to the optimized mooring system. A cost effective analysis was performed as well to determine the benefits of the optimized system. At the end of this chapter the final mooring line was achieved and it was generated a cloud point plot for easy verification of the optimized mooring line.

On the firs part of the fifth chapter of this work, a detailed design of a mooring line was performed. The details will focus on the most critical points of the mooring lines. The detailed design was performed using CAD software CATIA V5 R24 for both studless and stud link elements. Good practices of design were applied for offshore structures and metal elements.

Still on the chapter five, the stress analysis of the chain elements was performed. Material properties, criteria, conditions, loads, etc., was discussed according to suppliers as well as operational conditions in the element links. FEM analysis will be performed in thee steps, pre-processing, solver and post-processing. In both pre-processing and post-processing Altair software (Hypermesh and Hyperview) was used. The solver will be MSC Nastran. A mesh convergence was performed relating processing time with accuracy. FEM process was also described and results were compared with material allowable, both for Ftu (Tension ultimate) and Fty (tension yield). A fatigue analysis was performed and results were compared with DNV-GL standards.

Chapter six presents the general discussion and conclusions of the work developed during the present dissertation. It summarizes the most important achievements of this study and presents future work suggestions. It presents also the issues encountered during the development of the optimization process.

# Chapter 2

# Literature Review

The present chapter gives a macro description of the literature review performed during this work for mooring lines and anchoring systems. Theoretical framework and context basis of oil and gas as a whole, from the understanding of onshore and offshore industry (from economical point of view and maritime investment), passing to main components and infrastructures to the physical location of the specific oilfield is presented. In the final part of this chapter a literature review of mooring lines is introduced with the latest and updated developments in the research of mooring lines.

A comparison between the former and new FPSO is performed, as well as the comprehension of the full mooring system, from main components and equipments to international norms in the underwater industry of mooring equipment.

## 2.1 The Oil and Gas Industry

Nowadays there is a major dependence on petroleum and natural gas. World energy consumption has increased since 1950s. Non renewable energy (fossil fuel) is the most used energy worldwide with an average value up to 80% [1] of world energy consumption. The evolution of energy consumption and projection for the next years is presented in figure 2.1.

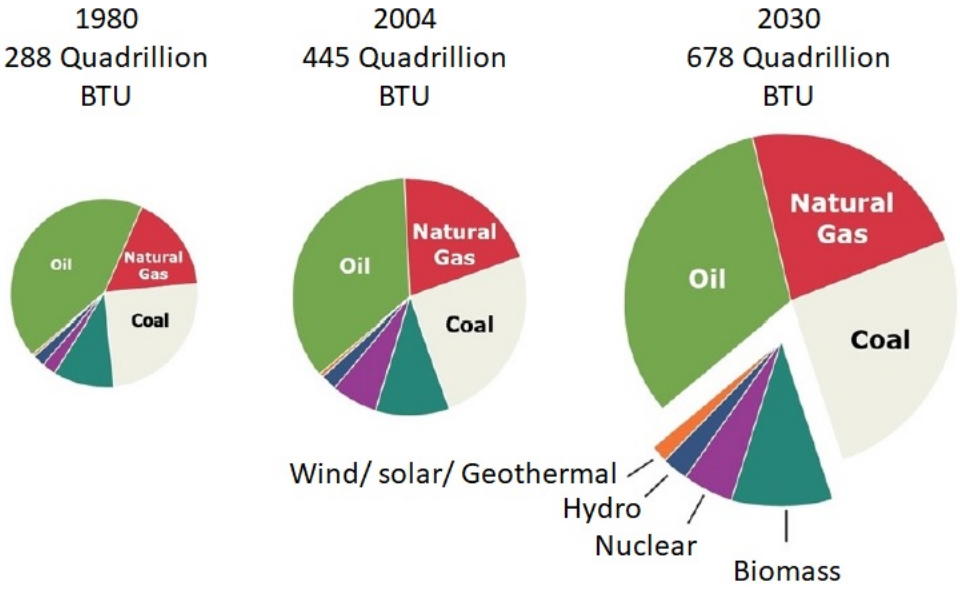


Figure 2.1: Consumption of Coal, Oil and Natural Gas (image from ref. [1])

The world consumption nowadays is about 97.7 million barrels a day, which means 35.6 billion

barrels annually or 1130,8 barrels per second [5]. The daily demand for crude oil worldwide is presented in figure 2.2.

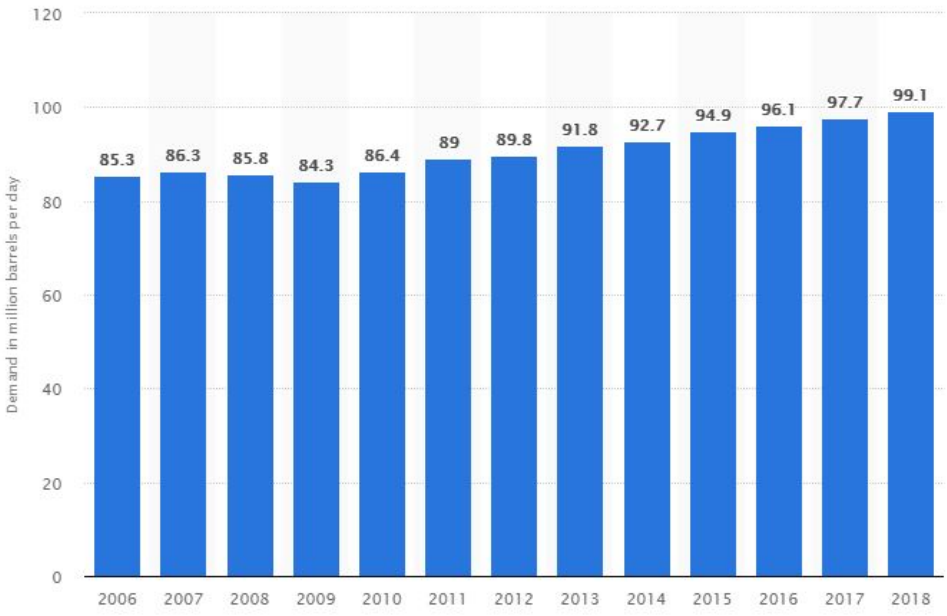


Figure 2.2: Daily demand for crude oil worldwide from 2006 to 2018 (in million barrels, image from ref. [5])

Since the world spins around that precious product hidden most of the times at several hundreds or thousands meters depth in a porous space of a special rock, the term oil and gas cover almost all concentrations of natural hydrocarbons wherever the physical state they are. In a former commercial way the liquid hydrocarbons are known as raw or crude oil, gas hydrocarbons are known as natural gas and the solid hydrocarbons products are known as asphaltenes and petroleum bitumen.

The industry of oil and gas industry is a millions industry, one of the biggest of all times it has the largest companies of the world, from oil refining to distribution of oil derivatives. In this context several small companies are dedicated to specific sectors of the industry, such as exploration and production (upstream), refining and distribution (downstream) and the critical sector of transportation crude oil, petroleum and liquified natural gas (midstream). This thesis will focus on the exploration and production (upstream sector) of oil and gas products.

## 2.2 The Offshore Oil & Gas

Between 1800 and 1900 onshore oil-wells were drilled through weight drops through a cable. This former technique worked for low depths in non full steady wells. With the need to exploit hydrocarbons at higher depths, it became necessary to implement more effective drilling methods such as rotating drills and circulating mud systems, this system is known as rotating rigs.

Rotary rigs started their activity between 1915 and 1938 in the United States using steam en-

gines. As more and more companies started to drill onshore hydrocarbons, the discovery of major wells started to decrease, exploitation of small wells increased, increasing costs. The next step was to drill in the sea. The process to explore and extract oil and gas through rotary rigs in open sea is known as offshore oil and gas production or just offshore production.

Although the first onshore well was drilled in 1859 by Colonel Edwin Drake [6], the beginning of offshore oil and gas exploitation started in 1947 when Kerr-McGee completed the first ever successful offshore well in the Gulf of Mexico off Louisiana in 4.6 meters of water. The whole concept of subsea oilfield was applied in the beginning of the seventies, by placing both injection and productions wells and production equipment under water at seabed. After processing hydrocarbons in the subsea wellhead, the produced hydrocarbons would flow to a nearby onshore processing facility by pipelines or vessels. This concept was the start of subsea offshore engineering [1].

Water depths less than 200 meters are defined as shallow-waters, greater than 200 meters but under 1500 meters are considered deep waters and above 1500 meters are known as ultra deep waters. In a shallow specific reservoir and one satellite well, the subsea costs are relatively flat with increasing depth. However, the cost increases with increasing water depth for more than one well.

Subsea costs as referred before, are the costs of the full project. Generally it includes capital expenditures (*CAPEX*) and operational expenditures (*OPEX*). Capital expenditures includes the total amount of costs necessary for the start of the project, as the required investment to put a project into operation from concept design, engineering construction to final installation. On the other hand the capital expenditures respects all the expenses during normal standard operation of an infrastructure or facility including man labor, utilities, materials and other related expenses. There are several points of interest in *OPEX*, such as operational, testing, maintenance etc.

The subsea oilfield production system is characterized either as wet tree or dry tree oilfield. In dry systems, trees are on the platform or close to the platform, wet systems can be everywhere else in a field development whether in a satellite well, a cluster of wells, template wells or tie-back wells [1]. Dry and wet systems can be seen in figure 2.3. Since the Schiehallion field is a Stand-Alone surface facility connected to several clusters, this work will focus only on Stand-Alone developments.

Stand-Alone layouts of offshore development are used most of the times for big reservoirs since both *CAPEX* and *OPEX* are very high and the return of investment versus the risk is very difficult to justify. In recent years due to the increase of the price of crude oil, there has been some popularity in the development of oil and gas subsea Stand-alone layouts since they are economically feasible. The operators verified that the overall capital expenditures can decrease if the same facility is capable to serve a cluster of wells and underwater structures rather than continue to build a new structure for every new discovered well.

Stand-Alone facilities are normally capable of having more than one field connected providing the flexibility for future satellites, however it has the disadvantages of requiring an early start up. They are only feasible for larger projects due to higher costs. For deep sea applications,

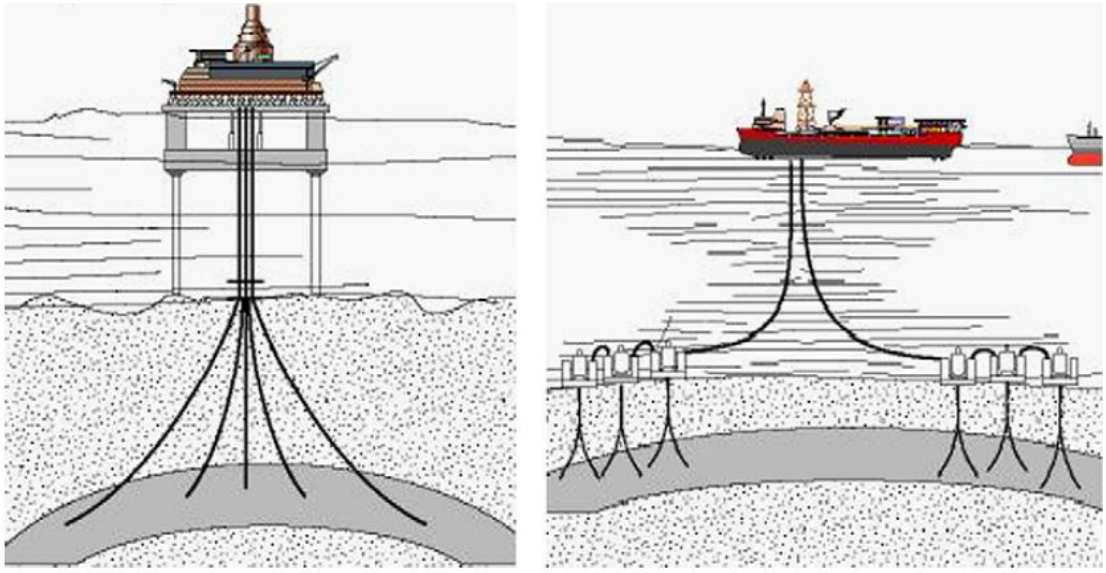

Figure 2.3: Dry Tree and Wet Tree Systems (image from ref. [1])

FPSOs are used as surface facilities rather than common Jack-Up rigs (figure 2.4).

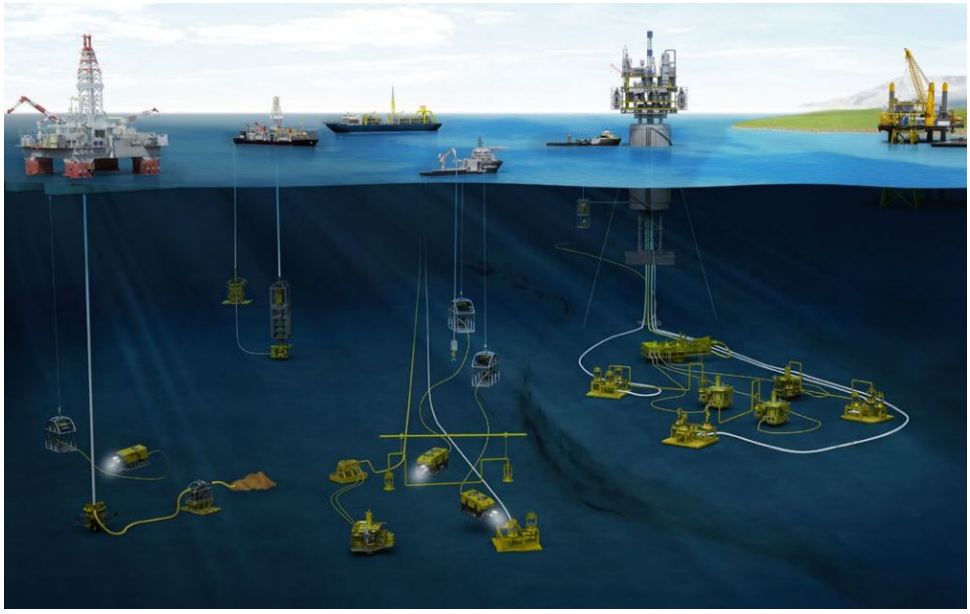

Figure 2.4: Courtesy of Oceaneering - Stand-Alone

In a proper way, the upstream process of offshore exploitation of hydrocarbons is a cycle, starting on the injection of salt water or carbon dioxide from the topside facility into the injection well and then the streaming from the production well to the surface facility of hydrocarbon products. In this context it is important to understand the main components of the oil and gas extraction as well as detailing the top facility vessel main components.

## 2.3 Oil Field Main Components and facilities

In order to detail the main components of an oil field it is important to separate the topside structures or facilities, the seabed components and the connection structural elements between them. This section will focus on the mechanical parts.

### 2.3.1 Topside structures

There are several topside structures or facilities depending on the size and operation depth [6]. There are shallow water facility complexes, gravity based complexes, compliant towers and floating production units (such as FPSOs, tension leg platforms, semi-submersible platforms and spars). In this work it will be taken in consideration only FPSO type facilities (in this case a vessel).

Since a FPSO is a stand-alone structure it does not need external infrastructure such as pipelines or storage compartments to be connected to other fixed facilities. The production unit has the storage within the vessel reducing the need for complex systems. Both crude oil, gas and solid hydrocarbons are offloading to tankers at periodic intervals depending on the capacity of the FPSO. The vessel is a tanker hull type vessel or a barge and due to new discoveries of new oil fields in higher depths they dominate almost all developments above 100 meters depth, such as Glen Lyon FPSO with a operational depth of 395 meters.

Both risers and wellheads from the seabed are located on a central point or on a bow-mounted turret so that the ship can weathervane and rotate freely to the sum of all external forces: wind, waves and current. The vessel is moored to the ground through segmented mooring lines with sheathed spiral strand wire and chain connection elements connected to several anchors (known as static position mooring - POSMOR), or it can also be dynamically positioned using thrusters (dynamic positioning - DYNPOS).

The main processing facility is placed on deck, while both storage and offloading is performed through the hull to a shuttle tank. It can also be used for transportation of equipment such as pipelines or risers [6]. An FPSO can be seen in the figure 2.5.

### 2.3.2 Seabed Components

The underwater systems used for hydrocarbons production are defined as Subsea production systems. The main components for subsea production systems consist of two wells (a completed well for injection and other completed well for production), subsea wellhead, subsea production trees (normally Christmas tree), subsea drilling systems, umbilicals and riser systems, manifolds, jumpers, tie-in and flowline systems, and control systems. Figure 2.6 shows a typical subsea production system with wet tree. This systems dictate the operation procedure. The reservoir is analyzed, then facilities are installed and drilling components are used. After the discovery of oil and gas the extraction process begins.

The subsea wellheads and Christmas trees are the most important components in subsea production systems. The wellhead is basically an end cap component sealing and supporting the

Figure 2.5: Courtesy of Keppel Corp - BW Offshore's Berge Helene FPSO

well. It also supports the BOP stacking during drilling and after completion. On the other hand the Christmas tree is a stack of devices and valves installed on the subsea well (wellhead) and provides an interface between the well and the production facility. The Christmas tree allows a controllable production.

The drilling system is a very important system in oil and gas exploration. This process is characterized by many components from drilling the well to wells completion. The main components are both drilling risers and drilling bits. The process can be applied through drilling submersibles or drilling ships.

A completion riser is normally used for running the tubing hanger and tubing through the drilling riser and BOP into the well-bore. The completion riser can be used to run the Christmas tree and its exposed to harsh external loads such as drilling risers curvature or the upper and lower joints connection.

In order to simplify the subsea systems, subsea manifolds have been used in the oil and gas industry. Manifolds have the purpose of minimize the use of pipelines and risers and optimize the flow of production in the system. The manifold is an arrangement of valves, pipes and tubes designed to combine, control, distribute and monitorize the fluid flow. They are installed at the seabed to gather product or to inject water or gas into wells. There are several types of manifolds in operation from a simple pipeline end manifold (PLEM) to large structures such as an entire subsea process system. In other words a manifold is a structural component (frame) with piping, control module, valves, pigging loop, flow meters etc.

The subsea system used to join two underwater components is called a tie-in system. For flowlines, tie-in systems are used to connect a tree or several trees to a manifold, trees between them, or a pipeline end to a tree or to a manifold. Between structures, jumpers, umbilicals and risers are used to connect components. Jumpers are short connection elements used to transport production fluids from one subsea component to another, for example a tree and a

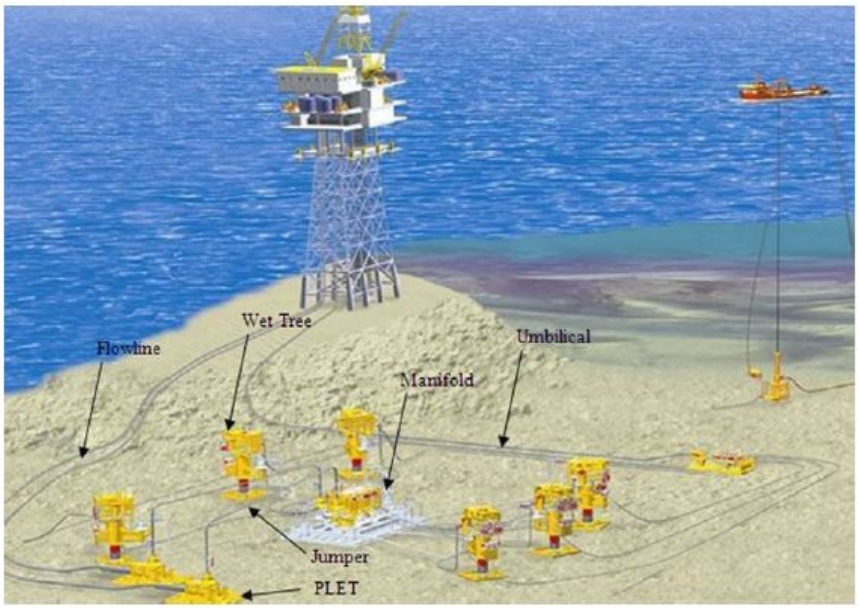


Figure 2.6: Typical Subsea Production System With Wet Tree (image from ref. [1])

manifold, or manifold and an export sled. Umbilicals are used to distribute energy while risers are components used to connect the underwater equipment with topside structures, they are pressurized and used to transport the hydrocarbon components. The connecting elements are described in the next section.

### 2.3.3 Connection between structural elements

The subsea control system receives and transmits the data between surface and seabed, it operates the valves and chokes on Christmas trees, manifolds/templates and pipelines. The subsea control system helps to monitorize the status of production by indicating in-situ conditions such as temperature, pressure, sand detection, hydrates, wax and asphalthenes, etc.

As mentioned before, both umbilicals and risers are the connection elements between subsea and surface components. Subsea umbilicals are used in many underwater applications. They are a combination of many components, fiber optic cables, electric cables, steel tubes and thermoplastic hoses, or just two or three of these components for specific operations. The umbilicals have several functionalities such as water injection, well work-over control, subsea manifold control, chemical injection and electrical power supply. Subsea production risers consists on conduction production pipes connecting the surface to the wellheads at the sea bottom. Risers can be rigid, flexible or hybrid, hybrid risers are a combination of both the previous types. There are four types of production risers, steel catenary risers (SCRs), top tensioned risers (TTRs), flexible risers and hybrid risers. In this work only flexible risers were considered.

## 2.4 The Schiehallion Oil Field

The Schiehallion oil field was discovered in 1993 by the semi-submersible drilling rig Ocean Alliance. Both loyal and Schiehallion fields are located in quadrants 204 and 205 of the UKTS, 130 km West of Shetland and 35 km East of Faroe-UK boundary in medium water depth 350-500 meters [7]. The oil reserves are estimated to be approximately between 450 and 600 million barrels. Although the discovery in 1993 the production only have started on 29 July 1998.

By operation in the Schiehallion field, the use of sharing helicopters and supply vessels is feasible due to nearest distance to the Foinavel and Loyal fields which lie within 15 km. The production life was estimated to be only of 17 years with a daily output (max) of 142 000 barrels a day. The field relies on subsea wellhead technology due to water depth. The system for oil flowing from pipelines to the FPSO is performed through the use of production risers [8].

Schiehallion and Loyal fields location can be observed in figure 2.7.

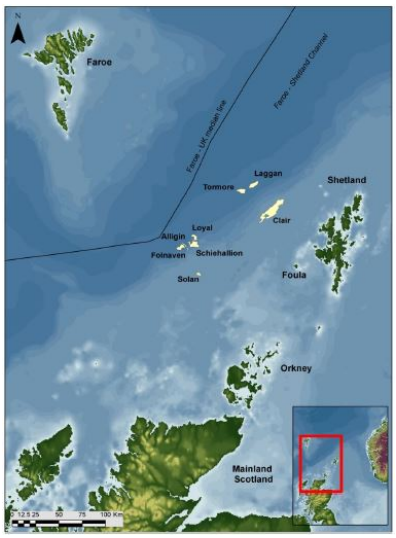


Figure 2.7: Schiehallion and Loyal Fields´satellite view (image from ref. [7])

The fields have been exploited through the use of the Schiehallion FPSO vessel via a multi-centre subsea infrastructure, and they have produced approximately 61 million standard cubic meters of oil (384 million barrels) and 4.6 billion standard cubic meters of gas (163 billion standard cubic feet) from 1998 to 2009. The oilfield comprises five drill centers with 53 active wells, 52 trees, 25 production wells and 28 water injection wells in a very extensive underwater infrastructure (Central, North, West, North West and Loyal) [4].

Both gas and water injection lines are connected to the Schiehallion FPSO through several risers, 10 production, 3 water injection, 1 gas import/export riser and 1 gas lift riser. As referred in the previous chapter both flowlines and risers have a number of subsea structures, including, jumpers, manifolds flowlines, among others. Table 2.1 shows the type of wells in the Schiehallion field.

All solid and liquid hydrocarbons are exported from the FPSO via Shuttle tankers. The gas export pipeline to Sullom Voe Oil Terminal in the Shetland Islands is connected to the FPSO [7], any

Table 2.1: Existing Production and Water Injection Wells associated with the development (image from ref. [9])

| Drill Centre | Number of active wells | Number of active water injection wells |
|---|---|---|
| Central | 16 | 9 |
| West | 6 | 9 |
| North West | 1 | 2 |
| North | 0 | 3 |
| Loyal | 4 | 4 |

excess gas remaining in the production is exported to Magnus on the East of Shetland via Sullom Voe [10].

The oilfield is operating since 1998, however recent discoveries, production history and experience from previous existing wells have confirmed that is still a very significant oil potential reserves in the fields ready to be exploited from these reservoirs. Other nearby oil reserves and gas discoveries have been pointed to have feasible potential to be developed in a nearby future by underwater tiebacks to Schiehallion and Loyal Infrastructures. In order to exploit the remaining reserves it would be necessary to keep the Schiehallion FPSO on-station for a further period then the projected design life of 25 years. The new FPSO shall withstand more 25 years operation in-situ. The subsea layout can be observed in figure 2.8.

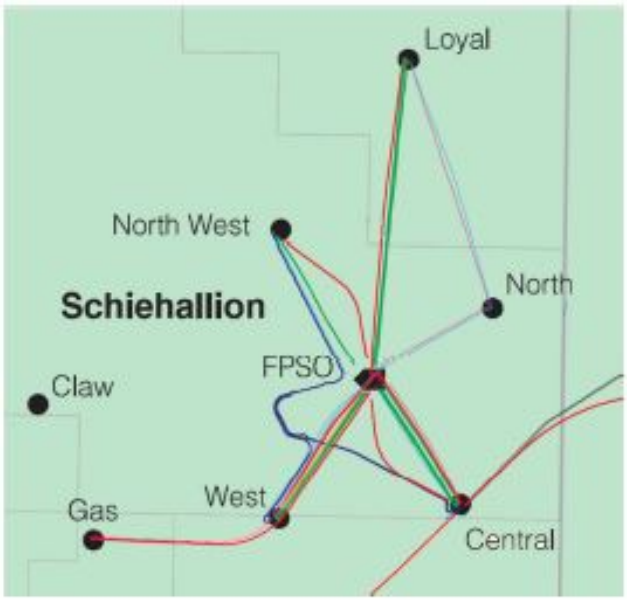


Figure 2.8: Schiehallion and Loyal Fields detailed view (image from ref. [7])

There has been a deterioration of the production operation efficiency due to the operational challenges in recent years. The existing FPSO in unable to fulfill the needs for processing requirements of the anticipated economic field life. The whole system and existing fields are being redesigned and redeveloped as ”Project QUAD 204”. With the additional wells and expansion of the subsea fields and infrastructure, the facilities will be re-used wherever possible. Hence, some will be disconnected, isolated and suspended for the moment, but they will be kept for future operational considerations due to its potential [4] [9].

The Schiehallion field development is performed throwout a consortium of several partners. The partners are BP, Shell, Amerada Hess, Statoil, Murphy and OMV. BP is the final operator responsible for the upstream process. The development of the oil field in expenditures is estimated to be around £1000million.

Both for the installation process of the vessel and in accordance with Petroleum Act 1998, BP is the operator for both former and new FPSO. Britoil limited is the operator of the fields alongside with the department of Energy and Climate Change.

In partnership with public stakeholders and regulatory consultation, the decommissioning programmes are submitted according with international and national regulations and DECC guidelines. The decommissioning project plan has a schedule outlined of three years. It was started in 2013 [7]. The layout of the Schiehallion Oil field is presented in figure 2.9.

## 2.5 Schiehallion FPSO VS Glen Lyon FPSO

For the development of the new oil field, it was imperatively necessary to replace the former FPSO for a new FPSO ready for production, yet, more robust and with more capacity than the previous one, capable to withstand the environmental conditions in the same location until 2035 at least. Within this context it is important to understand the main differences between them.

### 2.5.1 Schiehallion FPSO

Schiehallion FPSO was a new type of platform for oil and gas operated by BP. The FPSO was designed to withstand extreme sea conditions in the Schiehallion field, either waves, currents or wind loads. She was built and delivered to BP in 1996 by Harland and Wolff of Belfast, being the largest FPSO at that time. The hydrocarbon extracted arrives at the turret in the bow region of the vessel from underwater components or through on-vessel facilities via 15 dynamic risers.

The vessel has approximately 246 meters length, a breadth of 45 meters, a depth of 27 meters and an internal turret with 14 meters of diameter (size of the cylinder) [8]. The cylinder is installed in the bow region at the upper deck level supported by the turret collar. As mentioned before the vessel has a design life of 25 years and a theoretical fatigue life of 50 years for environmental loads [4]. All load cases will be discussed later on the next chapter. Several load cases will be defined according to standards and industry norms.

The full crude oil storage capacity has a combined amount of 950 000 barrels and the storage tanks are in the middle body region of the vessel. The vessel has ability to take on board daily 154 000 barrels of crude oil [4]. The on board processing facilities have 3 steps for the processes. The first one is for the recovery of reservoir products, the second is for cleaning and re-injection of water and gas into the wells and the third is the chemical treatments of the facilities. The export of oil from the FPSO is performed via shuttle tanker Loch Rannoch (Constructed at Daewoo's shipyard in South Korea, operated by BP) [8]. The offloading process of

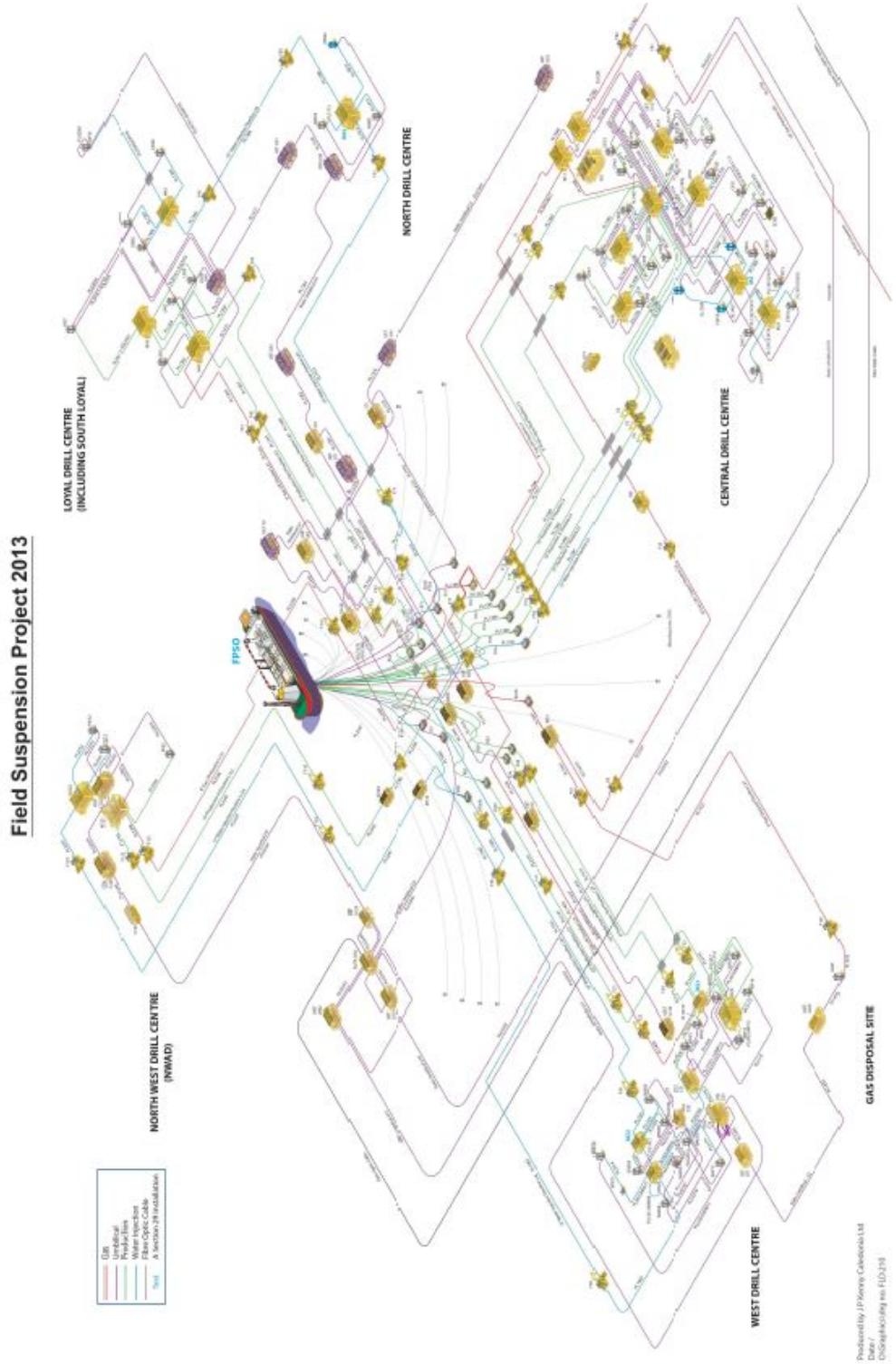


Figure 2.9: Schiehallion and Loyal layout (image from ref. [9])

Figure 2.10: Schiehallion FPSO (image from ref. [12])

oil crude from the FPSO takes place every 3 to 6 days. Loch Rannoch has DP (Dynamic Positioning) compatible with the Schiehallion oil field allowing an accurate positioning from the tanker to the FPSO helping to prevent the overall through-put oil supply from decreasing in production. As referred before both flexible risers carrying the oil and gas, the anchor lines and control umbilicals all reach the surface inside the turret. The Schiehallion FPSO has a accommodation on board for 123 personnel [11]. The Schiehallion FPSO can be seen in figure 2.10.

The mooring system from the seabed is connected to the turret and then connected to the vessel via the turret collar, the station keeping system has a weathervane turret allowing the turret free rotation movement. Table 2.2 shows the specifications of the Schiehallion FPSO [8]. This table is used for comparison between Schiehallion and Glen Lyon FPSO. In the next chapter all external forces will be discussed and analyzed.

### 2.5.2 Glen Lyon FPSO

The re-development of the Schiehallion oil field had 3 possible main approaches:

- Possibility of continuing with the existing FPSO with minimal modifications undertaken offshore;
- Bringing the existing FPSO ashore to be refurbished;
- Replacement of the existing FPSO with more storage capacity with new built facilities.

The winning concept was a new turret-moored FPSO since there was a need for a continuous oil production in-situ as well as the continuation of the exported hydrocarbon gases via the existing West of Shetland Pipeline system (WOSP). Both fluids and conditions at the Schiehallion and Loyal fields (the oils are not at high temperature or pressure) are favorable due to the quality of the crude oil (classed as medium crudes containing low proportion of volatile components).

The new FPSO would need to have increased storage and production capacity in order to achieve the optimum reservoir recovery and extending the service field life allowing any future expan-

Table 2.2: Specification of Schiehallion FPSO (image from ref. [8])

| | |
|---|---|
| Length | 246.00 m |
| Breadth | 45.00 m |
| Depth | 27.00 m |
| Draught (full load condition) | 19.70 m |
| Displacement | 194785 t |
| LCG From AP | 108.36 m |
| VCG from BL | 15.83 m |
| GMT | 3.13 m |
| Natural Surge Period | 125.54 sec |
| Natural Sway Period | 169.28 sec |
| Natural Heave Period | 11.65 sec |
| Natural Roll Period | 15.53 sec |
| Natural Pitch Period | 10.46 sec |
| Natural Yaw Period | 92.37 sec |
| Storage capacity | 950000 t |
| Peak | 154000 barrels of oil/day |
| Design Life | 25 years |
| Operating depth | 395.00 m |
| Turret | 14 m diameter with 360 rotation |
| Mooring | 14 anchor chain legs in groups |
| Type | 6.25 inch studless chain and wire rope |

sion. All the possible future expansions could potentially be developed by subsea tie-back to the new infrastructure as referred before.

Glen Lyon is larger than the existing Schiehallion FPSO and it was designed for 25 years. Glen Lyon FPSO has 270 meters in length, 52 meters in breadth with an operational draught of 14 to 20 meters depth[11]. The new FPSO has also more accommodation on board, 125 personnel although it is capable to accommodate during periods of high activity a total of 168 personnel (hook-up, commissioning and turnarounds).

One important parameter of the Glen Lyon FPSO is the double hull, double-sided, double-bottomed construction designed to better withstand fatigue and corrosion resistant suitable for harsh environmental operations.

Like the former FPSO, Glen Lyon is permanently moored in its operational location by the turret mooring system. It allows the vessel to weathervane around the cylinder in the turret system. Schiehallion FPSO had 14 mooring line system while the new FPSO requires 20 mooring lines arranged in four bundles connected to 20 suction pile anchors. The radius performed by the new mooring lines is greater than the previous ones. The installation of the new FPSO involved a re-attachment of the existing risers, umbilicals and flowlines.

Besides the size, Glen Lyon is able to process and export up to 130 000 barrels a day and store up to 800 000 barrels [13]. The Glen Lyon FPSO can be seen in figure 2.11.

Table 2.3 shows the specifications of the Glen Lyon FPSO [11] [15].

The comparison between the two FPSO can be observed in Table 2.4

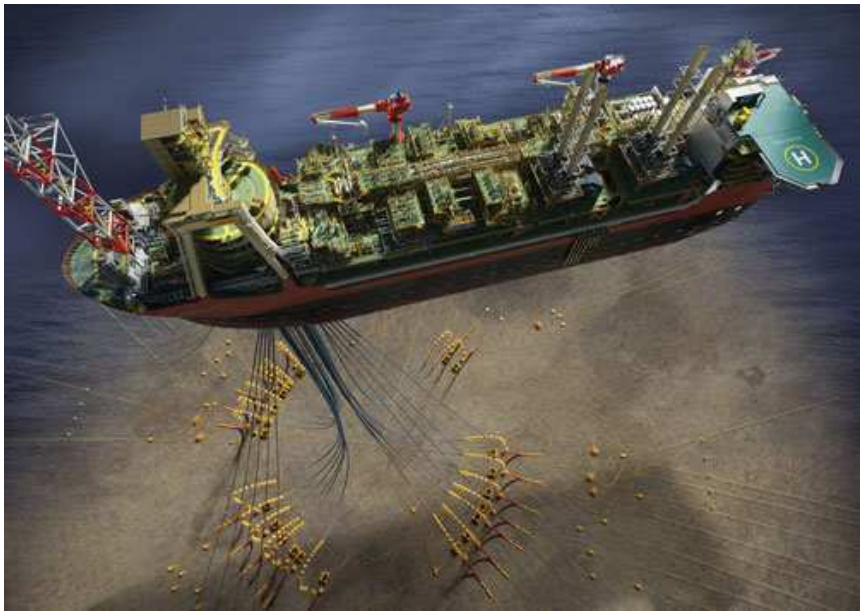

Figure 2.11: Glen Lyon FPSO [14]

Table 2.3: Specification of Glen Lyon FPSO (image from ref. [16])

| | |
|---|---|
| Length | 270.00 m |
| Breadth | 52.00 m |
| Depth | 30.00 m |
| Draught (full load condition) | 20.00 m |
| Displacement | 244342 t |
| LCG From AP | 126.66 m |
| VCG | 18.55 m |
| GMT | 3.39 m |
| Roll radius of gyration | 17.33 m |
| Pitch radius of gyration | 70.77 m |
| Yaw radius of gyration | 70.77 m |
| Natural Roll Period | 22.85 sec |
| Natural Pitch Period | N/A |
| Natural Yaw Period | N/A |
| Storage capacity | 1080000 t |
| Peak | 320000 barrels of oil/day |
| Design Life | 25 years |
| Operating depth | 395 m |
| Turret | 24 m diameter with 360 rotation |
| Mooring | 20 anchor chain legs in 4 groups |
| Type | 6.25 inch studless chain and wire rope |

Table 2.4: Existing Production and Water Injection Wells (image from ref. [10])

| Design capacity | Schiehallion FPSO | Glen Lyon FPSO |
|---|---|---|
| Oil fluids cubic meters/day | 50200 | 50900 |
| Oil production cubic meters/day | 35000 | 20700 |
| Gas production standard cubit meters | 3964300 | 6230000 |
| Produced water cubic meters/day | 35800 | 49300 |

## 2.6 Mooring Systems

There has been a consistent demand for offshore resources and hydrocarbon products. Unlike trading ships, FPSO's stay at pre-defined position, year after year without regular dry docking need for maintenance operations.

The powerful floating structures used for petroleum activities are maintained on station for a very long time by a variety of mooring line types and systems. For centuries, there has been the system of a single anchor mooring system from the bow [17]. However, with increasing depth, specific requirements and products associated with station keeping have increased. For floating structures used for offshore oil and gas operations, it has resulted in new and more developed materials and technology for different combination of mooring lines. A good example is the steel wire rope for deep water application like the ones used nowadays in TLP in order to improve horizontal and vertical plane responses.

Through the past years, the engineering operators of mooring design has been known by the experience developed of ship building and offshore structures [18]. The main objective of the mooring system in any vessel is to allow the relative movement of the ship according to external loads in-site ensuring that the ship remains very close to the point it was originally designed for, since both structural and functional inadequacy affects also the efficiency of energy conversion used in station keeping and offshore operations[19].

The mooring systems can be passive (if the movements have limited effect on the device efficiency and the purpose is just station keeping), active (if the system stiffness is the most important factor in the dynamic response of the device) and reactive (if the mooring provides a reaction force).

Mooring systems can also be classified based on the layout configuration: spread, turret, single point and dynamic mooring.

- The spread mooring systems consists on multiple mooring lines attached to the floating body. The movements are limited to horizontal excursion and they do not rotate about its hull. It comprises the catenary, multi-segmented lines and taut lines. These systems are very expensive;
- Catenary turret moored (internal or external) consists on several mooring lines connecting a floating vessel or structure allowing weathervaning around the turret;
- Single Anchor Leg Mooring (SALM) is a floating structure connected to a single or multiple buoy and it is able to weathervane around the buoy;
- Articulated Loading Column (ALC) on the other hand is a floating structure able to weathervane around a bottom hinged column;
- Fixed Tower Mooring is also a floating structure that can weathervane around the mooring point (composed by a anchored tower into the seabed).

In the context of this work only passive mooring system is considered with a catenary turret mooring system as it can be seen in figure 2.12.

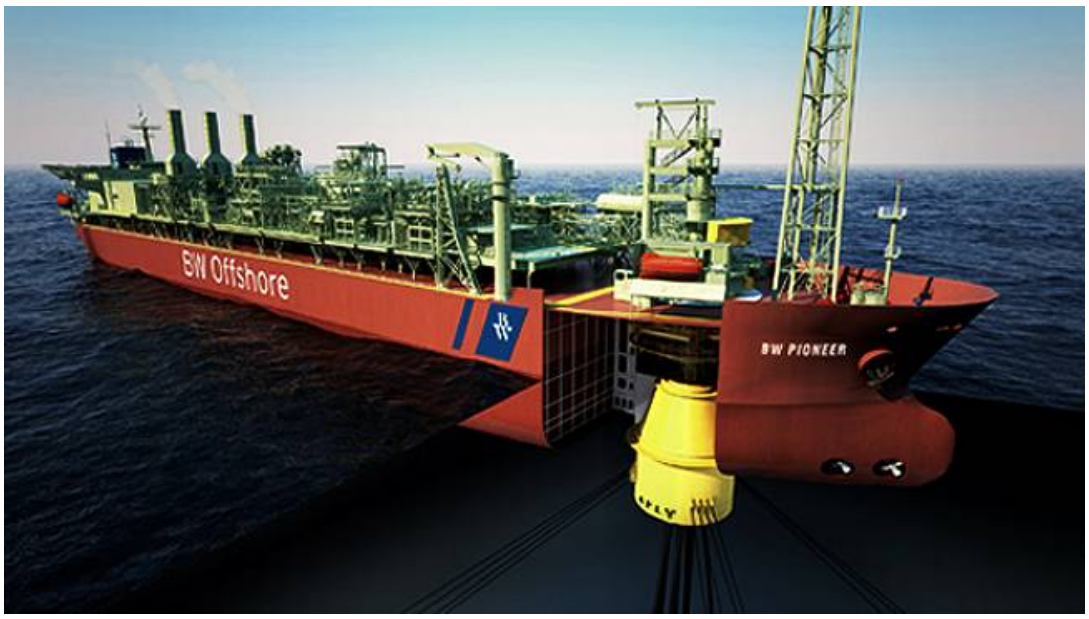


Figure 2.12: Turret Mooring System of BW Pioneer FPSO (image from ref. [20])

The mooring system consists of all the components required for anchoring the vessel from the turret to the seabed. The main components are the turret (as mentioned before), mooring lines (chains, shackles, steel wire rope, etc.), buoys (when applicable) and anchors. For Glen Lyon FPSO all anchors are suction pile type buried deep into the seabed.

The Glen Lyon FPSO is moored by a catenary wire and chain mooring line attached to a geo-stationary internal turret. The turret can be seen in figure 2.13.


Figure 2.13: Turret schematic (image from ref. [21])

The turret was placed at the Schiehallion field and is passively weathervaned with no thruster assistance. The anchor piles are located at a greater radius than the existing piles. The mooring was designed for a 100 year intact system with one line failed condition to avoid uplift at the anchor piles. The mooring system was designed for 25 years, however the target design life for

mooring components was designed for 250 years. The mooring system was designed to have 20 to 24 mooring lines in 4 identical bundles arranged at 90°. The mooring system is symmetrical with four bundles with twenty to twenty-four lines in total mooring lines. The mooring plan can be seen in figure 2.14.

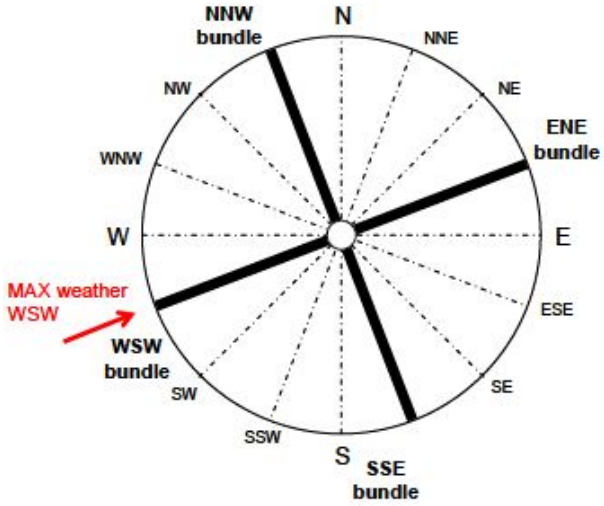


Figure 2.14: Mooring plan (image from ref. [16])

Besides the 24 meters of turret nominal diameter, the chain stoppers were re-arranged in two radii. Three lines from each bundle were placed on an outer diameter of 20 meters and an elevation of 0.5 meters above the hull baseline, while two lines placed on a outer diameter of 13 meters with an elevation of 1 meter below the hull baseline both coincident with the center of the turret. A scheme of the mooring lines location in the turret can be seen in figure 2.15.

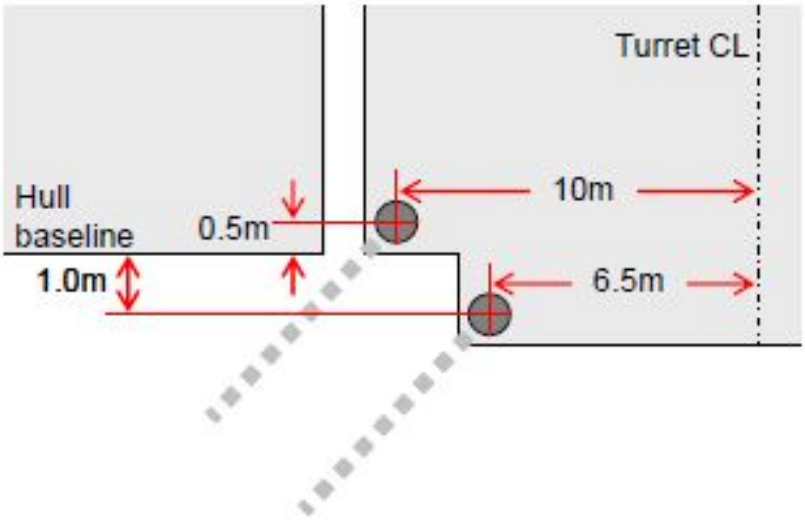


Figure 2.15: Mooring stopper arrangement (image from ref. [16])

On the other side, the turret has also the risers used for oil and gas operations (injection and production). The system has 20 risers in 4 identical bundles arranged at 90 °between them

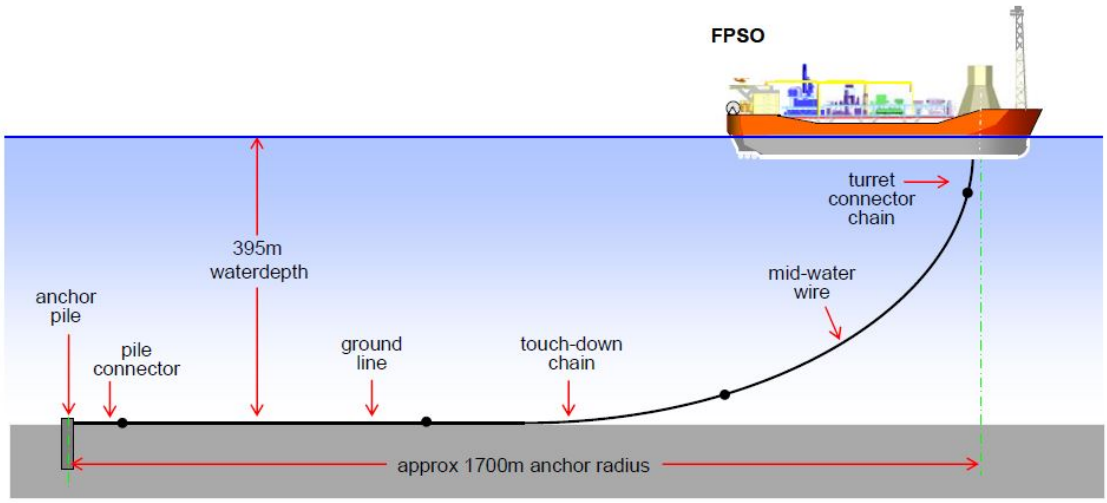


Figure 2.16: Principal mooring components (image from ref. [16])

with a mismatch of 45 °with the mooring lines. Although the purpose of this work was not the arrangement of the risers, for the mooring arrangement and FPSO positioning the riser characteristics of the risers are needed to be modeled with a standard precision to reflect the effects of inertia and drag from the mooring response. The riser properties and characteristics can be seen in Annex 1. Figure 2.16 shows the intended mooring segments.

## 2.7 Mooring Line Components

The mooring lines are generally composed by several segments. The discussion of mooring lines and mooring components are introduced in this section to help understanding the system as a whole.

Some components are suitable for certain operation conditions instead of others. Factor like durability, cost, compatibility with other systems and functionality under environmental conditions are taken into consideration to determine the types of mooring lines and components to use. Material properties understanding is needed in the design of such systems for the decision making process.

The referred components include metallic and nonmetallic ropes, chain links and connecting hardware in all types, sizes and materials. The choice of each component is a function of the life expectancy, precise application, restraints, vessel impact, etc. [22]. Tradeoffs between weight, ease to operate, cost and water depth must be performed in the development of the oilfield. The main components of the mooring system for Glen Lyon FPSO can be observed in figure 2.16.

After the turret, the mooring line is composed by 5 segments, from seabed to turret, chain, sheathed spiral strand, chain, sheathed spiral strand and chain again.

Both segment one and two are completely lying at seabed, the first segment should have short

length and be very resistant due to the fact that is connected to the suction pile subjected to high loads. The second segment is sheathed spiral strand since it does not withstand any expected load and it is connected to the third segment. The third segment is a very important segment since it is subjected to high loads both from environmental conditions and whiplashes, resulting from the difference of the height of the waves. It is the longest segment, and supports the main loads of the vessel, it is connected to the forth segment. The second-to-last segment is sheathed spiral strand since it only withstand tensional stress. The last segment is connected from the fourth segment to the turret since it shall withstand the loads from the impacts of the waves into the FPSO. In figure 2.17 it can be seen the segments of the mooring lines of the FPSO Glen Lyon.

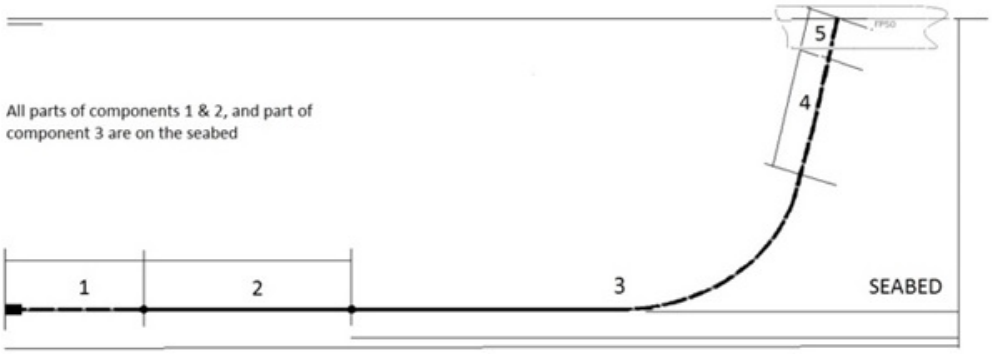


Figure 2.17: Glen Lyon mooring line segments

### 2.7.1 Studless Vs Studlink chain elements

Mooring system of floating structures consist of long lengths of chain, ropes or wires, or a combination between them. The mooring chain is the main component that contributes significantly to anchor the FPSO, in the precise position. The service life of the structural components is increased by the awareness of wear, corrosion, fatigue and resistance [23].

The chain is the component that has the better resistance both for bottom and FPSO abrasion (slamming). Besides having good catenary stiffness to horizontal and vertical excursions, it is suitable for long term mooring. It is only suitable if periodic maintenance and inspection operations are performed avoiding the bio-fouling responsible for increasing the weight per unit ratio, and the abrasion damage caused by links rotation [24]. Normally two types of mooring chains are used, open link (also called studless link) and stud link. The chain links are the most expensive component in the anchoring process [23].

- Studless link - Normally made of steel, reliable in terms of fatigue, although the tendency to get more entangled than stud links;
- Stud link - The Stud links are normally 10% heavier than studless links, however they have a higher breaking load.

The physical difference between stud link and studless links can be seen in figure 2.18 [25].

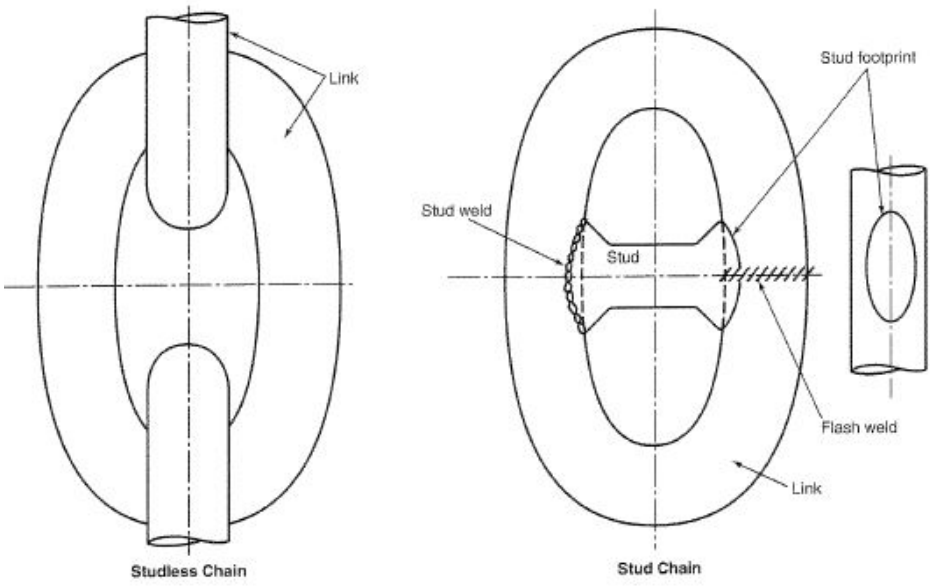


Figure 2.18: Stud Vs studless links (image from ref. [25])

For over 30 years stud chains have been used by the offshore industry. However the industry has experienced problems associated with studs including fracture of the stud, fatigue cracks and loose stud. In the nineties a new type of chain has started in the offshore industry, the studless chain links.Besides being 10% lighter it has about the same breaking strength however since it has a lower fatigue life [25].

Chains are obtained in several grades, each grade represents different proof tensile strength. Four grades are in general used for offshore anchoring systems (RQ3, R3, R3S and RQ4). The most common is RQ3 since has a very good performance.

Chain properties can be seen in table 2.5

For the minimum break load the constant c must be used:

- c=27.4 for Grade RQ4;
- c=22.3 for Grade R3 - RQ3;
- c=24.9 for Grade R3S.

In order to have a mooring system economically feasible, the mooring systems for deep water should be segmented in which the chain is connected to a sheathed spiral strand. In the next subsection spiral strand wires are analyzed.

### 2.7.2 Sheathed spiral strand steel wire rope

There are many applications in the offshore industry for steel wire ropes. For deep water, steel wires cables/ ropes are the second most used component for mooring systems [26]. In order to minimize the vertical loads, synthetic lines are an alternative solution to chains. The most used materials are kevlar, polypropylene, polyester, nylon and high density polyethylene. Mooring

Table 2.5: Chain properties (image from ref. [16])

| Designation | Symbol | Unit | studless | Stud link |
|---|---|---|---|---|
| Diameter of chain | D | [m] | | |
| Mass per meter | m | [te/m] | $19.9 * D^2$ | $21.9 * D^2$ |
| Total link length | | | 6.0*D | 6.0*d |
| Length within chain | | | 4.0*D | 4.0*D |
| Number of links/meter | N | | 1(4.0*D) | 1/(4.0*D) |
| Mass per link | m/N | te | $79.6 * D^3$ | $87.6 * D^3$ |
| Density of steel | $\rho$ | $te/m^3$ | 7.8 | 7.8 |
| Weight per meter chain | W | kN/m | $195.2 * D^2$ | $214.8 * D^2$ |
| Weight per chain link | | kN | $780.8 * D^3$ | $859.4 * D^3$ |
| Volume per meter chain | | m/$\rho$ | $2.551 * D^2$ | $2.807 * D^2$ |
| Volume per chain link | (m/N)/$\rho$ | m/$\rho$ | $10.2 * D^3$ | $11.2 * D^3$ |
| Young's modulus | E | kN/$m^2$ | $5.44 * 10^7$ | $6.40 * 10^7$ |
| 2*cross-sectional areas of bar | a | $m^2$ | $\pi * D^2/2$ | $\pi * D^2/2$ |
| Min. Breakin load | Fb | mN | $c * D^2(44 - 80 * D)$ | $c * D^2(44 - 80 * D)$ |
| Underw. weight p. meter chain | Wu | kN/m | $167.0 * d^2$ | $186.6 * d^2$ |
| Axial stiffness | EA | kN | $0.845 * 10^8 * D^2$ | $1.01 * 10^8 * D^2$ |

chains are resistant due to the weight of the elements while synthetic lines offers a different resistance depending on elastic characteristics [24]. Both weight and elastic properties makes the wire ropes suitable for deep water and tether applications.

There are many types of wire rope sections. The wire rope generally includes a number of strands wound in the same rotational direction around the center to form the rope. The number of strands and wires varies according to the specific application. There are non-sheathed spiral strand, non-sheathed spiral strand rope, sheath spiral strand rope, multi strand wire rope, 6 strand and 8 Strand wire rope types. A basic scheme of the structure of a synthetic line can be observed in figure 2.19.

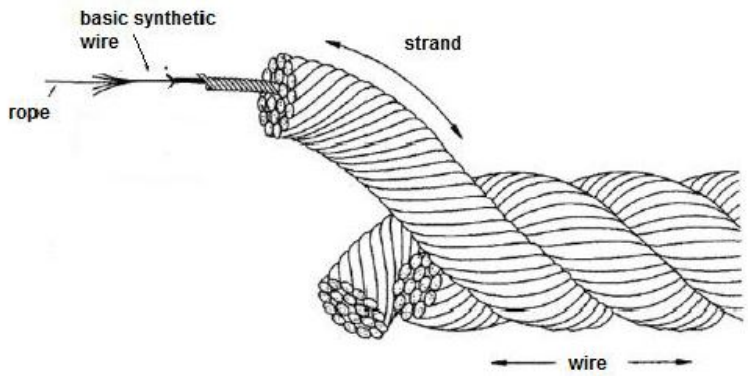


Figure 2.19: Structure of a synthetic wire rope (image from ref. [24])

The most important common type of failure modes for wire ropes are:

- Excessive abrasion;
- Corrosion due to lack of lubrication;
- Cathod corrosion;
- Extreme bending.

Since fish bites and environmental growth represents a serious problem, the fiber rope is normally protected by a outer jacket. The polymeric jacket provides long term mechanical properties and higher maintenance periods [27]. In the development of this thesis a Sheathed spiral strand rope is considered. A sheathed spiral strand can be seen in figure 2.20.

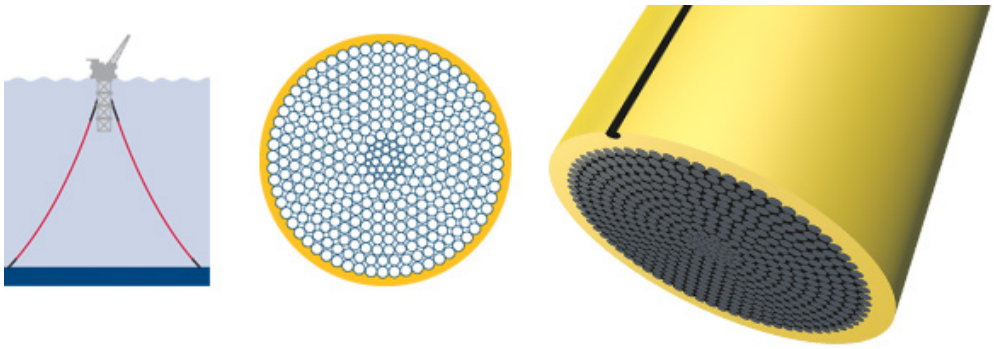

Figure 2.20: Spiral strand wire rope (image from ref. [1])

The properties proposed for spiral strand wire are detailed in table 2.6

Table 2.6: Wire properties (image from ref. [16])

| Spi. strand wire | MBL (kN) | D[mm] | Stiffness AE $kN * 10^6$ | Mass [kg/m] | Sub.weight (N/m)Te |
|---|---|---|---|---|---|
| Nominal 3.5 | 6418.00 | 88.90 | 0.690 | 42.00 | 349.80 |
| Nominal 4.75 | 14362.00 | 121.00 | 1.353 | 76.50 | 585.70 |
| Nominal 5.50 | 19180.00 | 140.00 | 1.799 | 102.40 | 799.50 |
| Nominal 5.75 | 20469.00 | 146.00 | 1.940 | 110.20 | 860.30 |
| Nominal 6.70 | - | 170.20 | 2.079 | 123.00 | 1050.00 |

### 2.7.3 Suction piles

Suction pile anchors were conceptual designed by Shell in the seventies, however the first prototype is believed to have been installed in 1981. In the nineties, one was installed at 1450 meters depth. In the 2000s, subsea foundations were installed and in 2010s heavy subsea modules emerged [28].

The suction piles are the predominant elements for anchoring the chain to the seabed. The are used in majority for oil and gas projects. The suction pile elements are basically cylindrical boxes embedded by suction, which means that they are lowered to the seabed followed by a suction process applied to the valve located at the top. The process requires the installation of underwater pumps assisted by divers (for very-shallow waters) or ROVs (for shallow, deep and ultra deep waters) [29].

The main advantages of suction pile anchors are the quicker installation (about one hour), ease to install and noise free installation process compared to other systems. The remove process during decommissioning is also easier than other systems since the fast retrieval by reversing the pumps pulling the foundation into the ground. The mooring lines connected to the suction

pile are at optimal load attachment since they are generating lateral forces. A Suction pile can be seen in figure 2.21.

Figure 2.21: Suction pile (image from ref. [30])

### 2.7.4 Regulation and Norms

Since the oil and gas activities are very pollutant to the environment, they shall meet very precise norms and regulations in order to avoid the hazard risks of oil spilling or any other dangerous activities to human beings or to the environment under extreme environmental loads. The mooring system for deep oil production is a very important system in the development of the oil and gas fields, as well as the engineering sector which is responsible for the application of those strict norms and legislation into the project [24].

In the development of this work several industry norms are applied to the mooring systems. It is important to take into consideration that there are several entities defining norms and legislation, the most important in the oil and gas activities are DNV-GL, API, ISO and NORSOK. The norms and standards used for this work are described below:

- DNV-OS-E301 - Position Mooring [31];
- DNV-OS-E302 - Offshore Mooring Chain [32];
- DNV-OS-E303 - Offshore Mooring Fiber Ropes [33];
- DNV-OS-E304 - Offshore Mooring Steel Wire Ropes [34];
- Bureau Veritas - NI 604 DT R00 E - Fatigue of Top Chain of Mooring Lines due to in-plane and out-of-plane bending [35];
- API RP 2SK - Design and analysis of stationkeeping systems for floating structures [25];
- API RP 2SM - Design, Manufacture, Installation, and Maintenance of Synthetic Fiber Ropes for Offshore Mooring [36];

- ISO 19901-7 - Petroleum and natural gas industries — Specific requirements for offshore structures - Part 7 - Stationkeeping systems for floating offshore structures and mobile offshore units [37];
- ISO 1704- Ships and marine technology — Stud-link anchor chains [38];
- NORSOK M-001- Materials Selection [39];
- NORSOK N-001- Structural Design [40];
- NORSOK N-002- Collection of Metocean Data [41];
- NORSOK N-004- Design of steel structures [42].

## 2.8 Environmental condition

The FPSO will have to be in the same place for 25 years. For that reason, an accurate environmental data gathering is necessary for a better design of the mooring system. It is then important to understand the environmental conditions/ loads that will actuate on the vessel during all operation times. This information is required both for engineering and design purposes.

The data is normally required for operator's own needs, or by imposition of NPD or by any maritime authority. The standard data covers several types of information, weather forecasting, helicopter traffic, tanker loading, climate statistics, marine operations, etc. [41].

The offshore environmental data can vary from simple observation of the sea for aviation purposes, to complete and detailed acquisition of data from several platforms and sensors. The environmental offshore data is known as metocean data or metocean conditions. Metocean data means Meteorology and Oceanography data.

In the development of this thesis, only weather and oceanography data will be taken in consideration. The weather observation in metocean collection refers to wind direction, wind speed, air pressure, air temperature, sea surface temperature, humidity, wave height, wave period, clouds, weather and icing while the oceanography refers to ocean currents at specified depths, water level, sea temperature at specific depths, salt content, oxygen, icebergs size and drift, and sea ice.

In the development of the load cases, the worst condition will be analyzed. In the next subsubsections both waves, wind and current will be analyzed as well. For the development of the environment, some basic considerations must be taken in order to have an accurate analysis.

The sea water (salt water) is assumed to be incompressible, inviscid and irrotational. The velocity potential $\phi$ is used to describe the velocity vector V(x,y,z,t)=(u,v,w) at a certain time $t$ at a precise point x=(x,y,z). The equation can be expressed as:

$$V = \nabla\phi = i\frac{\partial\phi}{\partial x} + j\frac{\partial\phi}{\partial y} + k\frac{\partial\phi}{\partial z} \quad (2.1)$$

Both i, j and k are unit vector along the x, y and z axes. There is no physical meaning in the velocity potential, however is important for the mathematical analysis of irrotational fluid motion. Considering the fluid as irrotational, the vorticity vector is zero alongside in the fluid, such as:

$$\omega = \nabla \times V \quad (2.2)$$

The sea water is also incompressible, i.e. $\nabla \times V = 0$, which satisfies Laplace equation:

$$\frac{\partial^2 \phi}{\partial x^2} + \frac{\partial^2 \phi}{\partial y^2} + \frac{\partial^2 \phi}{\partial z^2} = 0 \quad (2.3)$$

Adding the pressure parameter to the equation, it is important to follow Bernoulli's equation. Assuming z-axis to be vertical and positive we can write:

$$p + \rho g z + \rho \frac{\partial \phi}{\partial t} + \frac{\rho}{2} V \cdot V = C \quad (2.4)$$

C is an arbitrary function of time. In the former equation the only external force field is gravity. C can be related to the atmospheric pressure or ambient pressure. The mean sea free surface level will be assumed for z=0.

### 2.8.1 Waves

The most difficult part in mooring ship design is due to the fact of the sea irregularities. The acquisition of ocean data requires the use of several elements of probability and statistics. The wave acquisition data is based on a random distribution process. It describes the possibility/likelihood probability to a random process to occur. The typical random process distribution is Gaussian distribution [43].

In the wave design, it is important to analyze a series of points from ten to one hundred years of height and wave period. In the Schiehallion field the WSW direction is the predominant wave direction. In figure 2.22 the WSW form curves can be seen.

The maximum wave height in association with lower wave periods should be limited to the 1/12 steepness curve [16]. For long time analysis (fatigue analysis) an one hundred year return period is considered. In figure 2.23 a 100 year wave criteria is presented.

The representation of the sea surface is performed statistically. Is evident the highly irregular and random sea state under all types of conditions, either calm or stormy. For the sea representation a typical sinusoidal wave may be represented as:

$$\zeta(x,t) = a \sin(-kt - \omega t + \theta) \quad (2.5)$$

a =Wave amplitude
k $= 2\pi/\lambda$ =Wave number
$\lambda$ =Wave length
$\omega = 2\pi/T$ =Wave frequency
T =Wave period

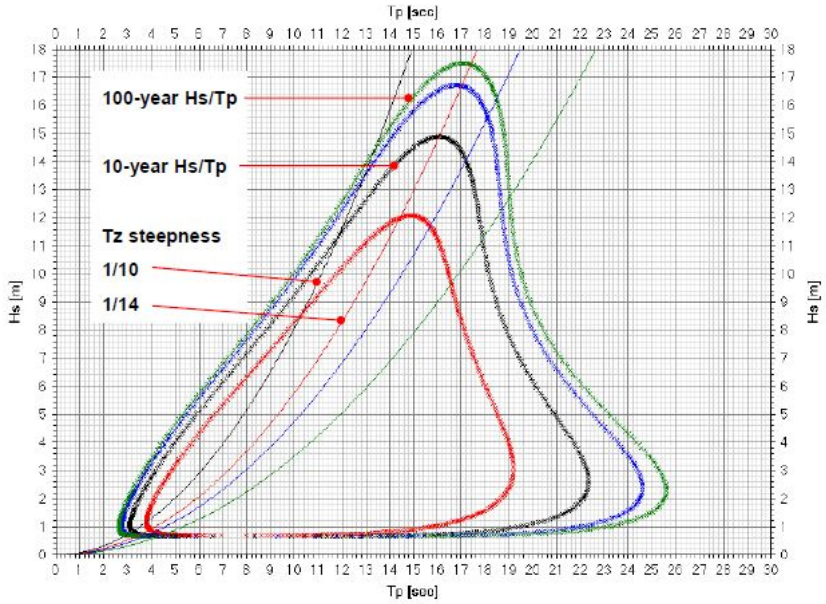


Figure 2.22: WSW wave form parameters (image from ref. [16])

$\theta$ =Phase angle

The representation for irregular sea of surface elevation h(x,t) can be represented as:

$$h(x,t) = \lim_{n\to\infty} \sum_{i=1}^{n} a_t \sin(-k_t x - \omega_t t + \theta_t) \quad (2.6)$$

For several decades, there has been a long acquisition of oceanic wave data. In 1959 Bretschneider [45] proposed two parameters for wave spectrum, significant wave heigh $H_s$, and the modal wave frequency $\omega_M$. The modal wave frequency reaches its peak when wave spectrum maximum height occurs. The most common spectra for ocean engineering was proposed by Pierson and Moskowitz in 1964 [46]. The Pieson and Moskovitz spectra assumes a deep sea and a sea-state fully developed condition. On other hand for coastal waters, the Joint North Wave Project (JONSWAP) spectrum was used in 1973 by Hasselman [47] and in 1976 by Ewig [48].

In 1987 Chakrabarti [49] defined the following wave spectrums.

- Philips;
- Newmann Spectrum;
- Pierson-Moskowitz Spectrum;
- Bretschneider Spectrum;
- ISSC Spectrum;
- ITTC Spectrum;
- Unified Form;
- JONSWAP Spectrum;
- Scott Spectrum;

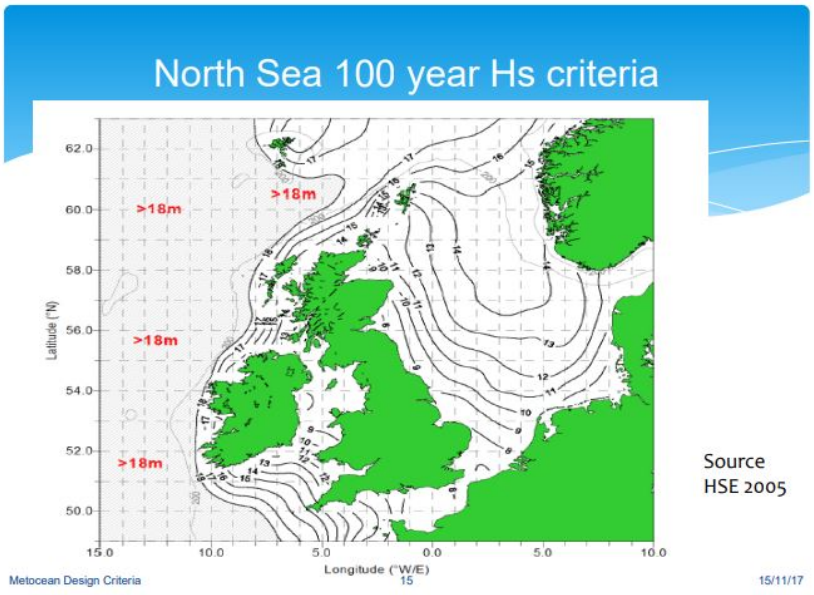


Figure 2.23: North Sea 100 year Hs criteria (image from ref. [44])

- Liu Spectrum;
- Mitsuyasu Spectrum;
- Ochi-Hubble Spectrum.

The analysis of the wave conditions in the Schiehallion field assumes that:

- Wave parameters such as Hs, Hs sea and Hs swell are taken from NEXTRA;
- Wave periods from NEXTRA were compared to measured data taken from directional wave buoy off Faroe islands;
- JONSWAP spectra has the main interest since its gamma values (peak enhancement) of the spectral fits when compared with Pierson-Moskowitz spectrum. The spectral width parameters $\sigma a$ and $\sigma b$ have been fixed at values of 0.07 and 0.09 respectively.

In the development of this work only Pierson-Moskowitz and JONSWAP will be considered due to BP requirements.

The Pieson-Moskowitz spectra can be expressed as:

$$S(\omega) = \frac{\alpha g^2}{\omega^5} exp\left[-0.74\left(\frac{\omega V_w}{g}\right)^{-4}\right] \quad (2.7)$$

$\omega$ = Spectral ordinate in $cm^2$ sec g = acceleration of gravity in $cm/sec^2$ $\omega$ = Frequency in Rad/sec $\alpha$ = 0.00810 $V_w$ = Wind speed in cm/sec (19.5m above the sea level) Modifying the P-M spectrum, JONSWAP spectrum can be written as:

$$S(\omega) = \frac{\alpha g^2}{\omega^5} exp\left[-1.25\left(\frac{\omega}{\omega_m}\right)^{-4}\right] \gamma^{exp\left[-\frac{(\omega-\omega_m)^2}{2\sigma^2\omega_m^2}\right]} \quad (2.8)$$

$\gamma$ = equal to 3.3
$\sigma$ = 0.07 and 0.09 for $\omega < \omega_m$ and $\omega > \omega_m$ respectively

$\alpha$ = $0.076e^{-0.22}$
$\omega_m$ = $2\pi\frac{3.5\overline{x}^{-0.33}g}{V_{w10}}$
$V_{w10}$ = wind speed 10m above the sea level
$\overline{x}$ = $\frac{gx}{V_{W10}^2}$
x in the above equation denote fetch.

#### 2.8.1.1 Wave Height and period statistical determination

In the time-domain analysis:
The Wave heigh $H_s$ is the average height of the highest one-third of all waves and is referred as $H_{1/3}$.

$$H_{1/3} = \frac{1}{N/3}\sum_{i=1}^{N/3} H_i \quad (2.9)$$

N is the number of wave heights and $H_i$ is a series of wave heights from highest to lowest.
In the frequency domain analysis:
Significant wave height $H_s$ is related to zero moment $m_0$ which is the area below the energy density spectrum curve.

$$H_s = 4\sqrt{m_0} \quad (2.10)$$

The root mean square (rms) in the time domain analysis is defined as:

$$H_{rms} = \sqrt{\frac{1}{N}\sum_{i=1}^{N} H_i^2} \quad (2.11)$$

The roor mean square (rms) in the frequency domain analysis is defined as:

$$H_{rms} = 2\sqrt{2m_0} \quad (2.12)$$

In the time-domain analysis, the largest wave height is known as maximum wave height record $H_{max}$. In the frequency domain, this parameter is a probabilistic value defined by Longuet-Higgins in 1952 [50]. For a small range of the wave spectrum:

$$H_{max} = \left(\sqrt{\sqrt{\ln N}} + \frac{0.2886}{\sqrt{\ln N}}\right) H_{max} \quad (2.13)$$

In the time-domain analysis, mean zero period $T_{0,2}$ is the total length of time divided by the point zero up-crossing in the record of values. Other important value is the mean crest period $T_{0,1}$, which is calculated as total length of time divided by the number of crests in the record. The mean wave period in the frequency domain is defined as:
$T_{0,1}$=$2\pi\frac{m_0}{m_1}$

$T_{0,2}$=$2\pi\sqrt{\frac{m_0}{m_2}}$

### 2.8.2 Wind

In the offshore mooring design, the wind is a very important factor. The wind conditions were collected in advanced in order to be consistent with other environmental conditions. Two common methods are used to access the effects of wind in design:

- The wind forces are considered to be constant and calculated based on one minute average velocity;
- The fluctuating wind forces are analyzed from a steady component, the one hour average velocity plus a time-varying component calculated from an empirical wind gust spectrum.

A 10 meters elevation above the mean sea level is considered for wind speed design. Both rapid changes in wind and resulting dynamic loads should be considered in the offshore structures design. In figure 2.24 can be seen the wind spectral density curves. A wind spectra of one hour mean is analyzed.

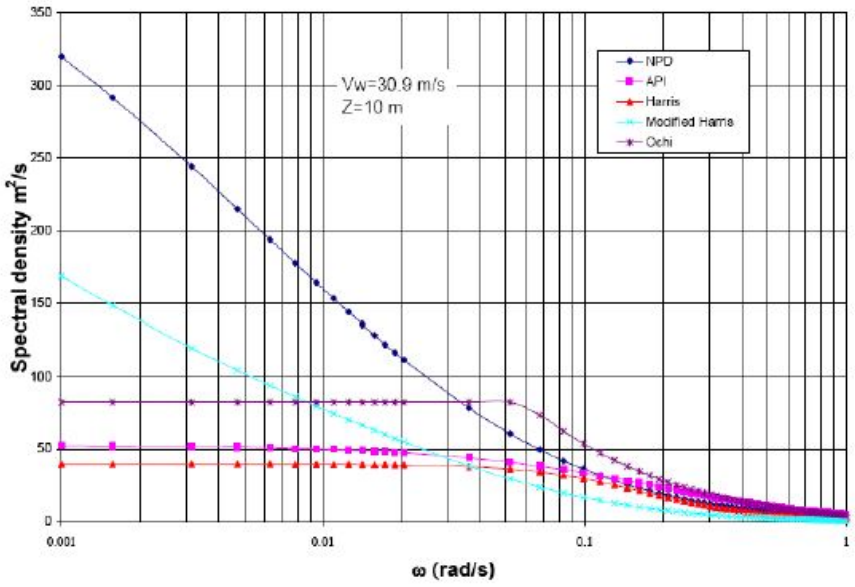


Figure 2.24: Spectral densities following the formulation of NPD, API, Harris-DNV and Ochi-Shin (image from ref. [16])

In table 2.7 an one hundred year wind speed (at 10 meters elevation) is detailed [41]. In table 2.8 the exposed area subjected to wind loads is assumed.

Table 2.7: 100 year wind velocity (image from ref. [16])

| Direction | 1 hour mean | 1 minute mean |
|---|---|---|
| WSW | 40.0 [m/s] | 51.0 [m/s] |
| SSE | 37.4 [m/s] | 47.2 [m/s] |

Table 2.8: Operation Draught (image from ref. [16])

| Windage [m] | 12.2 | 16.1 | 20.0 |
|---|---|---|---|
| Longitudinal area(Ax) $area[m^2]$ | 2600.0 | 2387.0 | 2184.0 |
| Transverse area(Ay) $area[m^2]$ | 11067.0 | 10014.0 | 8961.0 |

The dynamic properties of the wind depends on the stability of the atmospheric boundary i.e. wind turbulence. The stability depends on the difference of the temperature between the air, sea and mean wind speed. The fluctuating wind speed $u_w(z,t)$ in the frequency domain can be described by a wind spectrum. The spectral density function on the longitudinal wind speed fluctuation in a specific point in space can be described by the one-point turbulence spectrum equation.

$$S(f,z) = \frac{\left(320m^2/s\right)\left(\frac{U_{w0}}{U_{ref}}\right)^2\left(\frac{z}{z_r}\right)^{0.45}}{\left(1+\tilde{f}^n\right)^{\frac{5}{3n}}} \quad (2.14)$$

S(f,z) is the wind spectrum at a frequency f and reference elevation z;

$U_{w0}$ is the 1 hour sustained wind speed at the reference elevation z;

$U_{ref}$ is the reference wind speed (10 m/s);

f is the frequency in cycles per second (Hertz) over the range 0.00167 Hz $\leq$ f $\leq$ 0.5 Hz;

z is the height (above mean sea level);

$z_f$ is the reference height (above mean sea level 10 meters);

$\tilde{f}$ is a non-dimensional frequency where the numerical factor 172 has the dimension of seconds [s] defined as:

$$\tilde{f} = (172s)\, f\left(\frac{z}{z_r}\right)^{\frac{2}{3}}\left(\frac{U_{w0}}{U_{ref}}\right)^{-0.75} \quad (2.15)$$

n is a coefficient equal to 0.468.

#### 2.8.2.1 Mean wind speed

At the height of 10 meters the wind mean speed can be estimated by the formula:

$$u_{10}(t) = C_t U_{ref}(tr) \quad (2.16)$$

t is the averaging time [minutes]

$C_t$ is the wind speed averaging factor

$$C_t = \left[1 - 0.047\ln\left(\frac{t}{t_r}\right)\right] \quad (2.17)$$

$t_r$ is the reference averaging time, 10 minutes

The wind speed averaging time factors can be seen in table 2.9.

Table 2.9: Wind speed averaging time factors (image from ref. [51])

| Averaging time t [s] | $C_t$ |
|---|---|
| 3 | 1.249 |
| 5 | 1.225 |
| 15 | 1.173 |
| 60 | 1.108 |
| 600 | 1.000 |
| 3600 | 0.916 |

### 2.8.3 Sea Currents

One important parameter to take in consideration for mooring lines are the sea currents. The sea currents produces high loads in the surface structures leading to components failure [49]. The most common type of sea currents are:

- Tidal currents;
- Circulation currents, associated to oceanic-scale circulation patterns;
- Storm generated currents.

Some authors indicated that the surface speeds are up to 15% greater than the speed at 60 meters [16]. The direction of the currents are the same as at 60 meters depth. A bathymetry indicating the depth in the Schiehallion field can be seen in figure 2.25. The green dot on the green line indicates the location of the Schiehallion field while the green line indicates the depth profile on that straight line. On the other hand the white lines indicates the topology depth for the remaining seabed.

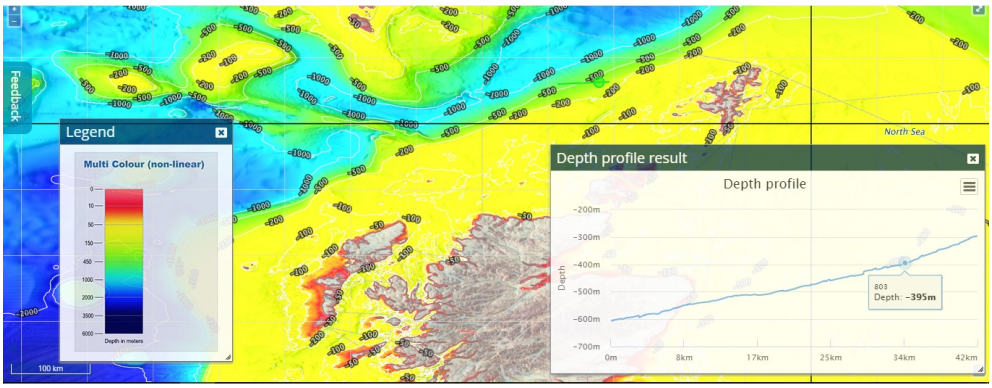


Figure 2.25: Bathimetry of Schiehallion fields (image from ref. [52])

Currents may have several directions, however one is predominant. In some areas, such as North sea, both tidal and wind driven currents are dominant, though for West of Shetland other type become important. In comparison with any natural frequencies of the platforms, currents are considered to have long periods, so they can be considered as steady for at least on hour period [17]. Submerged components will be affected by generated wind vortices at surface as they interact with the platform, the vortices might result in vortex inducted vibrations (VIV).

The characterization of the sea currents can be divided in:

- Near-surface currents (wind/wave generated currents);
- Sub-surface currents (tidal and thermosaline currents);
- Near-shore currents (wave induced surf currents).

#### 2.8.3.1 Near-surface currents

Near-surface currents are in general wind induced. The design velocity can be characterized as:

$$u_w(z) = k(z) \cdot us \quad (2.18)$$

$u_w(z)$ is the near surface current velocity [m/s]
k(z) if the factor, dependent of the vertical coordinate z. 0.01 for z=0m; 0 for z$\leqslant$ -15m
us is the sustained wind speed used for design [m/s]

#### 2.8.3.2 Sub-surface currents

The design velocity for sub-surface currents is based on the velocity at sea level (z=0). The vertical velocity distribution can be expressed as:

$$us0(z) = [(z+d)/d]\,1/7 \cdot uso \quad (2.19)$$

us0 is the sub-surface current velocity in [m/s]
d is the water depth
z is the vertical coordinate axis [m]
us0 is the current velocity at sea level [m]
A current profile can be observed in the figure 2.26.

#### 2.8.3.3 Near-Shore currents

Near-shore currents have the direction to the shore line, the design velocity at breaking waves section can be detailed as:

$$u_{nS} = 2 \cdot s \cdot \sqrt{g \cdot H_b} \quad (2.20)$$

$u_{nS}$ is the near shore current velocity [m/s]
s is the beach slope $\tan \alpha$
$\alpha$ is the inclination of beach g is the acceleration of gravity 9.81 $m/s^2$
$H_B$ is the breaking wave height [m], for very small slopes, $H_B$ can be assumed to be 0.8$d_b$
$d_B$ is the water depth at the location of the breaking wave [m]

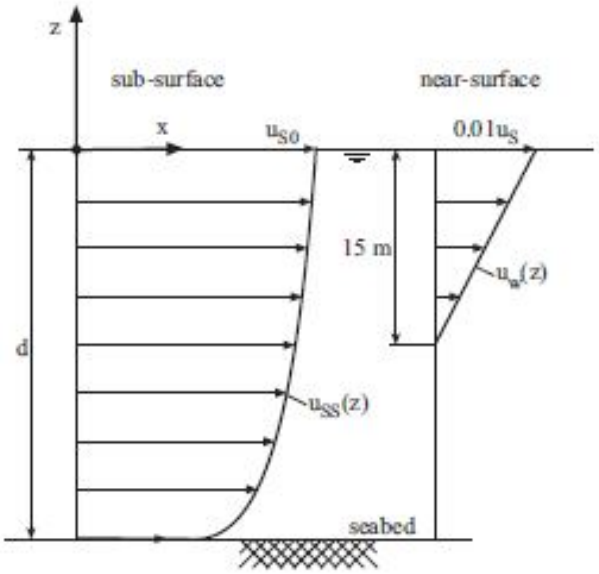


Figure 2.26: Current depth profile (image from ref. [51])

## 2.9 State of the art - Mooring Systems

The study of optimization of mooring lines have been performed for several years in order to improve the mooring systems either as a system or components. In this section the most relevant works in the last 30 years are presented from the former theories to recent and computational studies.

In the state of the art analysis it is crucial to refer the most important references. This literature review is based on that sentence.

Ansari 1980 [53] have conducted a study in mooring systems with multi-component cable systems. The work presents a general discussion of the several mooring lines available to use an analysis tool to determine the stiffness characteristics of a multi-component cable including the effects of the line stretch.

In the year 1982 Nakajima et al [54] set out a study to analyze multi-component mooring lines through both theoretical and experimental studies. The author took in considerations the dynamic behavior of the mooring line under the movement caused by the verified motion of offshore floating platform. It was verified in this study that in higher frequencies the dynamic tension is significant and has enough magnitude to cause a failure.

The dynamic behavior of mooring lines was set on a study by Van den Boom in 1985 [55]. In this study the results from an algorithm based on a lumped mass method was compared with results from harmonic oscillation tests. The results shown clearly the importance of dynamic analysis for mooring configurations. It was verified that catenary effects amplified the dynamic tension.

In 1986 Najeeb and Ansari [56] chose to study the dynamics of a multi component mooring line. This former study on segmented mooring lines took into consideration the importance of dynamic station-keeping response of a moored offshore platform or vessel. This method serves as a

useful tool in developing realistic mooring line analysis of floating platforms (vessels) anchored by multi-point.

In 1988 Singh and Verma [57] performed an evaluation of force-displacement relationship for multi-component mooring cable by finite element method. In this study the cable force versus excursion curves have shown the importance of non linear effects in the case of horizontal loads. The axial rigidity of the cable on the mooring line response is high but decreases with the increased value of axial rigidity. The stiffness behavior range of the mooring segment increases with the increase in the length of the mooring line.

Ansari 1991 [58] presented a study on the design of multi-component cable systems for moored offshore vessels. The equations of motion of a moored vessel was presented and methods of generation the restoring forces were discussed. The author verified that in a realistic manner, the cable dynamic effects must be included in the dynamic of the vessel as well as added mass.

Dercksen in 1994 [59] obtained important results from the analysis of mooring systems. Fast developments in synthetic ropes lead to alternative design of traditional catenary mooring systems. The author studied the feasibility of a synthetic rope compared with a wire rope for 800 meters depth. The results showed a reduction of the number of lines for the same vessel, a shorter length of the lines and approximately the same breaking strength per line compared to steel.

William Webster in 1995 [60] verified the mooring-induced damping. The study aimed to determine the energy absorption by a mooring system from an offshore platform as a result of its motion. Horizontal motions (surge, sway and yaw) and vertical motions (heave, roll and pitch) induced damping were presented and it was verified the very different phenomenon between them.

1996 was the year Mavrakos et al. [61] presented a work on deep water mooring dynamics. The dynamic of mooring lines with buoys attached are studied both experimentally and numerically. A good correlation was obtained and the beneficial effects of the buoys in reducing mooring line dynamic tension was verified.

Balola 1999 [62] obtained important results in analyzing the mooring line damping in very large water depth. The author have verified that with the increasing depth, the trend of mooring system design is shifting from classic cable mooring, to synthetic rope solutions. It was verified that synthetic ropes are cheaper, not only the material cost but also installation process. Since the amplitude of the motions does not vary from one mooring line to the other, the damping becomes a second stage consideration. The pretension on the synthetics proves that the maximum tension in the lines was not a critical issue. Even with low tension synthetic mooring solutions proved to have excellent dynamic properties which reinforces its feasibility.

The work of Vaz and Patel 1999 [63] investigated the pipe in pipe systems, known as double piping systems. An analytical formulation for couple buckling instability was considered for pipe in pipe systems with high temperature hydrocarbons. The solutions was verified to have high accuracy.

Macfarlane 2001 [64] focused a study on the statics of a three component mooring line. The author used a typical deep water mooring configuration connected to a moored floating platform required for the preliminary design of mooring systems. In conclusion the author verified that the stability measurement system should be used to minimize sources of errors.

Gobat and Grosenbaugh 2001 [65] have presented a simple empirical model for heave induced dynamic tension in catenary moorings. Although the model is applicable for waves frequency (in opposition to low drift frequencies), both standard deviation of the tension as the sum of an inertial term proportional to heave acceleration and a drag term proportional to quadratic heave velocity is calculated. The yield maximum error ranges from 8 to 11% and the root mean square of the lazy wave presents errors between 2 and 3%.

In 2002 Pacheco, Kenedi and Jorge [66] have studied the elastoplastic analysis of the residual stress in chain links. Since the traditional design does not take into consideration the residual stress, the authors have verified the influence of residual stress along the chain links before and after operation. The results have shown the importance of the residual stress in the design of fatigue live.

In 2002 Kreuzer and Wilke [67] focused a study of mooring systems from a multi-body dynamic approach. The study is performed in the time domain and the interaction between the fluid and the floating structure is taken into consideration using linear potential theory. They have concluded that this method is valid in the design of offshore platforms or pontoons under operational conditions.

In 2003 Ong and Pellegrino [68] focused a study on the modeling of seabed interaction in frequency domain analysis of mooring cables. Since the time domain integration was too far expensive for all load cases, the authors generated a new modeling method for the interaction with the seabed in the frequency domain, but without considering the frictional effects and impact. The model based on springs was analyzed in the frequency domain and the results from this method shows an increase of the accuracy compared with typical domain analysis in cases with affordable computational analysis.

In 2003 Pacheco et al. [69] executed a finite element residual stress analysis applied to offshore stud-less chain links. Considering three different approaches between two bi-dimensional finite element model, two three-dimensional finite element methods and analytic model. This study presents a comparative study on the stress distribution prediction in stud-less chain links. The author addresses two major phenomena that was influenced the stress prediction, plasticity and contact.

Harris, Johanning and Wolfram 2004 [27] have performed a review of design issues and choices in mooring systems for wave energy converters. In this work it was verified that overall performance characteristics of the WEC mooring should be taken into consideration in the design due to its expenses.

Vargas et al. [70] Studied the stress concentration factors for stud-less mooring chain links in fairleads. In this work the stress concentration factors were analyzed in a specific seven pocket fairlead. The study shows the maximum stress concentration factor of 1.15, a value very

different from the standard value in the DNV of 2.5 [31].

In 2005 Hobbs and Ridge [71] performed a study of the torque in mooring chains. In this work (divided in two papers) a frictionless theory that predicts the resultant torque in mooring chain is presented as well as the lift in the links as functions of the angle of twist. A comparison between chain specimens (theory and experimental) was performed resulting in large differences in the prediction of the angle of twist without friction, it emphasizes the need for friction contact.

In 2005 Jean et al. [72] performed a study of the failure of chain elements by bending on deep water mooring systems. This paper was executed to analyze the failure in mooring system of an Angolan platform designed based on norms and standards from offshore industry. The failure was caused by bending fatigue mode. This paper summarizes the applied methodology developed to estimate the damage from fatigue in the chain subjected to bending.

In 2005 in his bachelor Lacerda [73] performed a system analysis of anchoring and floating platforms. The author verified the need of the elasticity as the loads increased in the line. The displacements shall be taken into consideration due to accurate determination of loads. The inelastic approach can lead to higher errors than elastic approach however for conceptual design the inelastic approach is a very good approximation for first definition of the geometry.

In 2006 Ridge et al. [74] studied a methodology to predict the torsional response of large mooring chains. The authors presented a frictionless theory to predict torques and end-shortening in the chain as non-dimensionalised functions of twist angles. The results were compared with experimental data. The obtained design curves are given for typical stud-link chain geometries to allow designers to estimate torque and end-shortening for any bar diameter.

Yang 2007 [75] in his PhD analyzed the hydrodynamic analysis of mooring lines based on optical tracking experiments. The author performed an experimental investigation of the hydrodynamic characteristics of mooring elements through the use of oscillation and free tests, since the mooring coefficients are very hard to obtain experimentally. The author concluded that experimental coefficients were well estimated through the theoretical analysis performed in this study.

From the University of Oslo in 2008 Wingerei [76] performed a study on dynamics and damping of mooring lines for offshore windmills at 300 meters water depth. The author performed a comparison between the use of damping and the effects without the use of the damping in the analysis both in Matlab (without damping effects) and SIMO (with damping effects). The author concluded that SIMO was a better option for dynamic analysis for a longer period of time while Matlab was the best option for detailed analysis for shorter period of time.

In 2008 Udoh et al. [77] developed a numerical tool STAMOORSYS for the design of statically equivalent mooring systems in order to improve results from the challenge of direct scaling of mooring systems in controlled environmental. In the hybrid method a results comparison with Orcaflex was performed and analyzed. The potentiality was verified as well as the economic advantaged of the STAMOORSYS although the limitation from the actual version of the numerical tool.

Lassen, Storvoll and Beck 2009 [78] presented a study on the fatigue life prediction of mooring chains subjected to tension and out-of-plane bending. The behavior of segments subjected to pretension and rotation angle were investigated experimentally and by the use of finite element modeling. The authors verified that out-of-plane bending stresses were fairly linear with the response to the deviation angle, furthermore the out-of-plane bending stresses are related to the pretension.

Samad 2009 [79] verified the performance of catenary mooring system. The author investigated both performance and technical analysis of catenary mooring systems for a Spar platform. Samad carried out the study with a finite element approach and programming with Matlab for the mooring connection with the turret.

Neto et al. 2009 [80] have studied the effects of buried pipelines subjected to buckling with finite element method. Computational models and methods plays an important part in the prediction of undesirable situations since they are able to predict the behavior of pipelines, mooring lines and risers in the offshore industry actuated by harsh environments. The authors applied the use of spring elements in nonlinear analysis of pipelines for both materials and the efficiency of the numerical implementation was analyzed. The finite element formulation was proved to be worth-full for pipelines with nonlinear material which kinematic nonlinear effects such as buckling effects.

Song, Lee and Choung in 2009 [81] underwent a series of studies for the optimization of an FPSO riser support using moving least squares response surface meta-models. The paper relied on a reliability based-design for the riser support installed on the FPSO, being actuated by standard and extreme situations, damaged operations and line failure case. This method was proved to improve probabilistic design performance under very harsh sea conditions (14 meters wave height).

Yassir, Kurian, Indra and Nabilah 2010 [82] performed a parametric study on multi-component catenary mooring lines for offshore floating structures. In this study an implicit iterative solution was used through the use of catenary equations using multi-component catenary mooring systems. The authors have verified that horizontal restoring force is directly proportional with pre-tension and unit weight parameters and inverse proportional with pre-tension angle for positive excursions. The vertical pre-tension and pre-tension angle is proportional to vertical restoring force.

Ridge, Smedley and Hobbs 2011 [83] studied the effects of twist on chain strength and fatigue performance for small scale test results. This study verifies the effect of initial twist on the static strength in a stud-less chain and fatigue life in the design phase of the chain element. The authors verified that the proof load applied to the chain during manufacture is far lower than the load applied to the equivalent stud-less mooring chain at operational conditions. The breaking load measured test of the chain between 0 and 24 degrees showed a insignificant decrease in strength compared to standard untwisted chain.

Vicente et al. [84] in 2011 carried out a study to analyze the slack-chain mooring configuration analysis of a floating wave energy converter. It was performed different mooring configurations with slack chain mooring lines of a floating point absorber. It was concluded that catenary chain

elements rely on its weight to provide the necessary horizontal force.

Tai-pil Ha 2011 [8] set up an important study on the frequency and time domain motion and mooring analysis for a FPSO operating in deep water. The author used two different methods for the time domain. One method used a fast practical time domain approach using a first order motion responses, and the second through the use of six coupled equations of motion based on potential damping for the FPSO. The author performed his study in the Schiehallion FPSO in the Schiehallion field. The author verified that different catenary equations can be used for static mooring analysis or a quasi-static analysis since the Schiehallion FPSO operates in 400 meters depth. Both effects of line dynamics and line tension are significant and needed to be considered in the mooring design.

In 2011 Wales and Santosa [85] have investigated the impact of catenary embedment of the mooring performance of a deep water floating production unit. In this work it was investigated the impact of the slackening caused by severe loading conditions such as hurricanes as well as offset integrity during this events.

In 2012 Kurian et al. [86] performed a nonlinear dynamic analysis of multi-component mooring lines incorporation line-seabed interaction. In this study a dynamic analysis of a multi-component mooring line was formulated using a deterministic approach. The authors have considered the floater motions responses as upper boundary conditions while anchored point was considered as pinned. The results were compared with published results and a good agreement with numerical simulation was verified. It was verified that mooring line dynamic tension was directly proportional to the upper end motion frequency.

Ba 2012 [87] presented an analysis of mooring and steel catenary risers system in ultra deep water. A quasi-static and dynamic analysis for multi-component mooring and steel catenary risers was performed with Fortran. The author compared his results with published works and validated his new methodology for the Schiehallion FPSO.

Kiecke 2012 [88] simulated fatigue damage index on mooring lines of a Gulf of Mexico truss spar determined from recorded field data. Through the use of environmental platform response monitoring system, the study found out that events such as hurricanes accounted higher fatigue damage index than total damage during 20 year service life of the vessel. The one hundred year hurricane should be take in consideration in the design of station keeping systems similar to guidelines found in Norsok [41].

A finite element model for subsea pipeline stability and free span screening was performed by Elsayed, Fahmy and Samir in 2012 [89]. The proposed approach proved to be a valuable tool for pipeline design assessing the operator on bottom stability and free spans.

Sadovnikov et al. in 2012 decided to analyze the requirements for maintaining integrity of FPSO mooring system. This work focused on the importance of having a mooring integrity management plan. The methodology for advanced mooring defines a mooring residual capacity study for a FPSO and the need for a disconnectable turret mooring. The importance of a rapid response after a mooring line failure was verified theoretically for up-to-date analytical models.

Wang in 2012 [90] obtained important results in an evolutionary optimization study on offshore mooring system design. It was presented a feasible solution tool (Particle swarm optimization) for different performance characteristics. The optimization software was successfully tested by using in a mooring line design.

In the same year, Castro-Santos, González et al. 2013 [91] have studied the costs of position floating offshore platforms for marine renewable energies. The authors have defined a method to calculate the position keeping (both anchoring and mooring) costs of floating platforms, through this study the authors claimed that their method can be used to determine the feasibility and economic viability of offshore energy projects.

In 2013 Bastid and Smith [92] performed a numerical analysis of contact stresses between mooring chain links and potential consequences for fatigue damage. The work assumes a proof load to generate compressive residual stresses at the contact region as well as in the intrados point (point where fatigue has more probability to start). The work presents stresses applied at the contact regions and shows the fatigue sensitivity on the intrados point.

Farfan 2013 [93] performed a modal analysis of deep-water mooring lines based on a variational formulation. The effects of added mass and damping produced by water was analyzed since most studies considers the material as homogeneous which lead to errors. The author compared the natural period for two realistic models, one with the effects of added mass and damping and the other without. It was verified at the end of the study that the effects of added mass and damping are near the wave excitation periods causing fatigue loads in opposition to the analysis without the effects of added mass and damping pushing the wave excitation period far from wave excitation period reducing the fatigue loads.

Castro-Santos et al. 2013 [94] have performed a study to built a methodology to calculate both mooring and anchoring costs of floating offshore wind devices. The authors have identified the costs of the most important life phase cycles as being definition, design, manufacturing, installation, exploitation and decommissioning/ dismantling phases. The study was performed for offshore wind energy since this type of energy exploitation is one of the main European Union objectives.

Michael Chrolenko 2013 showed the importance of dynamic analysis and design of mooring lines [95]. Since mooring line responses may be calculated both in frequency domain and time domain, the work was performed to verify the compromise between accuracy and computational effort through the use of MIMOSA (frequency domain quasi-static and FEM method frequency domain dynamic), SIMO (time domain, quasi static), RIFLEX (time domain, dynamic and fully non-linear) and SIMA (Program for communication between programs). All developed by Marintek. A comparison was performed and a deviate of 4% was verified between them which verified the similar results between several softwares. Riflex showed the most precise results comparing to bench tests.

Bico 2013 in his study [96] analyzed the offshore mooring floating platforms with polyester cables. The aim of his study was to understand the characteristic of polyester ropes in typical oceanic loadings. The author concluded that new fibers in polyester cables are being used for the last 15 years with bigger elastic modulus than conventional steel ropes. However the technology

is considerable new with less information then required/existent to be fully implemented in most floating platforms.

Girón et al. analyzed in 2014 the implications of one single and fully integrated design methodologies both for risers and mooring systems for deep water. The traditional methods separate the mooring lines from production systems. the full interaction between both methodologies have lead to an efficiency gain and cost reduction [97].

Vineesh et al. 2014 [98] analyzed a mooring cable using a finite element method (Ansys). The authors studied the behavior of mooring cable attached to buoy and spar platform under extreme environmental conditions. Instead of typical steel and fiber rope, mooring cables CFRP material is used. In the analysis it was found that CFRP (polymer reinforced fiber carbon) is more effective for reducing the displacements of the buoy than steel chain and synthetic fibers.

In 2014 Evy Bjørsen [23] has studied how the structural components, mooring chains links work in a mooring system. In this study both offshore loading conditions, mooring failure detection and fatigue analysis was implemented and it was verified that residual stresses play an important role in proof testing. A comparison between stud and stud-less links was performed and it was verified that traditional design of mooring systems does not consider residual stresses which have resulted in this case in an increase of 3.65 and 3.30 times the nominal stress for stud and stud-less links.

Wang et al. 2014 [99] verified the structural reliability based dynamic positioning of Turret moored FPSOs in extreme seas. The authors presented first the mathematical model of the moored FPSO in therms of kinematics and dynamics, then they have applied catenary method in order to analyze mooring line dynamics. After the mathematical model of the whole turret mooring system was established, a structural reliability index was defined to evaluate both breaking strength for the mooring systems and mooring lines. Finally a series of tests were carried out.

A behavior of mooring systems for different line pretensions was used by Yenduri et al. 2014 [100]. In this study two different mooring configurations with and without mooring lines were considered in a Matlab code. The code was validated by experimental results and it was verified that with the increase of pretension of the mooring line, the restoring performance of the mooring system could be improved.

Fan et al. in 2014 [101] presented a study of an Innovative approach to design truncated mooring system based on static and damping equivalency. In this study the gravity, tension, current force and mooring line extension for the analysis of multi-component mooring lines was considered. The results shown that equivalent truncated system mooring design can solve multi-variable and multi-objective optimization problem in a large region for deep waters.

Gol-Zaroudi et al. 2014 [102] performed a study on the assessment of mooring configurations on the performance of a floating oscillating water column energy converter. He found that in deep water depth, catenary moorings are not capable of restoring considerable stiffness and restoring force.

Siow et al. 2014 [103] set up a series of studies in strength analysis of FPSO's mooring lines. This study intended to collect material properties of wire ropes from tensile tests experiments and through catenary theory equations. The stiffness curve of the mooring line in model was estimated and the difference between model scale experiments and theoretical data is acceptable at the defined range.

A finite element analysis of residual strength of degraded chains was performed by Rosen et al. 2015 [104]. This works analyzes the effects of microbiological influenced corrosion in mooring chains in tropical waters. The work verifies the strength loss and strength reduction in several segments of the chain element. In a second stage the author had the scope to predict the fatigue life according to residual degraded chain.

Gang, Liping and Chuanyun in 2015 [105] performed a study in order to develop an equivalent truncated intelligent optimization design for deep water mooring systems. The Matlab programing software was used to design the truncated mooring systems mathematical model based on static characteristics and compared with hydrodynamic software Orcaflex for accuracy. The feasibility of the model was verified.

Lars Stendal 2015 performed a study through her master thesis [106] on the common analysis methods for mooring systems with focus on accidental limit state. The author verified two common approaches, in frequency domain and time domain. In frequency domain both low frequency and wave frequency load effects were analyzed separately and combined later into characteristic values used for ALS and ULS design. The author concluded that both methods are comparable, however they are not identical. It was verified a more accurate precision in results when a low wave frequencies were combined. The frequency domain using MIMOSA gave consistent conservative results compared with time domain SIMI/ Riflex. It was verified also the increase of mean max tension of 21% and 25% with one mooring line broken in the accidental limit state.

Du et al. in 2015 [107] focused a study on a novel underwater measurement method for mooring system using self-contained technique. In this study a new prototype based on lumped mass method is proposed. System, design requirements, hardware design and installation mode are described in this study. The prototype proved to be a useful tool in gathering the load data from the mooring lines.

Bhinder et al. 2015 [108] modeled mooring line non-linearities for WEC converters using AQWA, SIMA and Orcaflex. A comprehensive design approach was performed in order to verify the impact on costs of the device in both operational and survival modes according to each software. The three main aspects in the analysis was the non-linear and temporal behavior of synthetic ropes, geometric mooring line non-linearities and non-linear viscous fluid damping. The results have shown the importance of the material non-linearities in simulated line tension. Both softwares had similar results, being Orcaflex the most conservative one with the higher loads.

Camarão et al. 2015 [109] analyzed the structural mechanics applied to mooring components design. The aim of this study was to develop a methodology for assessing the integrity of mooring components for offshore environment. The stress levels in stud-less and stud link elements were calculated in the critical regions of the mooring links. It as verified that studless links presents

a higher critical volume than the related to the stud chain link, in fact it justifies the presence of the stud.

Crudu, Obreja and Marcu 2016 [110] set out a study on moored offshore structures with an evaluation of forces in elastic mooring lines. A five different scale of elastic simulation are evaluated together with dynamic effects, in this paper a systematic diagram is presented as well as experimental results. The authors concluded that the influence of elasticity is very important for accurate results rather than inelastic analysis. However for preliminary analysis inelastic analysis are important due to computational expenses.

Qiao et al. in 2017 [111] presented a study of the Fatigue analysis of deep-water hybrid mooring line under corrosion effects. The study was performed numerically for 20 years time period corrosion actuation. It was verified that the fatigue damage occurred mostly on the chain elements. It was verified as well that upper element links were more damaged than bottom links. With the increasing corrosion years, the fatigue damage also increases.

In 2017 Omar et al. [112] reported the experience with design, analysis and installation of mooring ropes in polyester for deep water application. In the paper the authors described a series of full scale tests performed on polyester ropes in West Africa and Brazil. The main objective was to determine non-linear characteristics of the segmented mooring rope as well as the investigation of optimization parameters. The elastic property behavior of polyester ropes was verified and was proven to be important tools for mooring line optimization.

In the past year 2018 Potts et al. [113] performed some investigations into break strength of offshore mooring chains. This work is aimed to correlate finite element analysis of residual strength of chain links actuated by pitting corrosion. The study had the objective to determine an alternative formulation for the break strength of stud-less and stud link elements, to establish the origin and the technical basis for conventional minimum breaking load and assessing the validity of the MBL formula.

## 2.10 Remarks

In this chapter a revision of the oil and gas industry was performed, with specific detail in the offshore operations. The standard oil and gas components were detailed and the oil field was understood. The new developments in the oil field and the new discoveries were identified.

After a brief understanding of the necessity for the new developments in the oilfield, a comparison between the former and new FPSO was performed, from oil storage capacity, personnel capacity to anchoring systems, etc.

A detailed description of the major mooring systems was verified and compared with the previous systems. Environmental conditions of the oil field for collinear and non collinear loads were analyzed. For the specific case of this work, the most important loads considered were the waves, wind and currents. A brief explanation was given for sea water and for the referred loads. After understanding the necessity, cause and applicable industry norms and standards.

# Chapter 3

# Mooring analysis

In the previous chapter, the oil and gas upstream process was introduced as well as main components needed for hydrocarbons extraction. The Schiehallion field was also detailed and the requirements for mooring systems were defined. This chapter deals with design and analysis of mooring system considering the following issues:

- Statics of mooring lines;
- Dynamics of mooring lines;
- Single point moorings;
- Fatigue analysis.

In this chapter the positioning of the FPSO will be performed with the aid of CAE software Orcaflex. This chapter is divided in three subsections, the first one is the mathematical formulation of uni and multi-segmented catenary equations either for elastic and inelastic criteria both in frequency and time domain. The second subsection has all the requirements for the CAE model (considerations, materials, properties and constraints). At the end of the chapter the results will be presented and conclusions will be taken. The multi-segmented mooring line will be analyzed and compared with the existent one for validation.

## 3.1 Natural periods and frequencies

For the analysis of the mooring lines, it is important to find out the natural periods of the vessel. The resonance of the motions occurs when the natural period is near the excitation frequency. The natural period $T_n$ and the natural frequency $\omega_n$ for all degrees of motion (surge, sway, heave, roll, pitch and yaw) can be found by the formulae for moored FPSO [8].

$$T_n^{ii} = \frac{2\pi}{\omega_n} = 2\pi\sqrt{\frac{(M + A_{ii})}{K_{ii}}} \quad (3.1)$$

$$T_n^{surge} = \frac{2\pi}{\omega_n^{surge}} = 2\pi\sqrt{\frac{(M + A_{11})}{K_{11}}} \qquad \{k_{11} = \sum_{i=1}^{14} C_1 \cos^2\theta_1\} \quad (3.2)$$

$$T_n^{sway} = \frac{2\pi}{\omega_n^{sway}} = 2\pi\sqrt{\frac{(M + A_{22})}{K_{22}}} \qquad \{k_{22} = \sum_{i=1}^{14} C_1 \cos^2\theta_1\} \quad (3.3)$$

$$T_n^{yaw} = \frac{2\pi}{\omega_n^{yaw}} = 2\pi\sqrt{\frac{(I_{66} + A_{66})}{K_{66}}} \qquad \{k_{66} = \sum_{i=1}^{14} C_1 \left(x_1 \sin\theta_1 - y_1 \cos\theta_1\right)^2\} \quad (3.4)$$

The natural frequencies on the other hand can be found by:

$$\omega_n^{heave} = \sqrt{\frac{\rho g A W}{(M + A_{33})}} \quad (3.5)$$

$$\omega_n^{roll} = \sqrt{\frac{\rho g \nabla G M_T}{(I_{44} + A_{44})}} \quad (3.6)$$

$$\omega_n^{Pitch} = \sqrt{\frac{\rho g \nabla G M_L}{(I_{55} + A_{55})}} \quad (3.7)$$

$\nabla$ is the volume of the displacement of the vessel. With these parameters the vessel motions can be obtained according to environmental loads.

## 3.2 Current and Wind Loads on FPSO Structures

### 3.2.1 Current Loads on FPSO Structures

The current loads on vessels (barges, FPSO, etc.) are analyzed using theoretical formulas. Normally for a anchored/moored FPSO, the main loads are inducing surge and sway forces, as well as yaw moment on the structure. The drag forces in the longitudinal direction is the surge current force $F_1^c$ caused mainly by friction. From the estimation of the ship resistance (drag) in water, the force can be estimated. Then the *Froude* Number is:

$$Fn = \frac{U_c}{Lg^{\frac{1}{2}}} \quad (3.8)$$

$U_c$ is the current velocity, L is the ship length. The *Froude* number has a very small value, which means that the wave resistance can be neglected relative to the viscous resistance. Hence the approximate formulation can be used:

$$F_1^c = \frac{0.075}{(logR_e - 2)^2} \frac{1}{2} \rho S U_c^2 \cos\beta \left|\cos\beta\right| \quad (3.9)$$

$\beta$ is the angle between the current velocity and x-axis. S is the wetted surface on the ship. Then the *Reynolds* number must be taken:

$$R_e = \frac{U_c L \left|\cos\beta\right|}{\nu} \quad (3.10)$$

One important parameter to take in consideration is the skin coefficient $C_F$.

$$C_F = \frac{0.075}{(\log R_e - 2)^2} \quad (3.11)$$

$\nu$ is the kinematic viscosity of water $\nu = 1.19 * 10^{-6} m^2 s^{-1}$ in 15 degrees celcius water temperature. The current force (sway) $F_2^C$ in the transverse direction is found by the integral of the

drag force on a cross-section over the vessel using:

$$F_2^C = \frac{1}{2}\rho U_C^2 \sin\beta \left|\sin\beta\right| \left[\int_L C_D\left(x\right) D\left(x\right) dx\right] \quad (3.12)$$

$C_D(x)$ is the drag coefficient for a typical infinitely long cylinder with FPSO cross-sectional area, while $D(x)$ is the sectional draught. The yaw moment caused by the current $F_6^C$ is:

$$F_6^C = \frac{1}{2}\rho U_C^2 \sin\beta \left|\sin\beta\right| \left[\int_L C_D\left(x\right) D\left(x\right) dx\right] + \frac{1}{2} U_C^2 \left(A_{22} - A_{11}\right) \sin 2\beta \quad (3.13)$$

Both $A_{22}$ and $A_{11}$ are the added mass in the following directions (surge and sway).

### 3.2.2 Wind Loads on FPSO Structures

FPSO's are subjected to wind loads. The wind loads can be predicted similarly to the current loads using theoretical data. The steady mean loads $F_1^w$ and $F_2^w$ in x and y directions (in the FPSO Glen Lyon structure) and the Yaw moment $F_6^w$ can be estimated using the following formulae.

$$F_1^w = \frac{1}{2}\rho_{air} C_{XW} A_T V_Z^2 \quad (3.14)$$

$$F_2^w = \frac{1}{2}\rho_{air} C_{YW} A_L V_Z^2 \quad (3.15)$$

$$F_6^w = \frac{1}{2}\rho_{air} C_{XYW} A_L V_Z^2 L_{PP} \quad (3.16)$$

$\rho_{air}$ is the air density; $1.23 * 10^{-3} tm^{-3}$ in 15C air temperature; $C_{XW}$ $C_{YW}$ and $C_{XYW}$ are the lateral, longitudinal and yaw moment coefficients and they varies with the type of the FPSO/vessel. $A_T$ and $A_L$ are the areas (projected) in $m^2$ in directions x and y. $V_Z$ is the mean hour wind speed undisturbed in $ms^{-1}$.

$$V_Z = V_{Z_R}\left(\frac{Z}{Z_R}\right)^{0.125} \quad (3.17)$$

The height of the force centre above the surface (reference) is provided by the letter Z, $Z_R$ is the reference height. $A_{P_L}$ is the exposed projected area of the vessel and $L_{PP}$ is the distance between the perpendiculars.

## 3.3 Statics of mooring lines

A fixed mooring system applied on the vessel should block the vessel keeping her moored (safely), under specified design loading conditions [114].

Due to high costs, not every ship is fortunate to possess an all-wire or all-synthetic mooring outfit and is common to use a mixture of wires and chain ropes. As mentioned before the mooring line in the Schiehallion field is composed by steel chain elements and sheathed wire rope. The mooring line starts in the vessel and ends in the suction pile.

The catenary mooring legs are attached to the turret, which includes bearings to allow freely rotation around the anchor legs. The mooring system prevents the vessel from drifting away from a berth and keeps the ship in the designed place [115].

### 3.3.1 Method of Analysis

The typical and first method for evaluation the performance of a dynamic mooring system is a quasi-static analysis [82]. The effects of line dynamics are accommodated by the use of a relatively conservative safety factor [25].

In the design of a permanent mooring system, a more rigorous dynamic analysis is required. The safety factor is high to reflect some uncertainty in line tension prediction.

### 3.3.2 Maximum Design Conditions

The definition of specific design situations shall be performed in accordance with the requirements of a regulatory authority where one exists. The aspects shall include:

- Service requirements for mooring and station-keeping system;
- Service line design;
- Hazards (the loads that the system can be exposed during its design service life);
- Potential consequences of partial or complete system failure;
- Severity and nature of environmental conditions to be expected during the service line design.

The maximum design conditions are defined for the combination of extreme loads caused by winds, waves and currents. In practice, most of the times is approximated by the use of sets of design criteria, for 100 year design environment three sets are often investigated:

- The 100 year waves with associated winds and currents;
- The 100 year wind with associated waves and currents;
- The 100 year current with associated waves and wind.

The recommended analysis method can be seen in Table 3.1

Table 3.1: Recommended analysis methods and conditions (image from ref. [31])

| Type of mooring | Limit State | Conditions to be analyzed | Analysis method |
|---|---|---|---|
| Permanent Mooring | ULS | Intact/redundancy check | Dynamic |
| Permanent Mooring | FLS | Transition | Quasi-Static or dynamic |
| Permanent Mooring | SLS | No guidance given | No guidance given |

In general two methods are used to analyze the floating structures response (static-mode):

- The quasi-static frequency-domain approach;

- The quasi-static time-domain approach.

#### 3.3.2.1 Quasi-Static in Frequency-domain

In this approach, the known mooring equations of motion describes the response of the structure, analyzing it separately for mean, low and wave frequency responses. Mean responses are obtained from the static equilibrium between steady actions and mooring system's restoring forces. Wave frequency and low frequency structure motions are obtained from the frequency domain approach which yield motion response statics [37]. Extreme values are calculated based on peak probability density functions. The maximum expected values and significant values of wave frequency and low frequency when joined with the average response.

Due to constant changes in the environment (at sea), a number of variations of all wave directions and intensity is needed, which means irregular waves characterization. However, the environmental forces are most of the times considered as unidirectional. The stochastic analysis shall be considered for a better accuracy of the statistical characteristics of dynamic motion responses. To execute some frequency-domain analysis of a weathervaning structure, the structure's heading shall be fixed.

Both maximum significant values of first-order and second-order wave-induced motions are taken into consideration. The attachment point (x,y,z) of a mooring line in the infinitesimal mode of motion and can be obtained by the combination of the first-order and second-order wave-induced motion by the following approach [31].

$$X_j = \overline{\xi_j} + \hat{\xi}_j^{(2)} + \hat{\xi}_{j1/3}^{(1)} \quad ; \quad when \quad \hat{\xi}_j^{(2)} > \hat{\xi}_j^{(1)} \quad \textbf{(3.18)}$$

$$X_j = \overline{\xi_j} + \hat{\xi}_j^{(1)} + \hat{\xi}_{j1/3}^{(2)} \quad ; \quad when \quad \hat{\xi}_j^{(2)} < \hat{\xi}_j^{(1)} \quad \textbf{(3.19)}$$

Where,

$$\overline{\xi_j} = \overline{\xi}_j^W + \overline{\xi}^C + \overline{\xi}^{(2)} \quad \textbf{(3.20)}$$

Is the mean offset of the FPSO due to the environmental loads. These values can be obtained by the spectral analysis by:

$$\overline{\xi}_j^{(2)} = \frac{2\int_0^\infty \overline{F}_j^{(2)} S(\omega)\, d\omega}{K_{jj}} \quad \textbf{(3.21)}$$

Hence,

$$\xi_{j1/3}^{(1)} = 2\sqrt{m_0} \quad \textbf{(3.22)}$$

Here

$$\overline{\xi}_j^{(1)} = 2\sqrt{m_0 \ln(N)} \quad \textbf{(3.23)}$$

$$\xi_{j1/3}^{(2)} = 2\sigma_j \quad (3.24)$$

so

$$\hat{\xi}_j^{(2)} = \sqrt{2\ln\left(\frac{3600T}{T_{jn}}\right)} \quad (3.25)$$

In which

$$m_0 = \int_0^\infty \left|\xi_j\left(x, y, x, \omega, \beta\right)^2\right| S\left(\omega\right) d\omega \quad (3.26)$$

and

$$m_2 = \int_0^\infty \omega^2 \left|\xi_j\left(x, y, z, \omega, \beta\right)^2\right| S\left(\omega\right) d\omega \quad (3.27)$$

this equation can be integrated into;

$$\sigma_j^2 = \int_0^\infty \frac{S_{Fj}\left(\mu\right)}{\left\{K_{jj} - \left(M + A_{jj}\right)\mu^2\right\}^2 + B_{jj}^2\mu^2} \quad (3.28)$$

so it can be written as;

$$S_{Fj}\left(\mu\right) = 8\int_0^\infty S\left(\omega\right) S\left(\omega + \mu\right)\left[\overline{F}_j^{(2)}\left(\omega + \frac{\mu}{2}\right)\right]^2 d\omega \quad (3.29)$$

so:

$$N = 3600Tn' \quad (3.30)$$

$$n' = \frac{1}{2\pi}\sqrt{\frac{m_2}{m_0}} \quad (3.31)$$

$|\xi_j\left(x, y, z, \omega, \beta\right)|$ if the first order wave-induced motion amplitude operator of (x,y,z) at the wave frequency $\omega$. $F_j$ is the spectral density of low frequency drift force and $\sigma_j$ is the root mean square value of second-order motion. T is the time duration of the storm in hours, while n' is the average number of a motion response per unit time.

#### 3.3.2.2 Quasi-static in Time-domain

The equations of motion describe the combined mean, low and wave-frequency responses of the floating structures in the time-domain. The forcing functions include low-frequency, mean, and wave-frequency actions caused by wave, wind, current and thrusters. The equations for the floating structures, mooring lines, risers and thrusters behavior and their interactions are included in the time-domain simulation. These simulations should have enough time to yield stable statistical values.

The combination of extreme first-order wave-induced and second-order slow-drift motions in the frequency domain is an approximation performed for design purposes for a conservative mooring system. For an accurate design of mooring systems it is required a time-domain coupled motion. For this purpose the motion equations considers the six degrees of freedom of the FPSO

integrated in the time domain affecting the added mass as well as damping. The analysis for time domain simulations are very computational intensive in an irregular sea with storm duration of at least 3 hours. Assuming $\zeta$ as the wave elevation (based on the linearization assumption) at the origin of the co-ordinate system and the first-order motion $\xi_j^{(1)}$ at a Cartesian reference (x,y,z) of the FPSO. The amplitude sum of all frequencies can be written as:

$$\zeta(x,y,t) = \sum_{m=1}^{N} a_m \cos\left[\omega_m t \mp \varepsilon_m\right] \quad (3.32)$$

and

$$\xi^{(1)}(x,y,t) = \sum_{m=1}^{N} \left|\xi_j\left(x,y,z,\omega,\beta\right)\right| a_m \cos\left[\omega_m t \pm \varepsilon_m - \theta_{jm}\right] \quad (3.33)$$

where

$$a_m = \sqrt{2S\left(\omega_m\right)\delta\omega} \quad (3.34)$$

$a_m$ is the wave amplitude, $\omega_m$ is the wave frequency and $\varepsilon_m$ is the random phase. $\theta_{jm}$ is the angle phase of the first order motion also known as RAO (response amplitude operator) is $\left|\xi_j\left(x,y,z,\omega,\beta\right)\right|$. On the other hand N is the number of wave frequency components.

The displacement $\left|\xi_j\left(x,y,z,t\right)\right|$ at the infinitesimal mode can be assumed as the result of the first order motion $\xi_j^{(1)}$ at the exact point of the slow-varying drift motion $\xi_j^{(2)}$ of the FPSO as:

$$\xi_j\left(x,y,z,t\right) = \xi_j^{(1)}\left(x,y,z,t\right) + \xi_j^{(2)}\left(t\right) \quad (3.35)$$

Which can be found solving the equation

$$\left(M + A_{jj}\right)\ddot{\xi}_j^{(2)} + B_{jj}\dot{\xi}_j^{(2)}\left|\dot{\xi}_j^{(2)}\right| + K_{jj}\dot{\xi}_j^{(2)} = F_j^{(2)}\left(t\right) \quad (3.36)$$

By using Newton´s second order force approximation [116], the exciting force at slow drift can be written as

$$F_j^{(2)}\left(t\right) = \sum_{m=1}^{M}\sum_{n=1}^{N} a_m a_n \overline{F}_j^{(2)}\left(\omega_m,\beta\right)\cos\left[\left(\omega_m + \omega_n\right)t + \varepsilon_m + \varepsilon_n\right] \quad (3.37)$$

There are several contributions to the damping $B_{jj}$ of the FPSO mooring system, among some of them, they include viscous drag either on the FPSO or on mooring lines, wave drift damping caused by drift velocity, internal line and soil line frictional damping. For the analysis of this work only wave drift damping is considered. Hence,

$$B_{jj} = 2\int_0^{\infty} S\left(\omega\right) B_{jj}^{(2)} d\omega \quad (3.38)$$

$B_{jj}$ can be found by

$$B_{jj}^{(2)} = -\frac{\partial \overline{F}_j^{(2)}}{\partial U}\omega \quad ; \quad U = 0 \quad (3.39)$$

U is the speed of the vessel in forward direction.

### 3.3.3 Catenary equations - Inelastic

The mooring system is a conventional group of multi-segmented lines. Each of which is a single line or cable connecting to bottom anchor or multi-component combination of anchors. In this particular case there are twenty multi-segmented mooring lines connected to twenty suction pile anchors. The behavior of each line can be described as a non linear spring with tension-displacement characteristics that depend on its length, weight, elastic properties and water depth.

For a uniform line segment, hanging freely only due to its own weight (w) per unit length the governing differential equation is:

$$\frac{\partial^2 z}{\partial x^2} = \frac{w}{H}\frac{ds}{dx} \quad (3.40)$$

Where H is the horizontal component of the cable tension and ds is an infinitesimal element of the cable.

The segments for deep mooring are a combination of chain and rope/wire. This combination increases the stiffness in the mooring system, meanwhile getting a much more lighter cable system. Tension forces in the cables, which are the means of applying restraining forces on the floating structure are due to cable weight and elastic properties

The Catenary equations in offshore environment have been developed in the last decades due to the need to anchor vessels. In the preliminary design, the static catenary method is selected to anchoring a floating vessel, this method is based in the following assumptions [117]:

- The seabed is flat and horizontal;
- Bending stiffness of the mooring line can be neglected;
- The mooring lines are on a vertical plane comprising x-z coordinates only.

From figure 2.17 the five segments from a single mooring line could be seen.

From figure 3.1 can be verified that

$$dT - \rho g A dz = \left[ w \sin\phi - F\left(1 + \frac{T}{AE}\right)\right] ds \quad (3.41)$$

$$Td\phi - \rho g A z d\phi = \left[ w \cos\phi + D\left(1 + \frac{T}{AE}\right)\right] ds \quad (3.42)$$

In general, the equations are non-linear and an explicit solution might not be possible to find, however it is a good approximation to neglect the effects of both F and D. In this calculus, the elasticity effects are also neglected in order to simplify the analysis. However for extreme conditions, elasticity should be taken in consideration. Assuming the constant weight per unit length of the cable line we have:

$$T' = T - \rho g z A \quad (3.43)$$

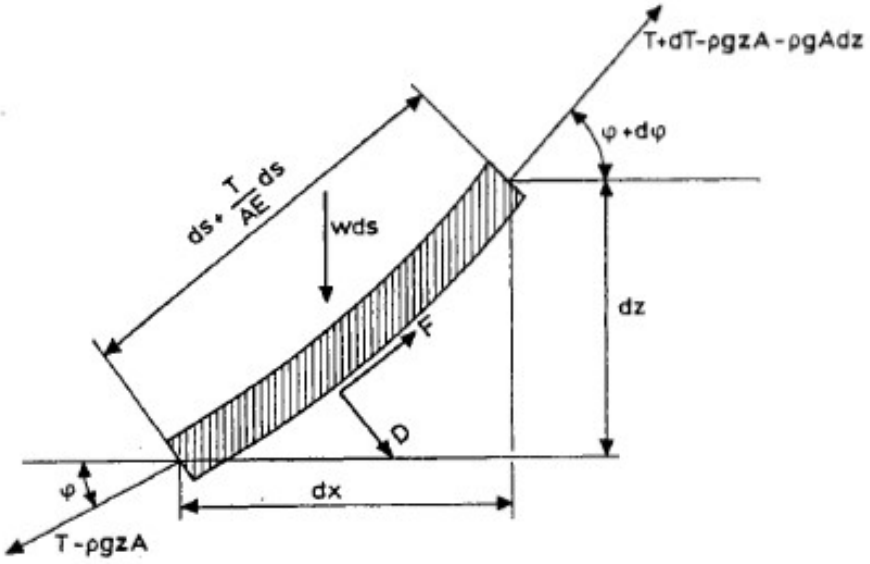


Figure 3.1: 2D forces acting on mooring line element

It can be writen as:

$$dT = w \sin\phi ds \quad (3.44)$$

$$T' d\phi = w \cos\phi ds \quad (3.45)$$

then

$$\frac{dT'}{T'} = \frac{\sin\phi}{\cos\phi} d\phi \quad (3.46)$$

i.e.

$$T' = T'_0 \frac{\cos\phi_0}{\cos\phi} \quad (3.47)$$

Using integration,

$$s - s_0 = \frac{1}{w} \int_{\phi_0}^{\phi} \frac{T'_0}{\cos\phi} \frac{\cos\phi_0}{\cos\phi} d\phi = \frac{T'_0 \cos\phi_0}{w} \left[\tan\phi - \tan\phi_0\right] \quad (3.48)$$

Since dx = $\cos\phi$ ds is obtained:

$$x - x_0 = \frac{1}{w} \int_{\phi_0}^{\phi} \frac{T'_0 \cos\phi_0}{\cos\phi} d\phi = \frac{T'_0 \cos\phi_0}{w} \left( \log\left(\frac{1}{\cos\phi} + \tan\phi\right) - \log\left(\frac{1}{\cos\phi_0} + \tan\phi_0\right)\right) \quad (3.49)$$

Since dz = $\sin\phi$ ds is obtained:

$$z - z_0 = \frac{1}{w} \int_{\phi_0}^{\phi} \frac{T'_o \cos\phi_0}{\cos^2\phi} d\phi = \frac{T'_0 \cos\phi_0}{w} \left[\frac{1}{\cos\phi} - \frac{1}{\cos\phi_0}\right] \quad (3.50)$$

$\phi_0$ is the contact point between the cable line and the bottom (seabed), i.e. $\phi_0$=0. Rewriting

the equation:

$$T_0' = T' \cos\phi \quad (3.51)$$

So the horizontal component of the line tension in the element(s) can be written as:

$$T_H = T \cos\phi_w \quad (3.52)$$

So we can write:

$$T_0' = T_H \quad (3.53)$$

The chosen coordinate system was $x_0$=0 and $z_0$=$-h$. Setting $s_0$=0, the angle $\phi$ can be eliminated from equations, which can be written as:

$$\frac{xw}{T_H} = \log\left(\frac{1+\sin\phi}{\cos\phi}\right) \quad (3.54)$$

i.e.

$$\sinh\left(\frac{wx}{T_H}\right) = \frac{1}{2}\left(\frac{1+\sin\phi}{\cos\phi} - \frac{\cos\phi}{1+\sin\phi}\right) = \tan\phi \quad (3.55)$$

$$\cosh\left(\frac{wx}{T_H}\right) = \frac{1}{2}\left(\frac{1+\sin\phi}{\cos\phi} - \frac{\cos\phi}{1+\sin\phi}\right) = \frac{1}{\cos\phi} \quad (3.56)$$

It can be written

$$s = \frac{T_H}{w}\sinh\left(\frac{w}{T_H}x\right) \quad (3.57)$$

$$z + h = \frac{T_H}{w}\left[\cosh\left(\frac{w}{T_H}x\right) - 1\right] \quad (3.58)$$

So the line tension is:

$$T - \rho g z A = \frac{T_H}{\cos\phi} = T_H + w(z+h) \quad (3.59)$$

i.e.

$$T = T_H + wh + (w + \rho g A)\, z \quad (3.60)$$

The vertical component $T_z$ of the tension is:

$$dT_z' = d\left(T'\sin\phi\right) = dT'\sin\phi + T'\cos\phi d\phi = w\sin^2\phi ds + w\cos^2\phi ds \quad (3.61)$$

$T_z'$=ws, which means $T_z$=ws, figure 3.2.

Assuming the use of gravity anchors, the anchors cannot be exposed to vertical forces from the anchor lines. This parameter will be used to determine the minimum length of the chain. To

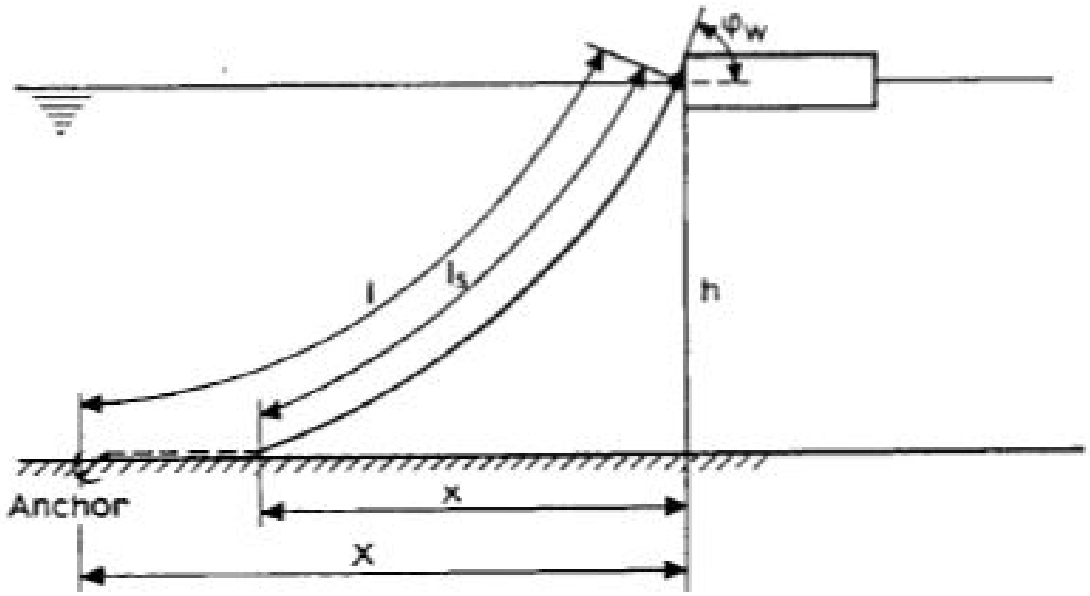


Figure 3.2: Moored vessel with one anchor line (image from ref. [8])

find the minimum length $l_{min}$ the following equations can be used:

$$l_s = a \sinh\left(\frac{x}{a}\right) \quad (3.62)$$

$$h = a\left[\cosh\left(\frac{x}{a}\right) - 1\right] \quad (3.63)$$

$a$ is a specific parameter in this chapter (horizontal tension per weight), it shall not be compared with other chapters. Where:

$$a = \frac{T_H}{w} \quad (3.64)$$

By combining equations the previous, so:

$$l_s^2 = h^2 + 2ha \quad (3.65)$$

The maximum tension in the cable line can be written as:

$$T_{max} = T_H + wh \quad (3.66)$$

So the minimum length of the cable is:

$$l_{min} = h\left(2\frac{T_{max}}{wh} - 1\right)^{\frac{1}{2}} \quad (3.67)$$

For a starting point, $T_{max}$ can be made equal to $T_{br}$ (i.e.breaking strength of the cable). To find the mean position of the vessel subjected to wind, waves and current. Knowing the horizontal force $T_H$ from the cable on the vessel as a function of the horizontal distance X between the anchor and the connection point on the vessel, the horizontal distance X is:

$$X = l - l_s + x \quad (3.68)$$

Using the former expression, the relation between X and $T_H$.

$$X = l - h\left(1 + 2\frac{a}{h}\right)^{\frac{1}{2}} + a\cosh^{-1}\left(1 + \frac{h}{a}\right) \quad (3.69)$$

It is important to know the environmental forces on the vessel in order to find the horizontal length of the mooring system. Due to the vessel's motion the offset of the vessel (oscillation of the vessel in x and y axis) will be larger or smaller. If the horizontal motions are not too large:

$$T_H = (T_H)_M + C_{11}\eta_1 \quad (3.70)$$

$(T_H)_M$ is the average horizontal force from the anchor line in the vessel. $\eta_1$ is the horizontal motion in the x-direction of the anchoring point on the vessel. $C_{11}$ is the derivative from $T_H$ with respect to X and $C_{11}$ at $(T_H)_M$. The analytical expression of $C_{11}$ by differentiating equation can be written as:

$$C_{11} = \frac{dT_H}{dX} = w\left[\frac{-2}{\left(1 + 2\frac{a}{h}\right)^{\frac{1}{2}}} + \cosh^{-1}\left(1 + \frac{h}{a}\right)\right]^{-1} \quad (3.71)$$

From this equation can be seen that the anchor line has a spring effect on the vessel. If the horizontal motion in the x-axis of the center of gravity of the ship $\eta_1$ is set, the surge equation of the motion of the ship follows that:

$$(M + A_{11})\frac{d^2\eta_1}{dt^2} + B_{11}\frac{d\eta_1}{dt} + B_D\left|\frac{d\eta_1}{dt}\right|\frac{d\eta_1}{dt} + C_{11}\eta_1 = F_1(t) \quad (3.72)$$

M is the mass of the ship, $A_{11}$ if the added mass in surge, $B_{11}$ is a linear damping coefficient, $B_D$ is the quadratic damping coefficient and $F_1(t)$ is the dynamic excitation force caused by all external forces. Surge will have resonance when the circular frequency of oscillation is equal to:

$$\omega = \left(\frac{C_{11}}{M + A_{11}}\right)^{\frac{1}{2}} \quad (3.73)$$

### 3.3.4 Catenary equations - Elastic

There can be very significant tension levels in the influence of the elastic material properties. In extreme conditions the effects of the elasticity in the cable lines shall be considered.

Previous static equilibrium equations do not change with elasticity, however the relationship between the horizontal tension and the vertical tensions to line length can be rewritten as [118] :

$$dx = ds\left(1 + \frac{T}{AE}\right)\cos\phi \quad (3.74)$$

$$dz = ds\left(1 + \frac{T}{AE}\right)\sin\phi \quad (3.75)$$

Since there is a chosen $\phi_0$ and $s_0$ to be zero (on the top connection with the vessel), it mean:

$$T' = \frac{T'_0}{\cos\phi} \quad (3.76)$$

$$s = \frac{T'_0}{w}\tan\phi \quad (3.77)$$

In order to find the x and y coordinates, the following relation must be considered:

$$dp = ds\left(1 + \frac{T}{AE}\right) \quad (3.78)$$

This means,

$$\frac{dx}{ds} = \cos\phi\left(1 + \frac{T}{AE}\right) = \cos\phi\left(1 + \frac{T'}{AE}\right) = \cos\phi + \frac{T'_0}{AE} \quad (3.79)$$

$$\frac{dz}{ds} = \sin\phi\left(1 + \frac{T}{AE}\right) = \sin\phi\left(1 + \frac{T'}{AE}\right) = \sin\phi + \frac{w}{AE}s \quad (3.80)$$

Assuming $z = 0$, the unstretched length $l_s$ of the cable when touches the ground at the bottom is given by

$$l_s = \frac{T_z}{w} \quad (3.81)$$

Integrating the equation can be assumed

$$h = \frac{T_H}{w}\left[\frac{1}{\cos\phi_w} - 1\right] + \frac{1}{2}\frac{w}{AE}l_s^2 \quad (3.82)$$

Where

$$\cos\phi_w = \frac{T_H}{\sqrt{T_H^2 + T_z^2}} \quad (3.83)$$

So

$$T_H = \frac{T_z^2 - \left(wh - \frac{1}{2}\frac{w^2}{AE}l_s^2\right)^2}{s\left(wh - \frac{1}{2}\frac{w^2}{AE}l_s^2\right)} \quad (3.84)$$

The tension at the attachment point can be simplified to

$$T = \sqrt{T_H^2 + T_Z^2} \quad (3.85)$$

So,

$$x = \frac{T_H}{w}\log\left(\frac{\left(T_H^2 + T_z^2\right)^2 + T_z}{T_H}\right) + \frac{T_H}{AE}l_s \quad (3.86)$$

Combining the elastic cable equations and obeying with Hooke's Law (zero angle at touch down

point):

$$x = \frac{T_H}{w}\sinh^{-1}\left(\frac{ws}{T_H}\right) + \frac{T_H s}{AE} \quad (3.87)$$

And,

$$h = \frac{ws^2}{2AE} + \frac{T_H}{w}\left[\sqrt{1+\left(\frac{ws}{T_H}\right)^2} - 1\right] \quad (3.88)$$

The suspended length for given fairlead tension

$$s = \frac{1}{w}\sqrt{T_z^2 + T_H^2} \quad (3.89)$$

The horizontal force for given fairlead tension

$$T_H = AE\sqrt{\left(\frac{T_Z}{AE}+1\right)^2 - \frac{2wh}{AE}} - AE \quad (3.90)$$

The horizontal scope can be set to

$$X = \frac{T_H}{w}\sinh^{-1}\left(\frac{ws}{T_H}\right) + \frac{T_H L}{AE} \quad (3.91)$$

And the vertical force at fairlead is

$$T_z = ws \quad (3.92)$$

## 3.4 Glen Lyon analysis methodology

As can be observed from figure 2.16, the multi component mooring line can assume several configuration types during operational or service life. The number and type of configurations depends on:

- Number of components;
- Type of anchoring system;
- For specific cases, the clump weight or buoy attached to the mooring line.

Each of the multi-segmented catenary mooring lines can have one of the following configurations:

- Totally lying at seabed, all its length $l_s$ is a part of $x_b$. for this specific case the mooring line conditions does not have any contribution on the station keeping of the FPSO;
- Part is on the seabed, and the suspended part with zero slope at the connection point of contact with seabed. For this specific case, some will have suspended length $s_i$ with projected lengths $x_i$ and projected high $h_i$ (horizontal and vertical projected lengths) and the rest is lying on the seabed;
- Completed suspended, making and angle of $\theta$ with the seabed. As it can be perceived the suspended length is equal to the total length, having projected lengths of $x_i$ and $h_i$.

### 3.4.1 Five component mooring line

From figure 2.17 the five segments can be seen. The following new multi-segmented catenary can be also verified in figure 3.3.

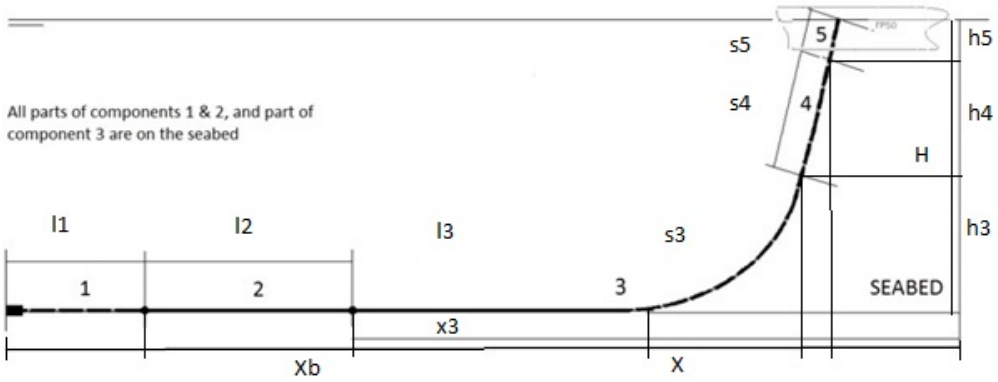


Figure 3.3: Multi-segmented catenary configuration

From this figure:

$$L = l_1 + l_2 + l_3 + l_4 + l_5 \quad (3.93)$$

As it can be seen the total length of each anchor system is the sum of all segments of the mooring line. $s_4 = l_4$ and $s_5 = l_5$, here,

$$S_1 = S_2 = \theta_1 = \theta_2 = T_{z_1} = T_{z_2} = h_1 = h_2 = 0 \quad (3.94)$$

$S_1$ $S_2$ are the suspended length of segment 1 and 2, $\theta_1$ and $\theta_2$ are the angles with the x-axis. X is the projected length of all mooring line in x-axis direction, hence

$$X_b = l_1 + l_2 + l_3 - S_3 \quad (3.95)$$

And,

$$X = l_1 + l_2 + l_3 + x_3 + x_4 + x_5 \quad (3.96)$$

$X_b$ is the mooring line in contact with the seabed, and X it the total projected length at the seabed, in the z-axis we have

$$H = h_3 + h_4 + h_5 \quad (3.97)$$

H is the full depth of the mooring line, $h_i$ is the projected height of each mooring segment. The typical vertical tension of each segment can be written as:

$$T_{z_i} = l_i \times w_i \quad (3.98)$$

Hence,

$$T_{z_5} = s_3 \times w_3 + l_4 \times w_4 + l_5 \times w_5 \quad (3.99)$$

$w_i$ is the weight per unit length of each segment. The projected suspended length of the segment 3 can be found using:

$$x_3 = a_3 \sinh^{-1}\left(\frac{s_3}{a_3}\right) \quad (3.100)$$

It can also be written as:

$$x_3 = a_3 \cosh^{-1}\left(1 + \frac{h_3}{a_3}\right) \quad (3.101)$$

The suspended length of the segment 3 can also be written as:

$$s_3 = h_3 \left(1 + \frac{2a_3}{h_3}\right)^{\frac{1}{2}} \quad (3.102)$$

$a_i$ is the ratio between the horizontal tension per weight of the segment i, $T_{H_i}$ is the horizontal tension at the specific point. The ratio is:

$$a_i = \frac{T_{H_i}}{W_i} \quad (3.103)$$

The vertical tension of the segment 3 can be written as:

$$h_3 = a_3 \left[\cosh\left(\frac{x_3}{a_3}\right) - 1\right] \quad (3.104)$$

The projected length of suspended length of the segment 4 is:

$$x_4 = a_4 \left[\sinh^{-1}\left(\frac{l_4}{a_4} + \tan\theta_4\right) - \sinh^{-1}\left(\tan\theta_4\right)\right] \quad (3.105)$$

It can be written as well as:

$$x_4 = a_4 \left[\sinh^{-1}\left(\frac{l_4}{a_4} + \frac{s_3}{a_3}\right) - \sinh^{-1}\left(\frac{s_3}{a_3}\right)\right] \quad (3.106)$$

The projected height of the $4^{th}$ segment is:

$$h_4 = a_4 \left[\cosh\left(\frac{x_4}{a_4} + \sinh^{-1}\left(\tan\theta_4\right)\right)\cosh\left(\sinh^{-1}\left(\tan\theta_4\right)\right)\right] \quad (3.107)$$

It can be written as well as:

$$h_4 = a_4 \left[\cosh\left(\frac{x_4}{a_4} + \sinh^{-1}\left(\frac{s_3}{a_3}\right)\right) - \cosh\left(\sinh^{-1}\left(\frac{s_3}{a_3}\right)\right)\right] \quad (3.108)$$

For the last segment, the projected suspended length of the segment 5 can be written as:

$$x_5 = a_5 \left[\sinh^{-1}\left(\frac{l_5}{a_5} + \tan\theta_5\right) - \sinh^{-1}\left(\tan\theta_5\right)\right] \quad (3.109)$$

It can be written as well as:

$$x_5 = a_5 \left[\sinh^{-1}\left(\frac{l_5}{a_5} + \frac{l_4}{a_4} + \frac{s_3}{a_3}\right) - \sinh^{-1}\left(\frac{s_4}{a_4} + \frac{s_3}{a_3}\right)\right] \quad (3.110)$$

On the other hand for the projected height:

$$h_5 = a_5 \left[ \cosh\left( \frac{x_5}{a_5} + \sinh^{-1}\left(\tan\theta_5\right) \right) \cosh\left( \sinh^{-1}\left(\tan\theta_5\right) \right) \right] \quad (3.111)$$

It can be expressed as well as:

$$h_5 = a_5 \left[ \cosh\left( \frac{x_5}{a_5} + \sinh^{-1}\left( \frac{s_4}{a_4} + \frac{s_3}{a_3} \right) \right) - \cosh\left( \sinh^{-1}\left( \frac{s_4}{a_4} + \frac{s_3}{a_3} \right) \right) \right] \quad (3.112)$$

## 3.5 Dynamic of mooring lines

### 3.5.1 Motion equations

Based on a 2D dynamic approach, the mooring line equations in a mooring line plane static equilibrium is:

$$m\frac{\partial v_t}{\partial t} - \left(m + m_a\right) v_n \frac{\partial \psi}{\partial t} = \frac{\partial T_e}{\partial s} - w\sin\psi + \frac{1}{2}\rho\pi d_0 C_{Dt}\left(U\cos\psi - v_t\right)\left|U\cos\psi - v_t\right|\sqrt{1+e} \quad (3.113)$$

and

$$\left(m + m_a\right)\frac{\partial v_n}{\partial t} + m v_t \frac{\partial \psi}{\partial t} = T_e \frac{\partial \psi}{\partial s} - w\cos\psi + \frac{1}{2}\rho d_0 C_{Dn}\left(-U\sin\psi - v_n\right)\left|-U\sin\psi - v_n\right|\sqrt{1+e} \quad (3.114)$$

Where:

- $T_e$ is the effective tension;
- $d_0$ and $\psi$ is the unstretched line diameter and angle with horizontal;
- m and $m_a$ are the mass and added mass per unit length;
- $C_{Dt}$ and $C_{Dn}$ are the frictional and drag coefficients;
- $v_n$ and $v_t$ are the velocity components of mooring elements, normal and tangential;
- U is the current velocity;
- e is the strain.

The mooring line elasticity is given by the relation with the material young modulus E

$$T_e = \frac{1}{4}\pi d^2 E e \quad (3.115)$$

The compatibility of deformations turns in to equations:

$$\frac{\partial e}{\partial t} = \frac{\partial v_t}{\partial s} - v_n \frac{\partial \psi}{\partial s} \quad (3.116)$$

$$\left(1 + e\right)\frac{\partial \psi}{\partial s} = \frac{\partial v_n}{\partial s} + v_t \frac{\partial \psi}{\partial s} \quad (3.117)$$

The dynamic effect has a relative high importance. The dynamic effect might be affected by damping from hydrodynamic drag and motion frequency increase, the mooring lines will not be

able to achieve the typical catenary form due to drag forces. Initially the drag equation is given by the *Morison* equation, so:

$$Drag = \frac{1}{2}\rho d C_d A v^2 \quad (3.118)$$

The dynamic effect is an inertia parameter:

$$\alpha = \frac{\frac{1}{2}\rho d C_d A}{m\left(1 + \frac{\rho}{\rho_l} C_a\right)} \quad (3.119)$$

For this case we can assume, A is the motion amplitude, $C_a$ and $C_d$ are the added mass and drag coefficients; m and $\rho$ are the mooring line mass and density and d is the line diameter. The motion amplitude has an average value of 5 to 10 meters, however if the line inertia effects are much below 1 and the effects can be neglected. For the line dynamics the Quasi-Static check can be expressed as:

$$\beta = \left(\frac{L}{TA}\right)\left(\frac{1}{2}\rho d C_d\right)\left(A^2\omega^2 L\right) \quad (3.120)$$

If beta is much bigger then 1, the dynamics are governed by hydrodynamic damping, if they are much below 1 it is a quasi-static problem. L and d are the suspended line length and diameter, T is the tension at the connection element, A and $\omega$ are the motion amplitude and frequency and $C_d$ is the drag coefficient.The solution methods for mooring dynamic can be classified in a Frequency Domain method and Time Domain Method.

#### 3.5.1.1 Frequency domain approach

In the frequency domain approach, the solution will assume a dynamic response around static equilibrium. All quantities are linearized. However partial differential equations of cable dynamics are transformed to ordinary differential equations by changing:

$$v_n = \mathbb{R}\left(V_n e^{i\omega t}\right) \quad , \quad v_t = \mathbb{R}\left(V_t e^{1\omega t}\right) \quad (3.121)$$

$$\psi = \psi_s + \mathbb{R}\left(\Phi e^{i\omega t}\right) \quad , \quad T_e = T_{es} + \mathbb{R}\left(\Theta e^{i\omega t}\right) \quad (3.122)$$

$$e = e_s + \mathbb{R}\left(E e^{i\omega t}\right) \quad (3.123)$$

Subscripts S are quantities at static equilibrium position, while capital symbols are the complex amplitudes. Rewriting the former equations in four coupled ordinary differential equations, we have:

$$\frac{d\Theta}{ds} = T_{es}\frac{d\Phi_s}{ds}\Phi - m\omega^2 P \quad (3.124)$$

$$\frac{d\Phi}{ds} = -\frac{1}{T_{es}}\frac{d\Phi_s}{ds}\Theta - \frac{1}{T_{es}}\frac{dT_{es}}{ds}\Phi\left[\frac{\left(m + m_a\right)\omega^2 + ib\omega}{T_{es}}\right]Q \quad (3.125)$$

$$\frac{dP}{ds} = \frac{\Theta}{AE} + \frac{d\Phi_s}{da}Q \quad (3.126)$$

And

$$\frac{dQ}{ds} = (1 + e_s)\,\Phi - \frac{d\Phi}{ds}P \quad (3.127)$$

From a numerical point of view, the frequency domain proved to be useful and efficient because it combines the nonlinear static solution with linear dynamic solution.

#### 3.5.1.2 Time domain approach

For the time domain approach, the mooring line is represented by a lump mass and spring model. The line discretization by mass points connected by weightless spring elements. This method will be used for the development of this work. The damp elements represents the damping effects. This methodology is used in the Orcina Orcaflex Software. An example can be seen in figure 3.4

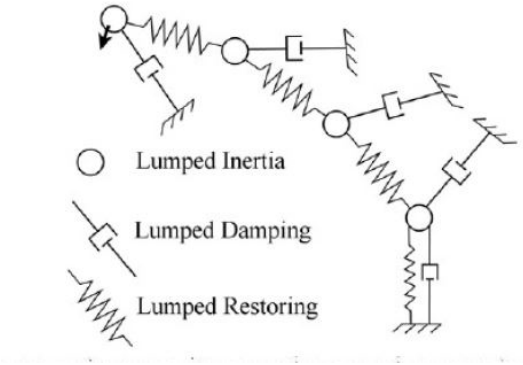


Figure 3.4: Finite difference method example (image from ref. [119])

The partial differential equations are then transformed into a set of ordinary differential equations for dynamics applied to each one of the lumped masses. The equations are solved by finite differences method. The method used is valid for large displacements, mass, added drag and mass of line elements, non-uniform or segmented cables, localized weights and buoys. The main advantages are the clear physical interpretation and the implementation is relatively simple, which means that computational effort is relatively small compared with other methods.

## 3.6 The model

### 3.6.1 The software: Orcaflex

In the development of this work, a 3D system modeling was used. The chosen software was Orcaflex 10.0 from Orcina Lda. Orcaflex is the leader software used for quasi-static and dynamic analysis of subsea and offshore fields. It is used by over 260 clients in several areas of expertise, such as naval, seismic, defense, subsea engineering, ocean engineering, oceanographic engineering, aquaculture and renewals. Some of the clients include Global Maritime, Aker solutions, CEiiA, etc. This software was developed initially for analyzing mainly the static and

dynamic behavior of engineering systems in offshore and marine environment. The program complies inputs from mechanical, structural, maritime and other sectors of expertise for all components of the system [120].

After the inputs, the software calculates the static equilibrium of the system as well as the response to dynamic loads. Outputs such as geometry, forces and moments throughout the system are given after processing. The model built from Orcaflex is a 3D model and is able to deal with large charges in system geometry. The system will comply several components such as vessels, lines,3D buoys and 6D buoys among others.

### 3.6.2 Initial considerations and assumptions

In the development of this work, several considerations were made. The first analysis of the mooring line system is based on the actual mooring system at Schiehallion field. In order to extract the estimated crude per day referred on chapter 2, the system needs to have 24 slots for risers (pliant wave) and umbilicals and the mooring system, composed by twenty segmented mooring lines (figure 3.5).

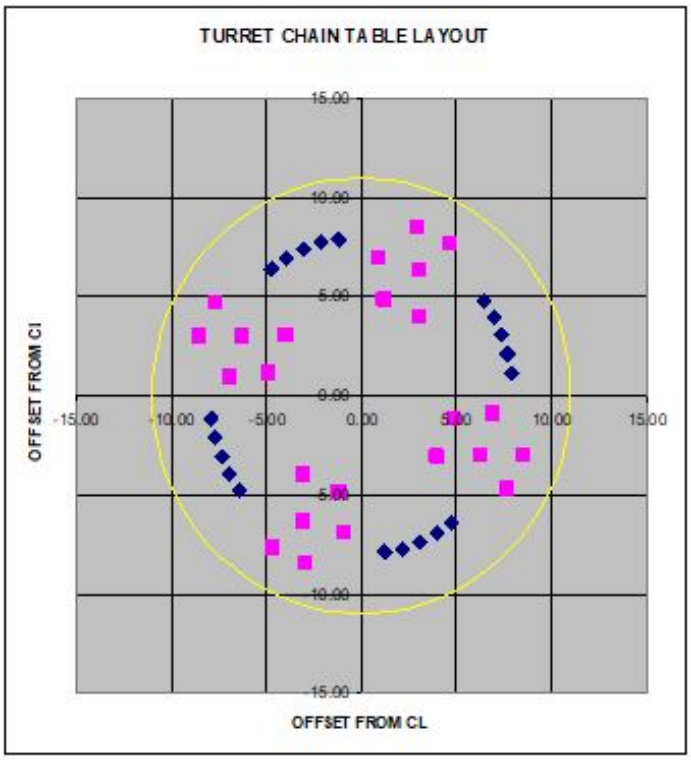


Figure 3.5: Mooring line Layout at turret (image from ref. [16])

Assuming the points from figures 2.13 and 2.14 and the geometry of the vessel in presented in annex A.2[121]. For the development of this work the first analysis will be performed according to parameters detailed in Model Basin Test Specification [122].

The recommended analysis methods can be seen in Table 3.2

Combining figures 2.14 with 2.15 results in the geometry presented in figure 3.6

Table 3.2: Mooring line data (image from ref. [122])

| Element | Type Stud-less | Diameter [mm] | Weight Air $[kg/m]$ | Weight Water $[kg/m]$ | Length [m] | MBL [kN] | EA Axial Stiffness [MN] |
|---|---|---|---|---|---|---|---|
| 1 | R3S Chain | 152.0 | 459.8 | 400.1 | 50.0 | 20156.0 | 1973.1 |
| 2 | Spiral Strand Wire | 144.0 | 106.3 | 84.6 | 490.0 | 19824.5 | 1868.5 |
| 3 | R3S Chain | 152.0 | 459.8 | 400.1 | 940.0 | 20156.0 | 1973.1 |
| 4 | Spiral Strand Wire | 144.0 | 106.0 | 84.6 | 390.0 | 19824.5 | 1868.5 |
| 5 | R4 Chain | 157.0 | 490.5 | 426.0 | 10.0 | 21234.0 | 2105.0 |

It means that each position for risers and mooring lines in the turret will have the coordinates (if the center of the turret has the value (0,0,0)) described in table 3.3 and table 3.4.

Table 3.3: Riser I-tube coordinates

| Riser | X turret [m] | Y turret [m] | X Seabed [m] | Y Seabed [m] | Location |
|---|---|---|---|---|---|
| 1 | 0.91 | 6.94 | 399.55 | 52.60 | North |
| 2 | 1.17 | 4.86 | 389.92 | 93.61 | North |
| 3 | 3.00 | 8.48 | 381.77 | 135.19 | North |
| 4 | 3.01 | 6.32 | 363.74 | 173.50 | North |
| 5 | 4.70 | 7.67 | 345.32 | 211.61 | North |
| 6 | 3.04 | 3.97 | 318.13 | 244.11 | North |
| 7 | 6.94 | -0.91 | -52.60 | 399.55 | East |
| 8 | 4.86 | -1.17 | -93.61 | 389.92 | East |
| 9 | 8.48 | -3.00 | -135.19 | 381.77 | East |
| 10 | 6.32 | -3.01 | -173.50 | 363.74 | East |
| 11 | 7.67 | -4.70 | -211.61 | 318.13 | East |
| 12 | 3.97 | -3.04 | -244.11 | 318.13 | East |
| 13 | -0.91 | -6.94 | -399.55 | -52.60 | South |
| 14 | -1.17 | -4.86 | -389.92 | -93.61 | South |
| 15 | -3.00 | -8.48 | -381.77 | -135.19 | South |
| 16 | -3.01 | -6.32 | -363.74 | -173.50 | South |
| 17 | -4.70 | -7.67 | -345.32 | -211.61 | South |
| 18 | -3.04 | -3.97 | -318.13 | -244.11 | South |
| 19 | -6.94 | 0.91 | 52.60 | -399.55 | West |
| 20 | -4.86 | 1.17 | 93.61 | -389.92 | West |
| 21 | -8.48 | 3.00 | 135.19 | -381.77 | West |
| 22 | -6.32 | 3.01 | 173.50 | -363.74 | West |
| 23 | -7.67 | 4.70 | 211.61 | -345.32 | West |
| 24 | -3.97 | 3.04 | 244.11 | -318.13 | West |

The location of the field was explained before. However the field location is subjected to high wind driven sea, combined with swell condition and strong currents. The RAO values for the vessel are not given, so they are estimated according to standard Orcaflex models for related FPSO's.

The riser arrangement is presented at Anex A.1. The weight of all the chain links must withstand all the added displacement of the vessel and the suction pile anchors shall not have any tension caused by the vessel system.

### 3.6.3 Boundary Conditions

The boundary conditions approximates the functions assuring the governing differential equations, not the boundary itself. In any model, the boundary conditions are required for the calcu-

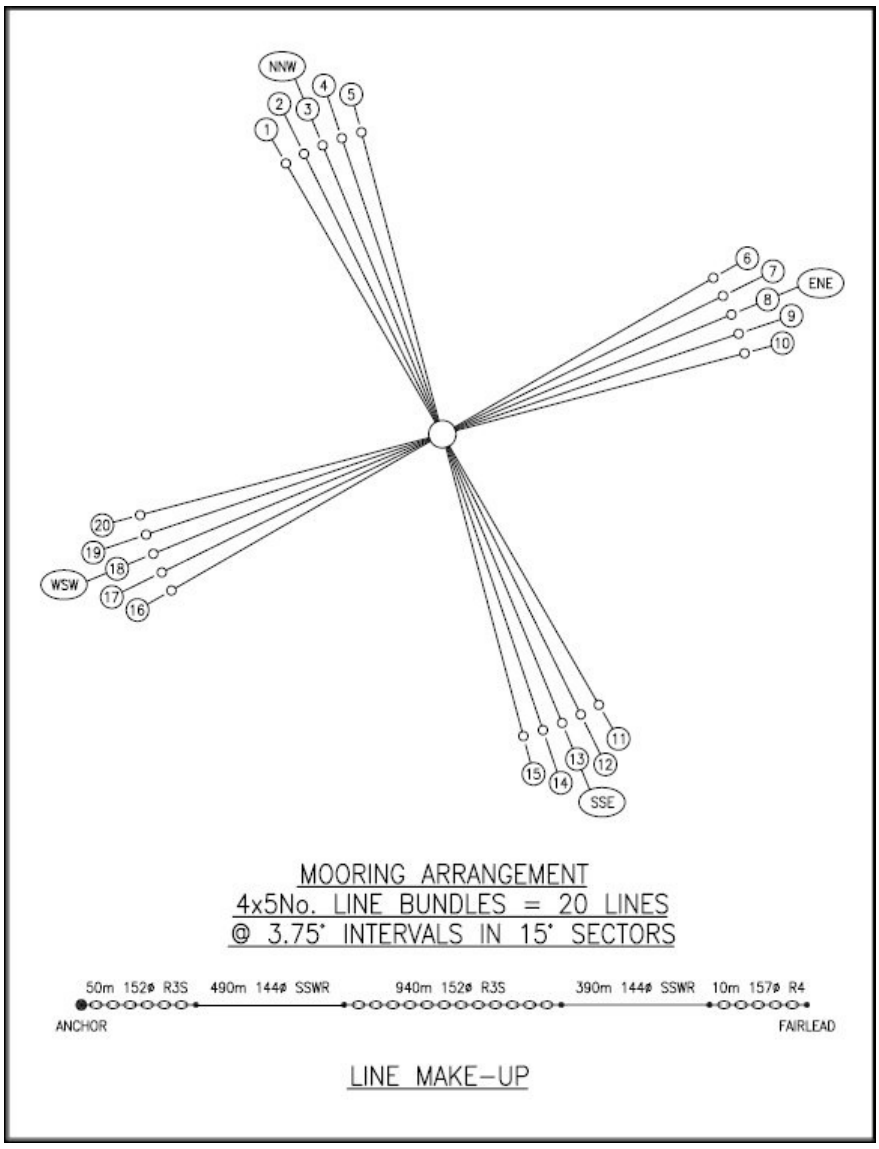


Figure 3.6: Mooring arrangement (image from ref. [16])

lation to start, these conditions are the start of the iteration process. The boundary conditions are divided in two main points, constraints and loads.

#### 3.6.3.1 Constraints

As explained before the boundary conditions (Orcaflex) are assumed to be fixed at the end of each mooring line. In the beginning of each mooring line there is a suction pile anchor with 30 meters length and 6 meters of diameter. The suctions pile anchors are assumed to be steady and fixed at the coordinate position referred before.

#### 3.6.3.2 Environmental Loads

Using figure 2.8 several load cases were performed. However only the worst case condition will be detailed. The load case can be seen in table 3.5.

Table 3.4: Mooring lines coordinates

| Mooring line | X turret [m] | Y turret [m] | X Seabed [m] | Y Seabed [m] | Location |
|---|---|---|---|---|---|
| 1 | -2.59 | 9.66 | -447.76 | 1671.05 | ENE |
| 2 | -2.09 | 6.16 | -556.09 | 1638.19 | ENE |
| 3 | -3.83 | 9.24 | -662.04 | 1598.31 | ENE |
| 4 | -2.87 | 5.83 | -765.16 | 1551.59 | ENE |
| 5 | -5.00 | 8.66 | -865.00 | 1498.22 | ENE |
| 6 | 8.66 | 5.00 | 1498.22 | 865.00 | NNW |
| 7 | 5.83 | 2.87 | 1551.59 | 765.16 | NNW |
| 8 | 9.24 | 3.83 | 1598.31 | 662.04 | NNW |
| 9 | 6.16 | 2.09 | 1638.19 | 556.09 | NNW |
| 10 | 9.66 | 2.59 | 1671.05 | 447.73 | NNW |
| 11 | 5.00 | -8.66 | 865.00 | -1498.22 | WSW |
| 12 | 2.87 | -5.83 | 765.16 | -1551.59 | WSW |
| 13 | 3.83 | -9.24 | 662.04 | -1598.31 | WSW |
| 14 | 2.09 | -6.16 | 556.09 | -1638.19 | WSW |
| 15 | 2.59 | -9.66 | 447.76 | -1671.05 | WSW |
| 16 | -8.66 | -5.00 | -1498.22 | -865.00 | SSE |
| 17 | -5.83 | -2.87 | -1551.59 | -765.16 | SSE |
| 18 | -9.24 | -3.83 | -1598.31 | -662.04 | SSE |
| 19 | -6.16 | -2.09 | -1638.19 | -556.09 | SSE |
| 20 | -9.66 | -2.59 | -1671.05 | -447.76 | SSE |

Table 3.5: Load Case

| Test | Hs[m] | Tp[m] | Wave Dir.[deg] | Cur.[m/s] | Cur. Dir.[deg] | U [m/s] | Wind Dir.[deg] |
|---|---|---|---|---|---|---|---|
| 1 | 12.20 | 14.00 | 180.00 | 2.00 | 180.00 | 40.00 | 180.00 |

### 3.6.4 Objects and elements

A mathematical computational model is built on the system by Orcaflex software [119]. The model has several objects that represents parts of the system e.g. vessels, lines, buoys, winches, etc.

A finite element model for line components is used by Orcaflex. A simplified model can be observed in figure 3.7.

In the model, the mooring line is divided into a series of segments connected with different materials and properties, and then modeled by straight mass-less model segments with a node in each end. The segments can only model axial and torsional properties in the line. However other properties (such as mass, weight, buoyancy, etc.) are lumped to the nodes (as indicated by the arrows).

The node is basically a straight rod that represents the two half segments on each side of the node. Each mooring line segment is divided in two halves and the properties (buoyancy, drag, mass, weight, etc.) of each segment are assigned and lumped to the node at the free edge of the segment.

In the development of the Orcaflex model, an object (vessel) is considered, placed at the center of the coordinates, the vessel is connected through a turret to the mooring lines and risers. The turret is implemented in the model as a 3D and 6D buoys (objects) and both mooring lines and

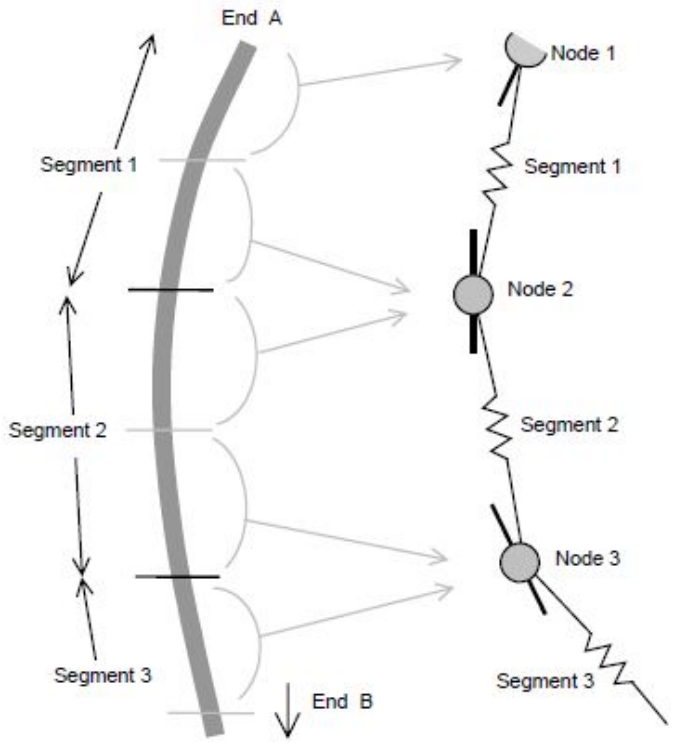


Figure 3.7: Default representation of Orcaflex Line model (image from ref. [119])

risers are implemented as lines. Between the turret and the vessel several winch element types are considered. In the development of this section, all used objects will be detailed. An example of an element (line element) can be seen in figure 3.8.

For the analysis with Orcaflex, the following flowchart represented in figure 3.9 must be taken in consideration for static analysis.

However for dynamic analysis of the case of the figure 3.8, the analysis is more complex. The model is separated in a number of consecutive stages. The stages have the duration specified in the data. The build-up stage is for the simulation to pass from static to dynamic, here both waves and vessel motion are smoothly ramped from zero to full size, the ramping of current is optional. In this stage the start of simulation begins helping to reduce the transients generated from the passage from static position to dynamic position.

The following stages are simply numerated for the intended main stages of the analysis. The stages are measured by time in seconds. In figure 3.9 and 3.10 both general static and dynamic Orcaflex flowchart is presented.

#### 3.6.4.1 Vessel

The object vessel is used to model several type of ships, floating platforms, barges, FPSOs etc. The objects are rigid bodies whose motions are detailed by the user. The motion of the Vessel object can be specified by a time history motion data file or by specifying the RAOs (response amplitude operators) for each of the 6 degrees of freedom (heave, sway, surge, yaw, pitch and roll). The information of the vessel can be verified in annex A.2.

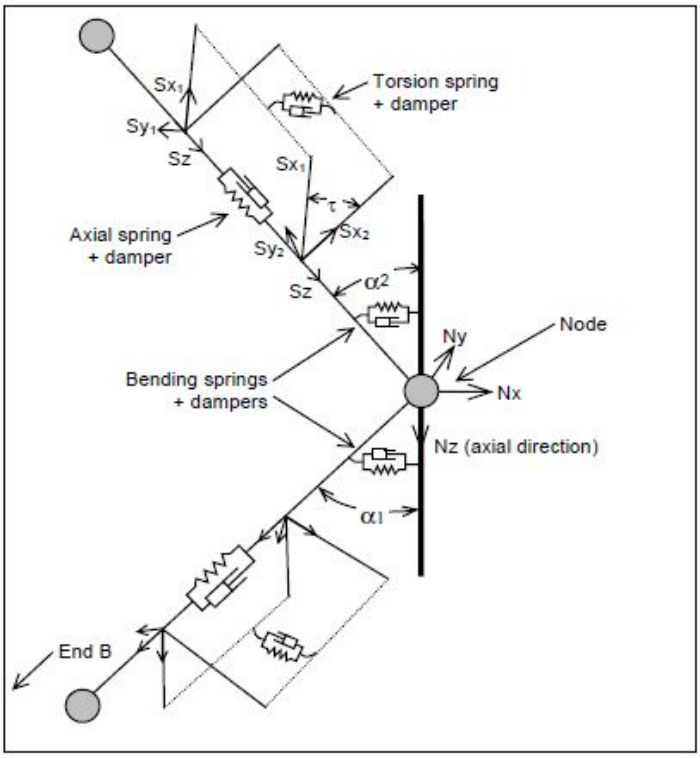


Figure 3.8: Default representation of Orcaflex Line model (image from ref. [119])

### 3.6.4.2 Lines

Lines are catenary elements used to represent mooring lines, cables, flexible hoses, pipes, etc. Buoyant element are represented as line elements, which are elements that may vary along the length. The end of the lines can be fixed or left free, they can also be attached to other objects such as buoys, vessels or shape type elements. The elements can be disconnected at the end of the simulation due to the convergence parameters.

Every line can have a number of attachments, which means that the elements can be attached to lines at user-specified locations. The elements can be attached to specific items, such as floats, clump weights, or drag chains.

### 3.6.4.3 3D and 6D Buoys

In the development of the Orcaflex model, The turret is modeled through the use of 3D and 6D buoys. Buoys are simple and single point bodies with 3 and 6 degrees of freedom.

The 3D buoy object has only translational degrees of freedom (x, y and z). The motion of the buoy is calculated by Orcaflex in opposition to vessel type objects whose response to waves is defined by the data. The object buoy 3D is not allowed to have rotation and is intended only for small objects.

The 6D buoy is a much more specific object than 3D buoy. Like 3D buoy, 6D buoy elements are rigid bodies but with full 6 degrees of freedom. Besides the translational degrees of freedom, rotation motion is also considered. Although the objects are called buoys, the objects do not

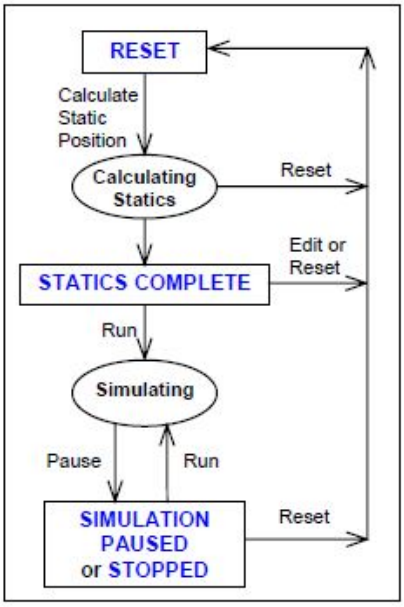


Figure 3.9: General Static Orcaflex Flowchart

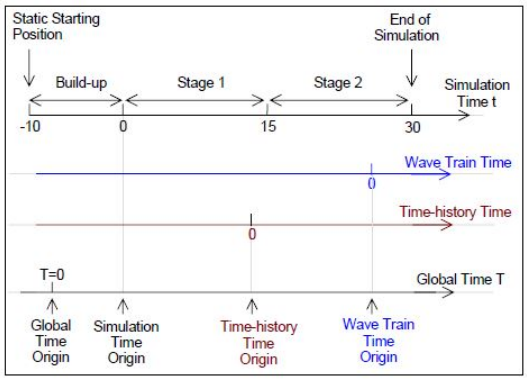


Figure 3.10: General Dynamic Orcaflex Flowchart duration

need to be buoyant which means it can used to model any rigid body whose motion is obtained by Orcaflex.

#### 3.6.4.4 Links

The link elements are mass-less connections used for linking two or more objects in a simulation. There are two types of link elements, tethers (simple elastic ties) and springs/dampers (combined linear and non linear elements), basically a combination of a spring plus damper units. This elements were used to connect the turret to the vessel, one in each quadrant.

### 3.6.5 Mesh elements

The model of the Glen Lyon FPSO can be seen in figure 3.11. the white long lines are the mooring lines, the vessel is the component in red, the other lines are the pliant waves (risers).

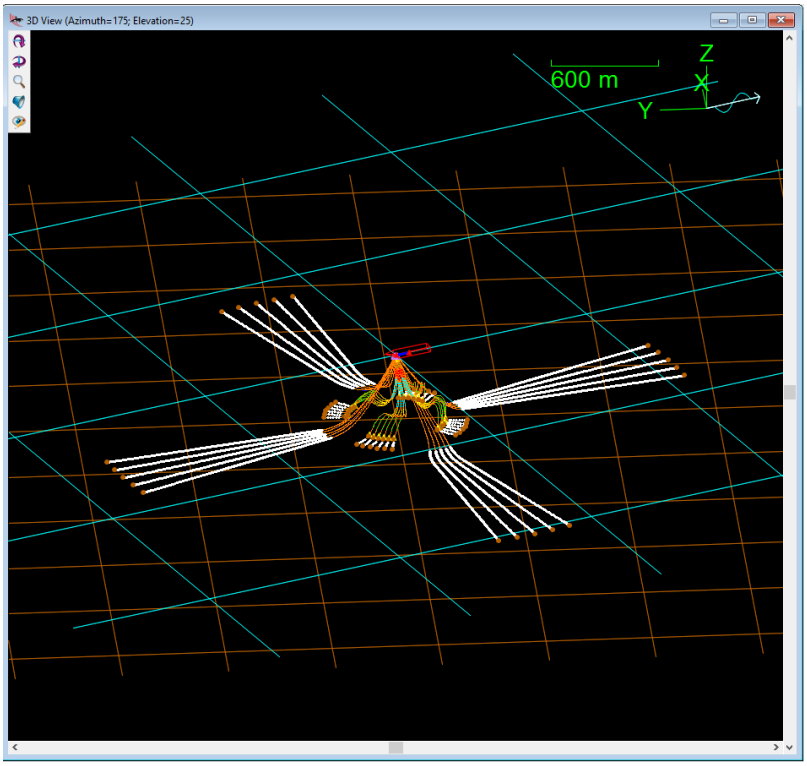


Figure 3.11: Developed model in Orcaflex for Glen Lyon FPSO

### 3.6.6 Mesh Convergence

In order to have a correct precision in the results, it must be demonstrated that the simulation converge to an accurate solution independent of the size of the mesh. Two terms must be taken in consideration, convergence and accuracy.

The convergence in a model, determines the number of necessary elements to ensure that the results are not dependent of the number and size of the elements assuring that the system response (stress, deformation, min and max principal will converge) while the mesh accuracy states that additional refinement does not affect the final results. The element type is an agreement between geometry size and shape, type of analysis and time allotted for project. In the development of this work the process is exhibited in table 3.6.

Table 3.6: Mesh Convergence

| Convergence and Mesh accuracy | | | | | | | | | |
|---|---|---|---|---|---|---|---|---|---|
| FEA mesh | Case N. of elem. | 1 10010 | 2 10330 | 3 10590 | 4 10670 | 5 10770 | 6 10870 | 7 10970 | 8 11150 |
| FEA Results | Error offset S. time[m] | 5.96e-2 66 | 4.42e-2 72 | 1.17e-2 81 | 9.02e-3 112 | 9.19e-6 132 | 1.93e-7 164 | 5.82e-9 214 | 0.00 223 |

Through the use of the former table, it is possible to analyze the convergence per solved time ratio according to full vessel offset. The mesh convergence can be verified in figure 3.12.

Within this context we can verify that the suitable mesh shall have 10770 elements, with a running time simulation of 132 minutes approx.

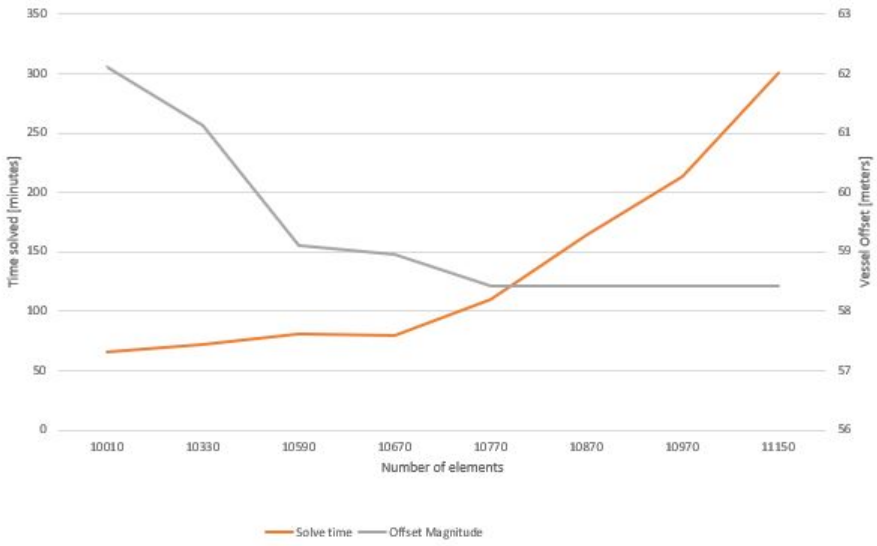


Figure 3.12: Mesh convergence Vs Solved Time

## 3.7 Results

For the analysis of the results, several parameters were analyzed. For the full system both Von Mises and effective tension of each mooring line was verified. The magnitude of the force for each direction (x, y, z) is described as well. The results will be shown for the system and separated in each of the four bundles. The results will be later compared with the results of the new optimized version, and the results will be compared. The results will also be used for the detailed analysis in FEM. The effective tension can be seen in figure 3.13.

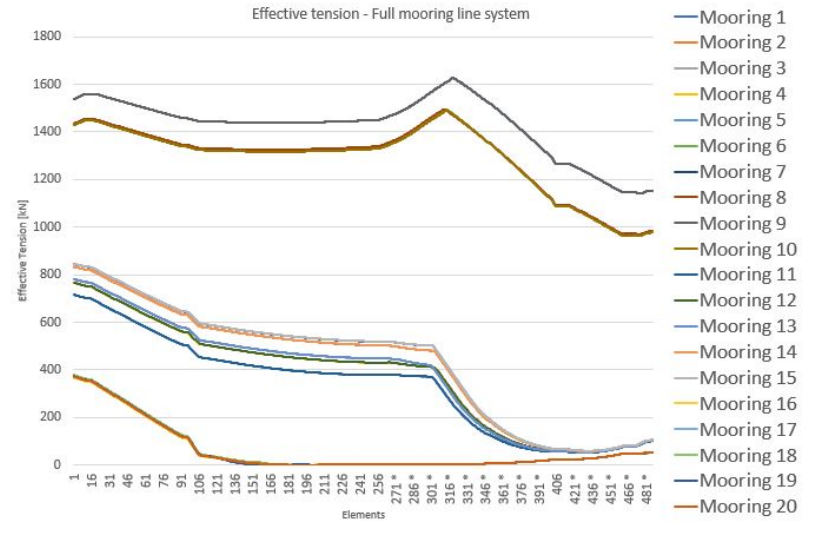


Figure 3.13: Effective tension in all mooring lines

Since the effective tension is analyzed according to each bundle it is expected that bundle 1 and bundle 3 to have similar behavior. Bundle 2 is expected to have the maximum load of the four bundles since the mooring lines have the same direction of the environmental condition in opposition to bundle 4 which was placed after the FPSO. The effective tension of the mooring lines according to each bundle can be seen in figures 3.14, 3.15, 3.16 and 3.17.

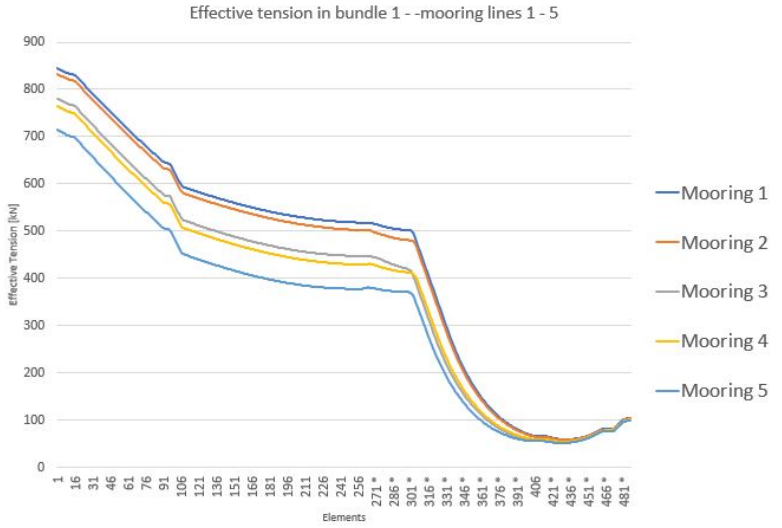


Figure 3.14: Effective Tension - Bundle 1

From figure 3.14 the most actuated mooring line in the bundle 1 is the mooring line 1, with a maximum effective tension at surface of 844.36 kN.

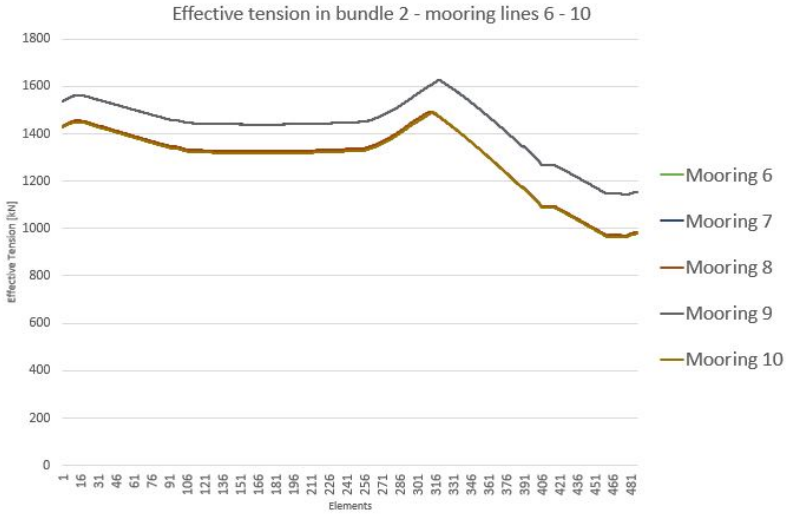


Figure 3.15: Effective Tension - Bundle 2

From figure 3.15 the most actuated mooring line in the bundle 2 is the mooring line 7, with a maximum effective tension at surface of 1626.11 kN. This mooring line withstand the most load of all the mooring system.

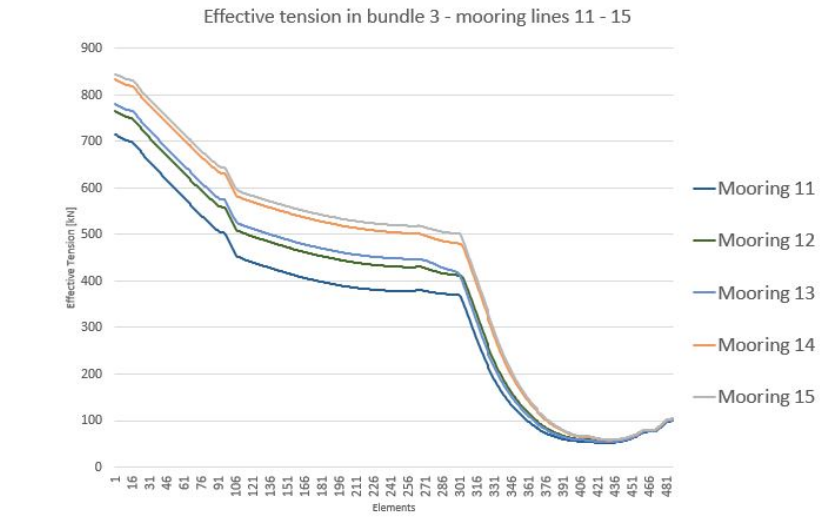


Figure 3.16: Effective Tension - Bundle 3

In figure 3.16 the most actuated mooring line in the bundle 3 is the mooring line 15, with a maximum effective tension at surface of 844.60 kN. This value is very closed the maximum value of the first mooring line as expected since they are symmetrical.

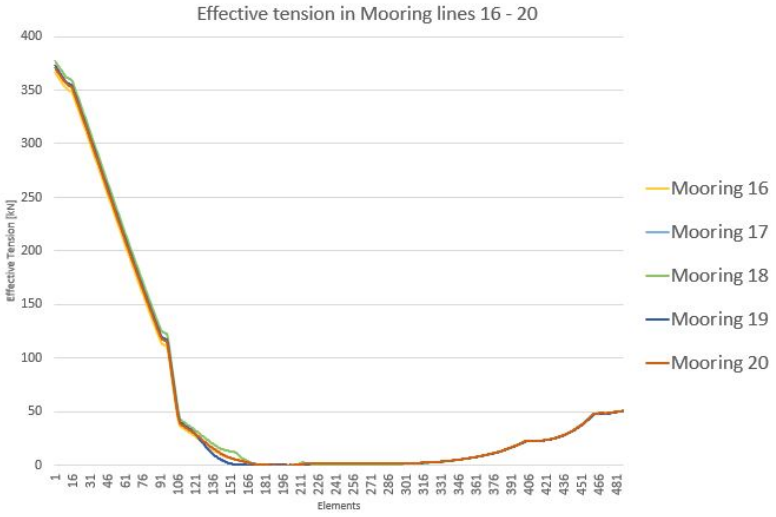


Figure 3.17: Effective Tension - Bundle 4

In the fourth bundle, the most actuated mooring line is the 18 with a effective tension of 376.87 kN. As expected the bundle four is the least actuated bundle of the entire system.

The other parameter that must be taken care into consideration is the Von Mises stress of each elements of all mooring lines. This parameter has a major importance and detailed analysis is made in Chapter 5. The full Von Mises stress of all Mooring Lines can be seen in figure 3.18. The figure correlates Von Mises stress of each node in each mooring line.

Like the effective tension above it is important to understand Von Mises stress in each bundle.

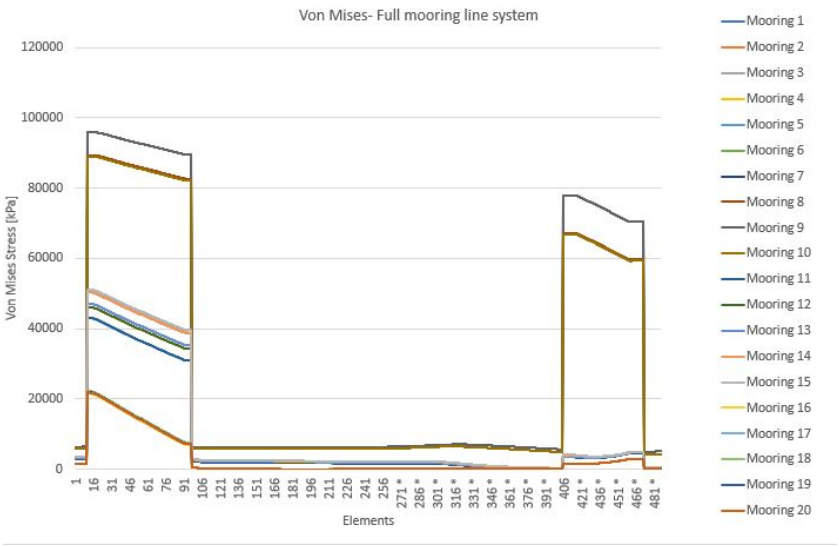


Figure 3.18: Von Mises Stress in all mooring lines

In this context for bundle 1 can be seen in figure 3.19.


Figure 3.19: Von Mises stress - Bundle 1

As expected, mooring line 1 has the most Von Mises stress of bundle 1 with 51148.97 kPa. In bundle 2 the Von Mises stress can be observed in figure 3.20

Again (like in effective tension) the most tensioned mooring line in bundle 2 is the number 7 with a maximum value of 95808.70 kPa in element 11. In bundle 3, Von Mises stress can be analyzed in figure 3.21.

Bundle 3 has the maximum stress in mooring line 15 with 51199.40 kPa in element 11. Bundle 4 can be seen in figure 3.22.

Finally the bundle 4 has a maximum Von Mises stress of 22233.42 kPa in mooring line 18 which

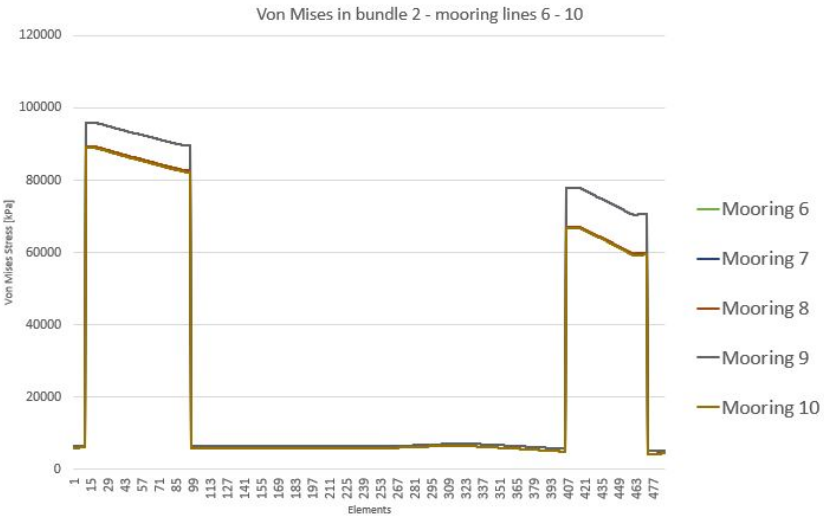


Figure 3.20: Von Mises stress - Bundle 2


Figure 3.21: Von Mises stress - Bundle 3

confirms to be the least tensioned mooring line of the entire system. One other important parameter to be analyzed is the maximum effective tension in the end connections. Figure 3.23 show the comparison between all mooring lines.

As it can be seen, the most actuated mooring line is number 9 at seabed, due to the mooring line being completely tensioned.

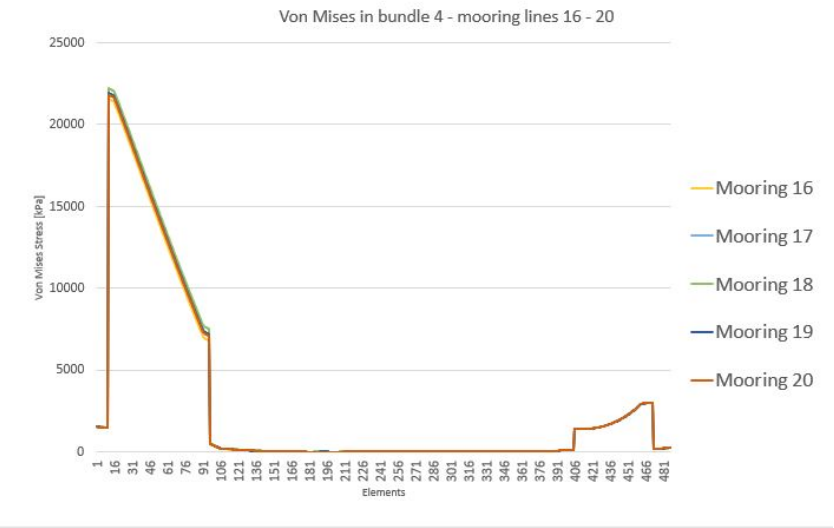


Figure 3.22: Von Mises stress - Bundle 4

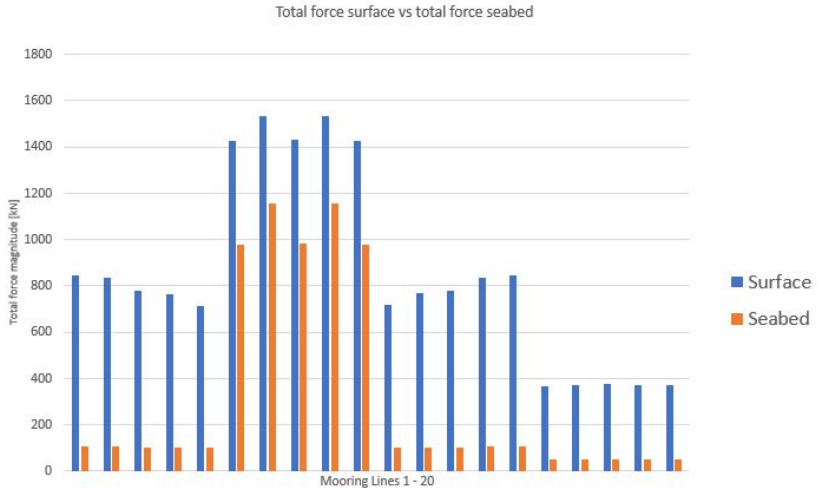


Figure 3.23: Surface Vs seabed - Effective tension (force)

## 3.8 Conclusions

The main objective of this chapter was to define the load conditions that actuates in the system, vessel and mooring lines and the model characterization.

In this chapter all the components and methodology for mooring the FPSO Glen Lyon at seabed was understood as well as the typical calculation process. The natural periods and frequencies were analyzed as well as current and wind loads for the offshore structure FPSO.

A detailed calculation process was performed for both static and dynamic (since the software requires static for positioning and dynamic for final results), either inelastic (as a first approach for convergence) and elastic (for final results). The mooring line of each mooring line was verified according to special requirements (chain for heavy segments and whip effect location

and spiral strand wire rope for light weight segments at inter-medium positions).

The model of the entire system was understood from software itself, to boundary conditions or to mesh elements. A mesh convergence was performed in order to precise the most suitable number of elements required for the analysis versus simulation time. It was verified to be 10770 elements for 132 minutes.

After running the analysis, results were verified and correlations were performed. It was verified that as expected, mooring line number 9 withstands the most harsh conditions of all mooring lines. In the previous figures, it was possible to perceive which bundles are subjected to the most environmental loads. It was also possible to verify that bundle 3 is placed both in front and in line with the vessel. Bundle 4 withstand the least loads of all the system for this collinear environmental, however for new directions of both wind, currents and waves, the vessel will adapt forcing the other bundles to support the loads. Both bundle 1 and bundle 3 are subjected to the same forces, which was expected since they are perpendicular (approx.) to the environmental loads.

One important point was the loads of the third bundle. As it can be seen it is the only bundle that has more effective tension at seabed instead of at the turret at seabed. Although the weight of the mooring line is very high, the suction pile of mooring line number 9 withstand high loads in opposition to any other suction pile. This condition happens due to the fact that the weight of the mooring lines are not enough to withstand all the loads.

According to reference [7] the offset of the vessel should be under 70.00 meters and an offset of 61.15 meters was verified for the Glen Lyon. In the development of these simulations, an offset of 58.36 meters was obtained, in which resulted in a difference of 4.78 %.

In the development of this chapter several parameters were obtained (though the mathematical model) in order to use them later in Orcaflex model. Natural periods and frequencies, current and wind loads on the structures were calculated and later used in Orcaflex. Quasi-static in frequency and in time domain alongside with dynamic of mooring lines were understood since it is the method used by Orcaflex. Catenary equations (either inelastic and elastic) were both calculated through Orcaflex and by hand and compared (1 simple case for validation).

## 3.9 Next steps

After the analysis of the mooring line system it is important to optimize it though an algorithm in Matlab. The objective in the next chapter is to reduce costs assuring the same conditions and load conditions of the model presented in this chapter.

# Chapter 4

# Mooring line Optimization

In the previous chapter, the entire mooring system was presented. The catenary mathematical process was detailed and the few official data (from reports) was analyzed for comparison. At the end of the chapter the loads and forces in the mooring line were presented and the results analyzed.

In this chapter the optimization of the mooring system is described. A parametric analysis will be performed through the use of a mathematical routine in Matlab software. In the first part of this chapter the standard cost of a mooring system will be presented in order to understand the need for improvement. Hence, the optimization process will be detailed and the methodology will be explained as well as the basis for genetic algorithms. Later in this chapter the new mooring line system will be achieved and the results will be compared with the previous system at chapter 3 both in loads, forces and cost.

## 4.1 Mooring line costs

As mentioned before, the mooring system is one of the major expenditures in the development of an oilfield. Most of this costs can be associated with the actual price of the heavy components in the mooring system such as chain links, steel wire ropes, shackles, thimbles, etc. For a optimization in therms of costs it is necessary to know the gross value of such elements from industry suppliers.

First, and as expected it will be verified that the cost can vary from supplier to supplier (like any COTS(components of the shelf)). In order to estimate the typical cost of a mooring line (stud-less and stud link chain elements and spiral strand wires) several quotation prices were asked to some mooring line suppliers. Most of them did not answer the e-mail, however one in particular was very helpful helping with the quotation price, typical evaluation of mooring chain links, differences between them, as well as, some more related information. In this context the quotation price for mooring line chain elements was asked to several companies both in UK and Norway. These companies are specialized in Oil and Gas or Aquaculture industries. A company in Norway was very helpful in giving the quotation price and some expertize advices to this work. This company was Global Maritime.

The quotation price of the mooring elements given by Global Maritime for Studless links can be seen in table 4.1

Since it is usual to consider that Studless chain elements are 10% lighter than stud links, and since the price of the components are in general associated with the weight of the elements, the price of the elements were considered in the same manner. On the other hand the quotation

Table 4.1: Quotation price of chain elements

| Type | Diameter [mm] | Price [€/kg] |
|---|---|---|
| R4 | 126.0 | 1.96 |
| R4 | 136.0 | 2.70 |
| R4S | 126.0 | 2.33 |
| R4S | 136.0 | 2.85 |

price of spiral strand wire elements given by Global Maritime can be seen in table 4.2. The spiral strand wire elements are sold in 6 or 8 lines with a standard length for a specific price.

Table 4.2: Quotation price of spiral strand wire

| Number of lines | Diameter [mm] | Segment length [m] | Price [€] |
|---|---|---|---|
| 6 | 122.0-144.0 | 250.0 | 1500000.0 - 2100000.0 |
| 8 | 133.0-155.0 | 100.0 | 1400000.0 - 1700000.0 |

Hence it is possible to establish a relationship between the costs from a reliable source and relating it to new diameters and weights. In figure 4.1 and figure 4.2 the main data can be seen. x is the diameter of the chain.

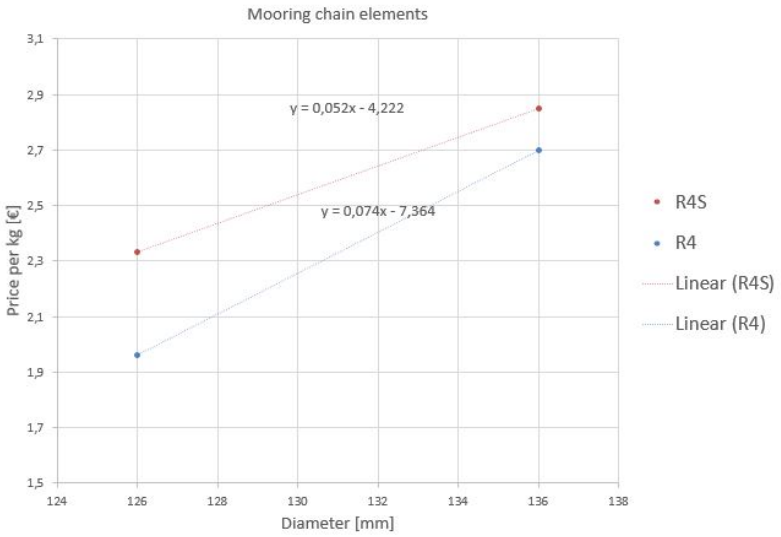


Figure 4.1: Mooring chain element cost per diameter

For chain elements and based on figure 4.1 the relationship for R4S and R4 chain type is given by:

$$y = 0.052x - 4.222 \quad \textbf{(4.1)}$$

$$y = 0.074x - 7.364 \quad \textbf{(4.2)}$$

On the other hand and based on figure 4.2, the relationship for spiral strand wire ropes for 8

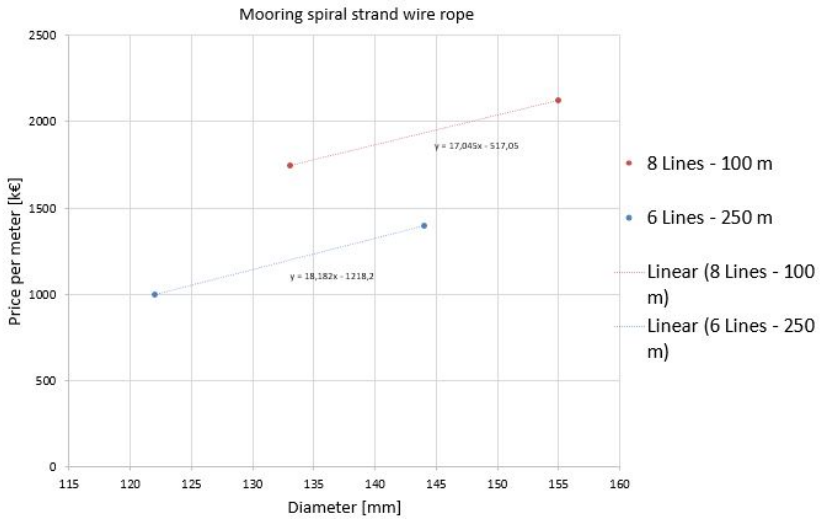


Figure 4.2: Mooring spiral strand wire rope cost per meter

lines with 100 meters and 8 lines with 6 lines with 250 meters are given by the equations:

$$y = 17.045x - 517.05 \quad \textbf{(4.3)}$$

and equation

$$y = 18.18x - 1218.2 \quad \textbf{(4.4)}$$

With these trend lines it is possible to estimate the cost of the mooring system.

## 4.2 Requirements & opportunities

For an optimization to occur it is important to understand the methodology behind it. After verifying the typical costs from a reference offshore mooring system supplier, it is important as well to understand from a macro point of view if the optimization if feasible. As it could be seen the chapter 3, the max tension will occur in mooring 7 with 1626.11 kN at the connection between the vessel and the chain element segment.

Figure 4.3 and 4.4 shows both proof load and minimum breaking load either for chain or wire elements. Within this context, it can be seen that if the loads at surface are either the same or below the values of the official mooring lines, the optimization can occur as long as margins of safety are valid and conservative. With this point we can verify the need for the optimization to occur.

Through the previous chapter, the importance of the question regarding the need of optimization is answered. If an optimization method is performed for mooring lines instead of the standard too conservative way, offshore companies could save a lot of money in the deployment of moor-

Table 4.3: Chain properties and allowables

| diameter | Proof load | | | | | | Break load | | | | Weight | |
|---|---|---|---|---|---|---|---|---|---|---|---|---|
| | R4-RQ4 | | R3S | | R3 | RQ3-API | R4-RQ4 | R3S | R3 | RQ3-API | | |
| | stud | studless | stud | studless | stud-studless | stud-studless | stud and studless | | | | stud | studless |
| mm | kN | kN | kN | kN | kN | kN | kN | kN | kN | kN | kg/m | kg/m |
| 105 | 8478 | 7497 | 7065 | 6829 | 6123 | 5495 | 10754 | 9773 | 8753 | 8282 | 241 | 221 |
| 107 | 8764 | 7750 | 7304 | 7060 | 6330 | 5681 | 11118 | 10103 | 9048 | 8561 | 251 | 229 |
| 111 | 9347 | 8265 | 7789 | 7529 | 6750 | 6058 | 11856 | 10775 | 9650 | 9130 | 270 | 246 |
| 114 | 9791 | 8658 | 8159 | 7887 | 7071 | 6346 | 12420 | 11287 | 10109 | 9565 | 285 | 260 |
| 117 | 10242 | 9057 | 8535 | 8251 | 7397 | 6639 | 12993 | 11807 | 10574 | 10005 | 300 | 274 |
| 120 | 10700 | 9461 | 8916 | 8619 | 7728 | 6935 | 13573 | 12334 | 11047 | 10452 | 315 | 288 |
| 122 | 11008 | 9734 | 9173 | 8868 | 7950 | 7135 | 13964 | 12690 | 11365 | 10753 | 326 | 298 |
| 124 | 11319 | 10009 | 9432 | 9118 | 8175 | 7336 | 14358 | 13048 | 11686 | 11057 | 337 | 308 |
| 127 | 11789 | 10425 | 9824 | 9497 | 8515 | 7641 | 14955 | 13591 | 12171 | 11516 | 353 | 323 |
| 130 | 12265 | 10846 | 10221 | 9880 | 8858 | 7950 | 15559 | 14139 | 12663 | 11981 | 370 | 338 |
| 132 | 12585 | 11129 | 10488 | 10138 | 9089 | 8157 | 15965 | 14508 | 12993 | 12294 | 382 | 348 |
| 137 | 13395 | 11844 | 11162 | 10790 | 9674 | 8682 | 16992 | 15441 | 13829 | 13085 | 411 | 375 |
| 142 | 14216 | 12571 | 11847 | 11452 | 10267 | 9214 | 18033 | 16388 | 14677 | 13887 | 442 | 403 |
| 147 | 15048 | 13306 | 12540 | 12122 | 10868 | 9753 | 19089 | 17347 | 15536 | 14700 | 473 | 432 |
| 152 | 15890 | 14051 | 13241 | 12800 | 11476 | 10299 | 20156 | 18317 | 16405 | 15522 | 506 | 462 |
| 157 | 16739 | 14802 | 13949 | 13484 | 12089 | 10850 | 21234 | 19297 | 17282 | 16352 | 540 | 493 |
| 162 | 17596 | 15559 | 14663 | 14174 | 12708 | 11405 | 22320 | 20284 | 18166 | 17188 | 575 | 525 |
| 165 | 18112 | 16016 | 15094 | 14590 | 13081 | 11739 | 22976 | 20879 | 18699 | 17693 | 596 | 545 |
| 168 | 18631 | 16474 | 15525 | 15008 | 13455 | 12075 | 23633 | 21477 | 19234 | 18199 | 618 | 564 |
| 171 | 19150 | 16934 | 15959 | 15427 | 13831 | 12412 | 24292 | 22076 | 19771 | 18707 | 640 | 585 |
| 175 | 19845 | 17548 | 16538 | 15986 | 14333 | 12863 | 25174 | 22877 | 20488 | 19386 | 671 | 613 |
| 178 | 20367 | 18010 | 16972 | 16407 | 14709 | 13201 | 25836 | 23479 | 21027 | 19896 | 694 | 634 |
| 180 | 20715 | 18318 | 17263 | 16687 | 14961 | 13427 | 26278 | 23880 | 21387 | 20236 | 710 | 648 |
| 185 | 21586 | 19088 | 17989 | 17389 | 15590 | 13991 | 27383 | 24884 | 22286 | 21087 | 750 | 685 |

Table 4.4: Wire properties and allowables

| Properties of spiral stand wire rope | | | | | | |
|---|---|---|---|---|---|---|
| Diameter mm (inch) | MBL kN | Axial Stiffness EA MN | Weight in air | | Submerged strand weight kg/m | Sheathing Thickness mm |
| | | | Unsheathed kg/m | Sheathed kg/m | | |
| 76 (3) | 5647 | 540 | 28.4 | 31.4 | 23.8 | 8 |
| 82 (3.25) | 6550 | 627 | 33.0 | 35.2 | 27.6 | 8 |
| 90 (3.5) | 7938 | 760 | 39.9 | 42.8 | 33.3 | 10 |
| 96 (3.75) | 8930 | 855 | 44.9 | 48.0 | 37.5 | 10 |
| 102 (4) | 10266 | 982 | 51.6 | 55.3 | 43.1 | 11 |
| 108 (4.25) | 11427 | 1059 | 57.6 | 61.4 | 48.0 | 11 |
| 114 (4.5) | 12775 | 1184 | 64.2 | 68.3 | 53.6 | 11 |
| 121 (4.75) | 14362 | 1331 | 72.2 | 76.5 | 59.7 | 11 |
| 127 (5) | 15722 | 1457 | 79.1 | 83.6 | 66.1 | 11 |
| 133 (5.25) | 17171 | 1599 | 86.8 | 91.5 | 72.5 | 11 |
| 140 (5.5) | 19180 | 1799 | 97.5 | 102.4 | 81.4 | 11 |
| 146 (5.75) | 20469 | 1940 | 105.1 | 110.2 | 87.7 | 11 |
| 153 (6) | 22070 | 2110 | 114.4 | 119.7 | 95.5 | 11 |
| 156 (6.25) | 23835 | 2277 | 123.6 | 129.0 | 103.1 | 11 |

ing lines, less material would be at sea and both repairs and maintenance would be easy (less weight per segment). The implementation of this new method could escalate to all mooring systems, either oil and gas, aquaculture, buoys etc. It is important to refer that each case shall be analyzed properly. It is important to refer also that these properties referred previously are general properties, which means that although they are detailed, for a proper understanding a FEM analysis is required.

## 4.3 Optimization

For the optimization process to occur, it is important to understand how the optimization will be performed, as well as how the software work. The assumptions of the optimization must be understood for results comparison.

### 4.3.1 Software

Matlab software is a powerful proprietary programming language, which means that it has its own language. It is a software mainly used for users with backgrounds in economics, science and engineering. It allows function plotting and data, matrix manipulation, algorithms implementation, etc. This software uses a variable system, allowing an easy integration with multiple syntax subroutines, treated as objects, constants or functions outputs. In the development of this optimization, genetic algorithms will be used, having the final cost per suspended catenary length as objective function.

In the development of this chapter, the optimization of the mooring system will be performed through several routines.

### 4.3.2 Methodology

In the development of this work, the optimization of the mooring system is the most important objective to achieve. Hence it is very important to define the strategy hereafter defined as the methodology of the optimization. In figure 4.3 the applied methodology can be observed and analyzed.

As mentioned in figure 4.3, the program starts by defining the mooring line initial properties. After retrieving the data from all mooring lines in Orcaflex, the mooring line that withstand the most load is analyzed, which means that the considered values for the optimization are the values from the worst case condition in the most actuated mooring line but with a factor of safety of 2 [31]. Then, the mooring line is divided into the five segments like in Orcaflex with different properties (diameters, stiffness, length, etc.).

After the definition of the identified properties and through the use of the catenary equations from chapter 3, a range for each parameters is defined. In this context, a map of discrete variables are defined as well as the constraints of the model. Here is important also to define

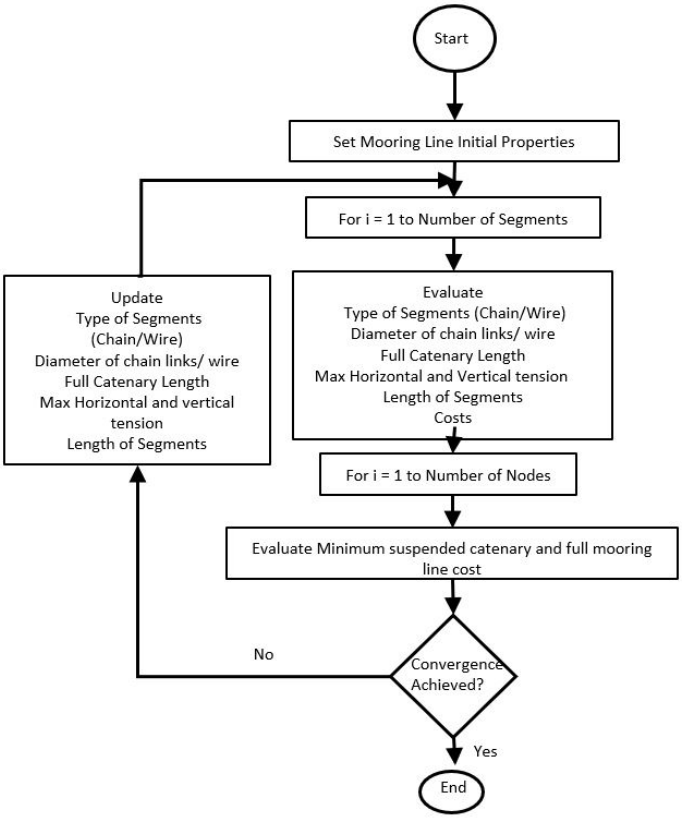


Figure 4.3: Optimization methodology flowchart

the upper and lower boundary inputs for each variable. The convergence parameters are also defined, for this case a convergence value of $1 * 10^{-8}$ is considered. It is also important to refer that this algorithm is based on stochastic method, meaning that we will not have the same solution every-time. The boundary conditions used for this specific work are the full length of the mooring line, the same location of the mooring line ends, the specific location for chains (beginning in the vessel and touching the seabed due to the whip effect and using spiral strand wire ropes for the connections between them). The connection with the suction pile anchor shall be connected to a mooring chain in order to keep the same suction piles already installed in place without having to re-install them [31].

In this context, 14 variables and constraints are defined as well as the matching of the total mooring length, max horizontal and vertical forces and costs. Then the iteration begins varying the number of elements in each mooring segment leading to the minimum cost for the minimum suspended catenary parameter.

Since a lot of possibilities are available, each time a simulation converges, a value is found and added to a txt file. Each time the convergence process does not converge to a solution, the iteration process leads to a new mooring line with updated segments. When 500 points are achieved, a cloud point graph is built. Through the use of this methodology it is possible to understand where can be possible to improve the mooring system. For the optimization process it is necessary to understand how the optimization work, since it uses genetic algorithms.

### 4.3.3 Genetic algorithms

The genetic algorithms (GA) are a family of computational models inspired in the natural evolution defended by Charles Darwin 1859 and they are used to find approximated solutions in optimization problems. The GA modeled a solution for a specific problem in a data structure, and with the use of genetic operators, both selection and cross data performed a parallel research, although mainly random. Although they have a random base they are not a simple random research since they are deterministic, which means they are based in deterministic data from former individuals from previous generations [123].

Its functioning assures that no analyzed point in the plane has the probability to be zero. Genetic operators are applied to a individual population, which can vary according to the analyzed optimization problem. GA consisted in the successive application of three processes: first, codification and decoding of variables; second, evaluation of aptitude of the problem; third, the application of GA to generate the next generation of solutions [124].

Most part of optimization methods involves the selection of values for certain variables which improves the behavior and performance of a problem in particular while obeying the requirements and specifications of the project. However most mathematical programming methods consider discrete variables, in the discrete optimization problems, the search for global optimum values become a much harder task. In the discrete problems, to find the optimum it just have to raise the function in the most inclination direction. The following genetic algorithm is presented in the diagram of figure 4.4 [123].

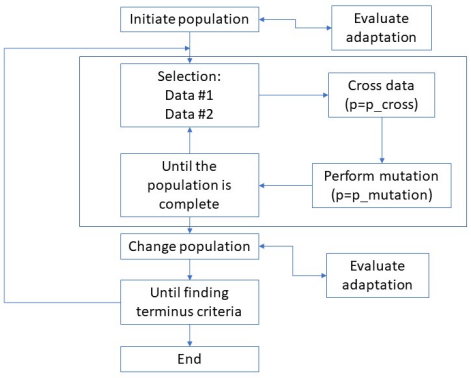


Figure 4.4: Genetic algorithm implementation diagram

The functioning of a GA is known as a Schema theorem. Which states that small groups of right information (also called construction blocks), or relevant data exponential rise in the next generation. while irrelevant data tend to disappear in next generations. This theorem can be expressed by the equation:

$$m(H,t+1) \geq m(H,t) \times \frac{f(H)}{f_{avg}} \left[1 - p_c \frac{\delta(H)}{L-1} - O(H)\, p_m\right) \quad (4.5)$$

Where $m(H,t+1)$ and $m(H,t)$ are the number of schemes H in the generation $t+1$ and $t$. $f(H)$ is

the medium value of the object function which includes the scheme H, $f_{avg}$ is the medium value of the object function of all population. $\delta(H)$ is the length of the scheme H, L is the full length of the data. $O(H)$ is the order of the scheme H and both $p_c$ and $p_m$ are the probabilities for cross and mutation. For the optimization of this work in Matlab of genetic algorithms, discrete values for the variables were used, instead of typical real values (as expected).

### 4.3.4 Script/code assumptions

In the development of the Matlab script/code, one of the major points is the definition of limitations, boundaries, element types and segments range for each mooring line. To understand the assumptions in the optimization, each lines is divided according to figure 2.17 and according to the element types as in reference in table 3.2.

As mentioned before, the script consist in evaluating the model of a mooring line used in Glen Lyon FPSO, check the standard price according to figure 4.1 and figure 4.2 and optimize it for a less expensive one but able to withstand the loads of the previous mooring line. This way the cost plays an important role in the optimization.

In order to use the same anchor points and location, it is important also to keep the full mooring line lengths equal. Through the use of the same length unnecessary costs will not be performed, the installation of the suction pile anchors are very expensive and passive to compromise the operation. The mooring lines shall have the same length as before 1880 meters long.

Another important point is the chain element type, studless vs stud link chain elements. Since the purpose of this optimization is to reduce costs it is expected to be mainly studless links. The loads at surface will be the same as represented in the previous chapter.

The segment line length elements and diameters are the major points for optimization. It is important then to understand which can be changed and which cannot. Segment 1 is the segment connected to the suction pile. This segment has the requirement to have high tensile strength since it is the last component to withstand the loads in case anything else fails.

The first segment will have the same length as before, or 50 meters long. For second segment the methodology is the same. Due to the fact that the segment is at the seabed, it is important to keep it at the seabed maintaining the segment's length the same as the previous length or 490 meters long. Both diameters of segment 1(chain elements) and segment 2 (wire elements) will be in the optimization script.

The diameter of chain segments 3 and 5 can vary from 133, 135, 137, 142, 147, 152, 157 and 162, while the diameter of wire segment 4 can vary from 121, 127, 133, 140, 144, 146, 153 and 156.

The length of the mooring segments 3 4 and 5 can vary according several characteristics, mooring 3 shall start after spiral strand mooring segment 2 and shall withstand the loads from whip effect (when touchs the seabed), on the other hand mooring segment 5 shall withstand the loads from hitting the vessel.

The mooring line length of segment 3 can vary from 700 to 1200 meters (to guarantee the chain elements are in the whiplash zone), segment 4 can vary from 300 to 450 meters (as a result) and segment 5 can vary from 6 to 15 meters (to guarantee the chain elements are in vessel slamming zone).

The optimized mooring line was applied to line number one, the line is not the most actuated one, since an average mooring load is preferable for optimization according to [98] and [43]. The reference mooring line has a force of 742.84 kN, for the optimization process a factor of 2 is used. However for FEM analysis the most actuated mooring line will be used and a factor of two will still be used.

Resuming the points referred before, we can divide the variables and their range like referred below.

- Mooring costs, like referred in the previous chapter (constraint);
- Individual full mooring line lengths, 1880 meters long (constraint);
- Chain element type - Studless vs studlink elements (free parameter);
- Chain inner diameter of elements at segment 3 and 5 (free parameter);
- Spiral strand wire rope inner diameter of elements at segment 4 (free parameter);
- Length of segment 3 - 700 to 1200 meters (free parameter);
- Length of segment 4 - 300 to 450 meters (free parameter);
- Length of segment 5 - 6 to 15 meters, preferable 10 meters (free parameter).

## 4.4 Results

The results are calculated according to FPSO Glen Lyon vessel case located at Schiehallion Field. The vessel will withstand all environmental applied forces, anchoring loads and mooring conditions (related to vessels dimensions). After the script ran, a cloud point was created and the results were verified. The cloud point relates the minimum catenary suspended length versus mooring line costs. The cloud point can be seen in seen in figure 4.5.

The recommended analysis results can be seen in table 4.5.

Table 4.5: Optimized mooring line results

| Element | Type Stud-less | Diameter [mm] | Weight Air $[kg/m]$ | Weight Water $[kg/m]$ | Length [m] | MBL [kN] | EA Axial Stiffness [MN] |
|---|---|---|---|---|---|---|---|
| 1 | R3S Chain | 137.0 | 373.5 | 325.1 | 50.0 | 16992.0 | 1602.9 |
| 2 | Spiral Strand Wire | 133.0 | 91.5 | 72.5 | 490.0 | 17171.0 | 1599.0 |
| 3 | R3S Chain | 137.0 | 373.5 | 325.1 | 922.0 | 16992.0 | 1602.9 |
| 4 | Spiral Strand Wire | 133.0 | 91.5 | 72.5 | 408.0 | 17171 | 1599.0 |
| 5 | R4 Chain | 157.0 | 490.5 | 426.9 | 10.0 | 21234.0 | 2105.02 |

As it can be seen, a curve is generated. This curve correlates the minimum length versus cost of the full mooring line for the presented conditions in this chapter. Comparing the mooring

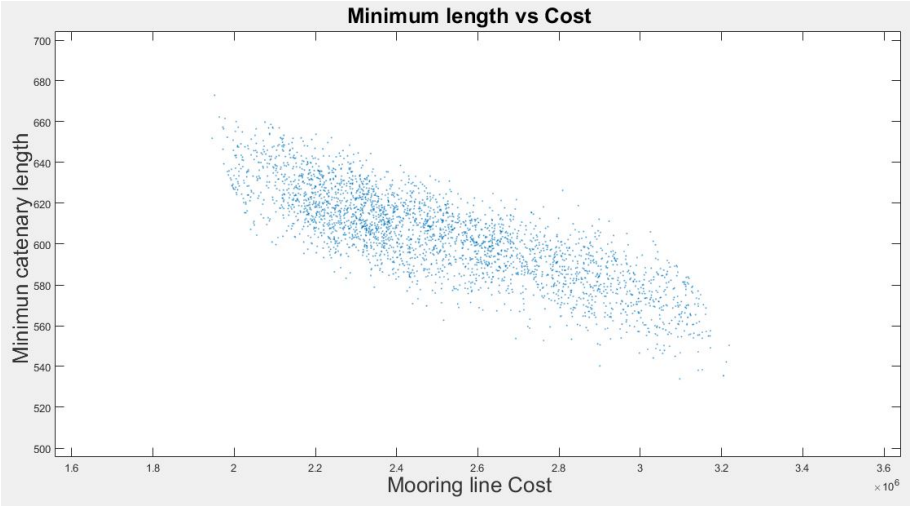


Figure 4.5: Minimum suspended catenary versus mooring line costs

line in chapter 3 with chapter 4 is possible to verify that the optimized mooring line is able to withstand the same loads but at a less expensive cost as it can be seen in figure 4.5. As it can be seen in chapter 4, each of the previous mooring lines, had a cost of 2.88 M€ while the optimized mooring line would cost 2.14 M€, or each mooring line would cost less 0.74 M€. Considering that the vessel has 20 mooring lines, the full reduction cost would be about 14.8 M€. This work and this optimization is justified from a system mooring cost saving point of view.

Although through the point cloud a curve can be visible, it is important to understand the offset difference between the former mooring line 1 and the optimized mooring line 1 in the . Hence in figure 4.6 the 2D offset difference between original and optimized mooring line can be visible.

It is possible to verify that the offset is very small compared to the cost difference. However it is important also to verify the offset difference in a 3D model as it can be seen in figure 4.7.

After the optimization in Matlab the new parameters were inserted in the Orcaflex model and results were observed. In order not to duplicate information only results from this chapter will be analyzed. It can be concluded that the offset is very small compared with the benefits of the optimization. On the other hand like in chapter 3 it is important to analyze both Von Mises and effective tension of each mooring line. The magnitude of the force for each direction is described as well. The result are presented as a whole and in bundles. The effective tension can be verified in figure 4.8

Like before, it is expected that bundle 1 and bundle 3 to have similar behavior. Bundle 2 is expected to have the maximum load while bundle 4 is expected to have the lowest value. The effective tension in bundle 1, 2, 3 and 4 can be seen in figures 4.9, 4.10, 4.11 and 4.12.

As it can be seen, mooring line number 1 has the most effective tension in bundle 1 with a maximum of 863.04 kN.

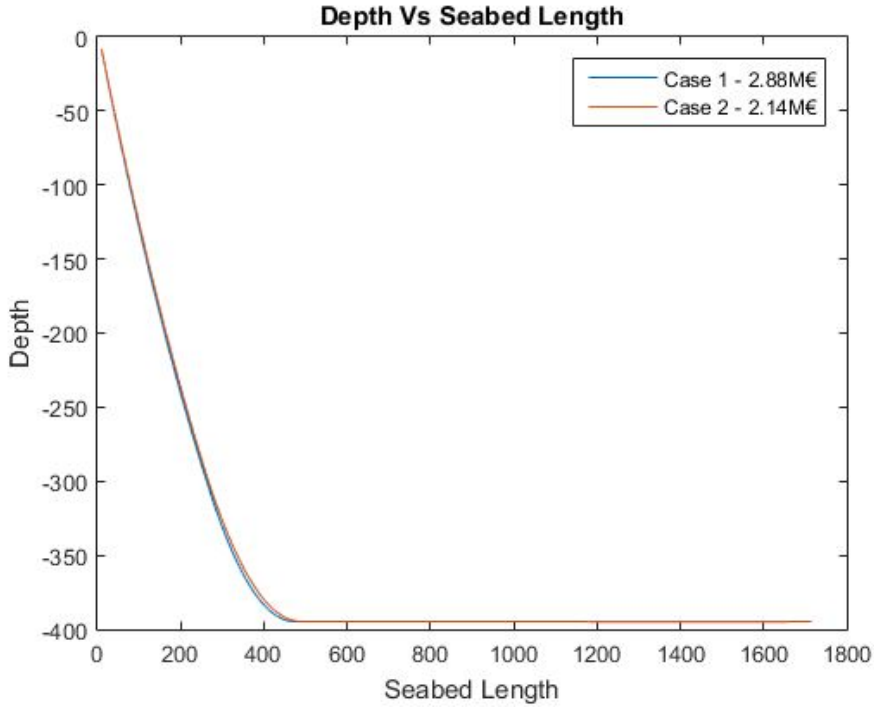


Figure 4.6: Mooring line offset - 2D view

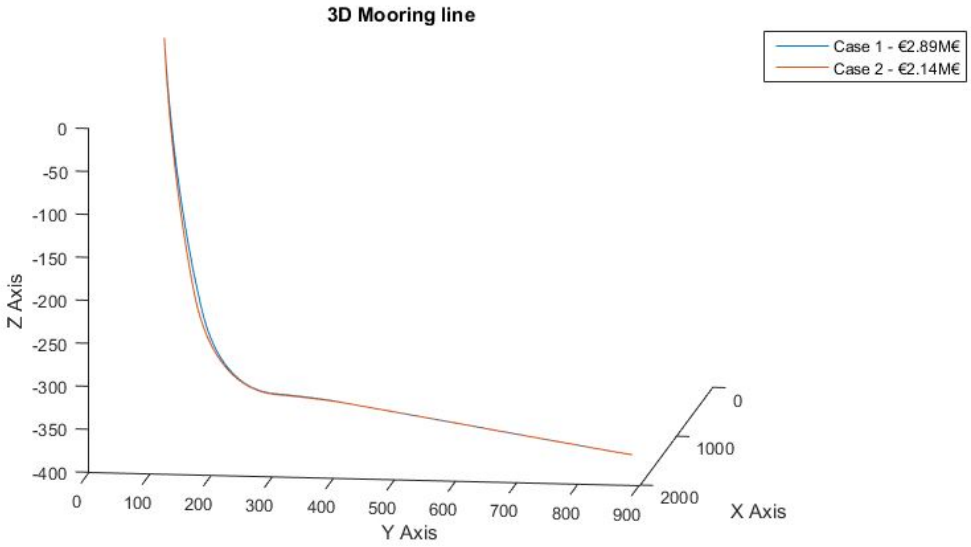


Figure 4.7: Mooring line offset - 3D view

Bundle 2, mooring line 7 has the most effective tension with a maximum of 1649.00 kN. Like in chapter 3 this mooring line is the most actuated in the whole system.

In figure 4.12, the mooring line number 15 is the most actuated one, with a maximum effective tension of 863.79 kN. This value is very close to the first mooring line in bundle 1. In the fourth bundle the mooring line number 19 has the maximum effective tension of 364.73 kN.

Regarding the Von Mises load, in figure 4.13, the maximum stresses can be seen.

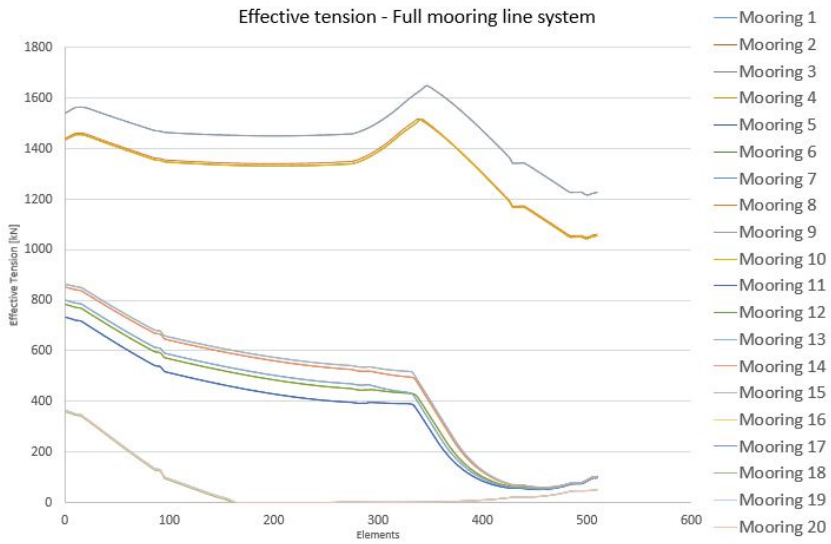


Figure 4.8: Effective tension in all mooring lines

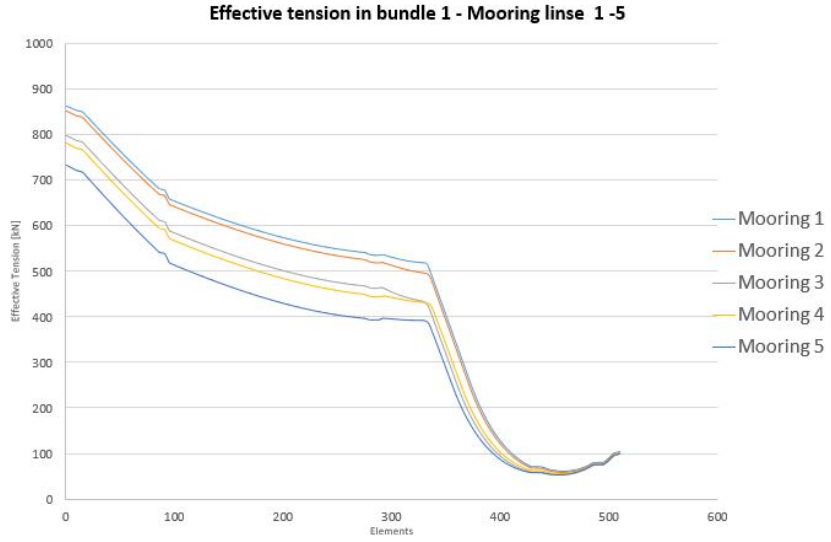


Figure 4.9: Effective Tension - Bundle 1

A detailed analysis according to each bundle can be seen in figures 4.14, 4.15, 4.16 and 4.17.

For the first bundle, mooring line number 1 is the most actuated one with a value of 55418.80 kPa.

In bundle 2, the seventh mooring line is the most actuated one with a stress of 101580.67 kPa. This mooring line withstand the most environmental loads of the whole system.

The mooring line number 15 withstand the most loads in bundle 3 with a stress of 55470.44 kPa. Once again it is very closed to the most actuated mooring line in bundle 1.

The last bundle as a maximum value of 22755.27 kPa in bundle 19. This bundle like referred in

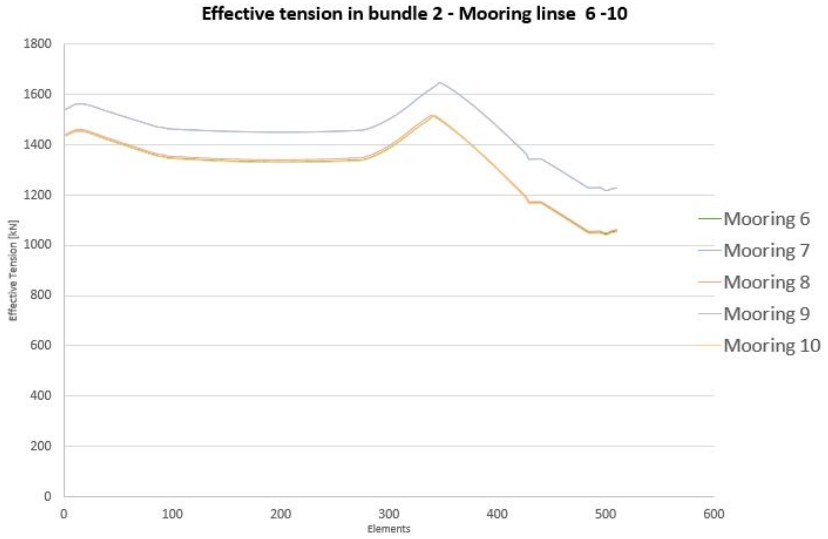


Figure 4.10: Effective Tension - Bundle 2

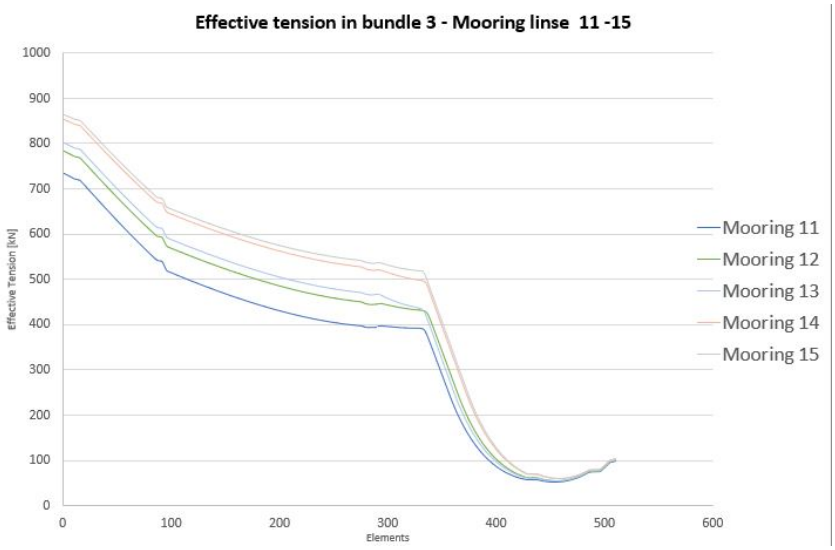


Figure 4.11: Effective Tension - Bundle 3

chapter 3 is the least actuated bundle in all system. Analyzing the maximum effective tension on the end connections is possible to verify and compare to the previous mooring system. In figure 4.18 the difference in the end connection can be verified.

## 4.5 Conclusions

After comparing and analyzing both effective tension and Von Mises stress in the first (installed) and second system (optimized). Several conclusions can be made. For a better comprehension of the results it is important to define the installed mooring system as ”Installed” and the new mooring system as ”Optimized”. In table 4.6 a comparison between the installed and the optimized mooring line is presented. The maximum difference between the former and optimized effective tension is 5.04 % while the Von Mises stress difference is 8.71 %. This results

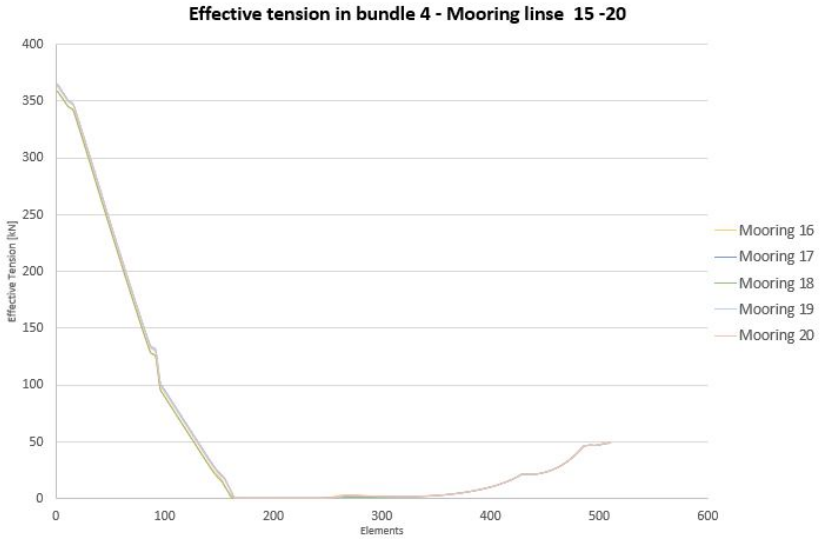


Figure 4.12: Effective Tension - Bundle 4

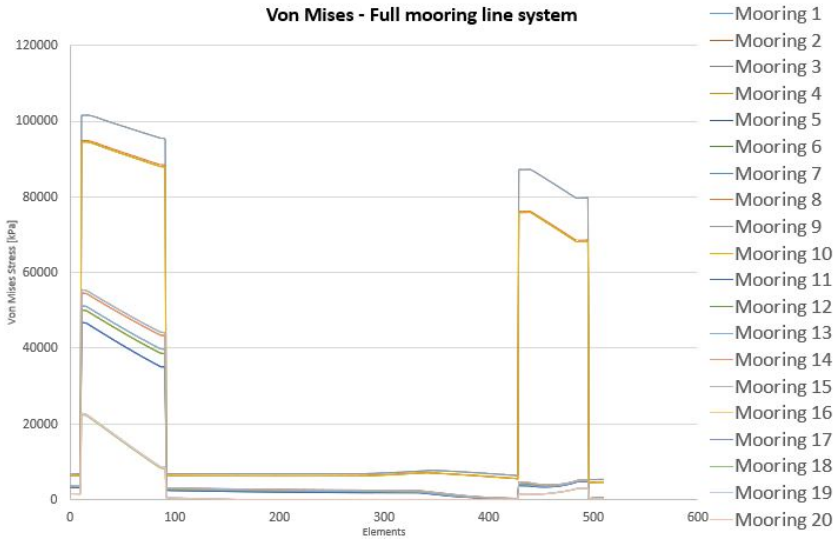


Figure 4.13: Von Mises Stress in all mooring lines

assures the correct optimization of the mooring line the offset is 59.7 meters.

As it can be seen, the new optimized chain is less expensive , the new optimized mooring line system layout can assure about the same results as the former one, both in Von Mises and effective tension in the lines. The effective tension in the turrets connection has a very small difference compared with the previous one although for the new optimized system a saving of 14.8 M€ is applicable.

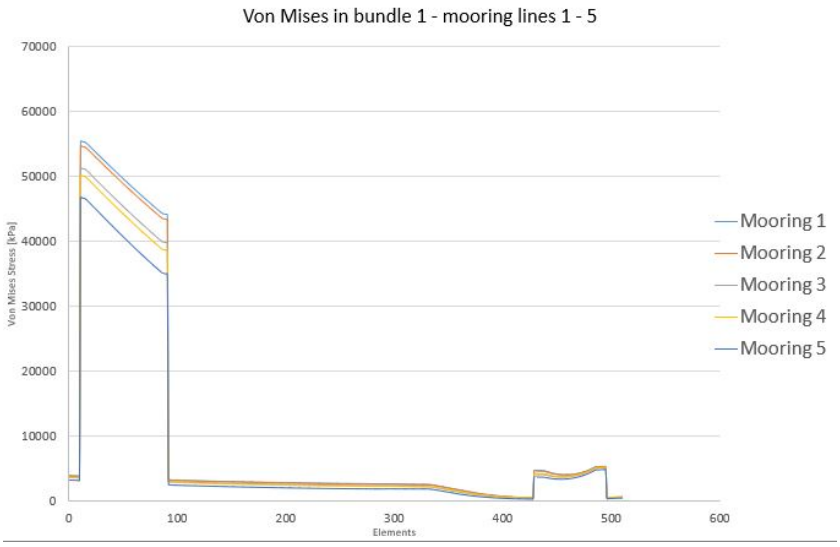


Figure 4.14: Von Mises stress - Bundle 1

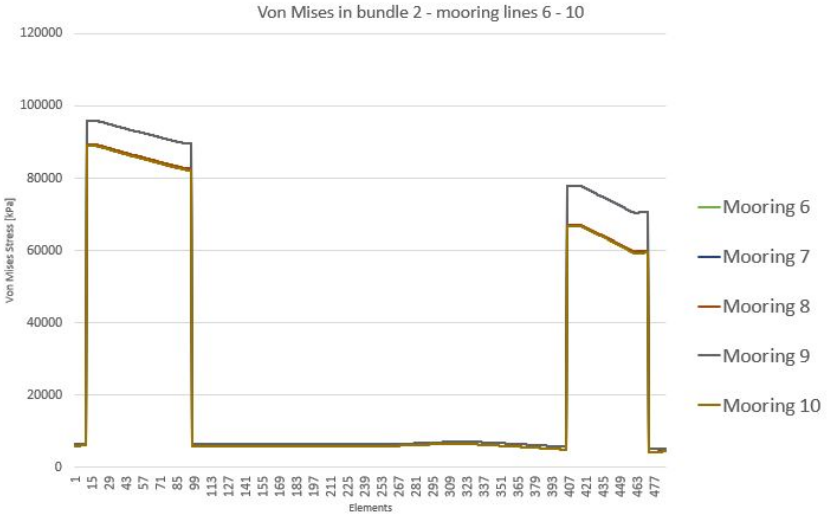


Figure 4.15: Von Mises stress - Bundle 2

## 4.6 Next steps

After the analysis of the new mooring system, it was possible to compare the differences between former and new optimized mooring line system. In this chapter the optimization was performed and the results were analyzed. Both the analysis in Orcaflex and further optimization in Matlab have proven that for macro analysis (conceptual and preliminar phases) the results have relevance with margin to improvement.

Although the mooring system of the FPSO Glen Lyon was very expensive due to the mooring design, for further installations the process can be enhanced, assuring the same considerations but lowering the capital expenditures.

In the next chapter the detailed model will be performed to verify the exact margins of safety

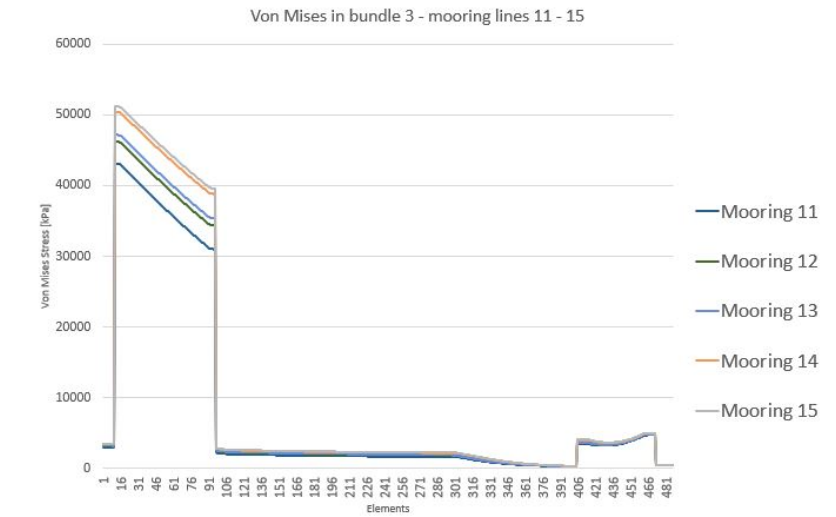


Figure 4.16: Von Mises stress - Bundle 3


Figure 4.17: Von Mises stress - Bundle 4

for both former and optimized mooring line system.

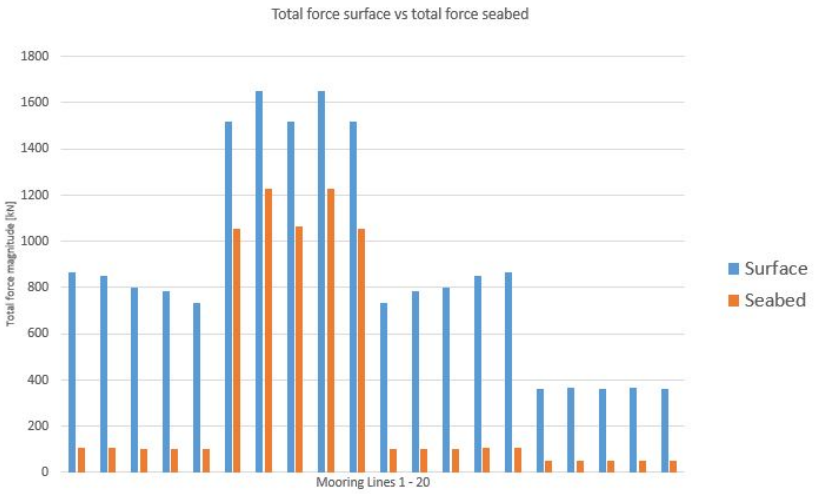


Figure 4.18: Surface Vs seabed - Effective tension (force)

Table 4.6: Comparison between former and optimized mooring lines

| Mooring line | Former EF [kN] | Optimized EF [kN] | Former VM [kPa] | Optimized VM [kPa] | ET difference [%] | VM difference [%] |
|---|---|---|---|---|---|---|
| 1 | 863.04 | 843.82 | 55418.80 | 51148.97 | 2.27 | 8.34 |
| 2 | 851.54 | 832.20 | 54613.80 | 50376.63 | 2.32 | 8.41 |
| 3 | 799.74 | 780.05 | 51213.41 | 47138.46 | 2.52 | 8.64 |
| 4 | 783.08 | 764.83 | 50085.35 | 46159.21 | 2.38 | 8.50 |
| 5 | 732.78 | 714.51 | 46800.20 | 43050.43 | 2.55 | 8.71 |
| 6 | 1517.32 | 1491.35 | 94509.52 | 88934.38 | 1.74 | 6.27 |
| 7 | 1649.00 | 1626.11 | 101580.67 | 95808.70 | 1.41 | 6.02 |
| 8 | 1517.54 | 1493.38 | 94899.57 | 89307.01 | 1.62 | 6.26 |
| 9 | 1648.82 | 1625.93 | 101568.20 | 95797.53 | 1.41 | 6.02 |
| 10 | 1516.85 | 1490.92 | 94478.70 | 88905.74 | 1.74 | 6.27 |
| 11 | 733.41 | 715.17 | 46843.73 | 43092.94 | 2.55 | 8.70 |
| 12 | 783.84 | 765.59 | 50136.08 | 46207.06 | 2.38 | 8.50 |
| 13 | 800.39 | 780.69 | 51258.33 | 47180.57 | 2.52 | 8.64 |
| 14 | 852.37 | 833.05 | 54668.58 | 50430.03 | 2.32 | 8.40 |
| 15 | 863.79 | 844.60 | 55470.44 | 51199.40 | 2.27 | 8.34 |
| 16 | 359.07 | 366.30 | 22426.53 | 21567.30 | 2.01 | 3.98 |
| 17 | 364.72 | 372.73 | 22754.34 | 21925.46 | 2.20 | 3.78 |
| 18 | 358.80 | 376.87 | 22431.53 | 22233.42 | 5.04 | 0.89 |
| 19 | 364.73 | 372.75 | 22755.27 | 21926.60 | 2.20 | 3.78 |
| 20 | 362.52 | 370.32 | 22672.23 | 21833.33 | 2.15 | 3.84 |

# Chapter 5

# Design and strength analysis

In the last chapter, the optimization process of the mooring system was detailed, based on the real mooring system already installed for the Glen Lyon FPSO in Schiehallion field. Last chapter consisted in the optimization of the entire mooring system from cost analysis to the optimization itself. The costs were estimated alongside with specialized companies. Requirements and opportunities were also verified and the optimization process was explained.

All the process was analyzed, from understanding the software, detailing the methodology to the verification of the actual scripts using some important code assumptions. At the end of the chapter, results were given and conclusions were taken.

It is also important to mention that most of the former chapters presented a type of conceptual and preliminary design analysis, while this new chapter presents the detailed design of the critical components. The main purpose of this chapter is then, to verify if the material can withstand the loads for the new mooring system. In this chapter the design of the mooring system will be performed through the use of a CAD software $Dassault\ CATIA\ V5^{TM}$, then the meshing process will be detailed for the FEM analysis with $Altair\ Hypermesh^{TM}$ and finally the results will be analyzed through the software $Altair\ Hyperview^{TM}$.

At the end of this chapter, the mooring system's margins of safety will be taken for chain elements. The analytical process of the strength analysis will be presented and conclusions will be taken. A structural comparison between studless and studlinks under the same load conditions will be also performed.

## 5.1 Structural design

In the development of this section it is important to understand the design principles behind the structural design. For the development of this dissertation both chain and wire are considered as marine structures/components and the objective is to summarize the engineering practices, research and design codes and engineering considerations before the next section entitled structural analysis.

Both in chapter 3 and later in chapter 4, the wave calculation and load combinations gave the first steps for the marine design. It was of a major importance to have the basic concepts of waves, motions and design loads [43]. The standard separation for underwater structural components is normally performed for beams, plates and shells under several type of loads, such as concentrated loads, hydrostatic pressure and bending loads. Is is usually assumed one of the three levels in the structural design phase.

- Design by rules;

- Design by analysis;
- Design based on standards of performance.

If design by rules was used in the seventies, nowadays the design by analysis is used based on the finite element method (FEM). It has been the most used approach for all engineering areas, such as aeronautical, mechanical and maritime fields for complex systems like aircrafts, ships and offshore structures. FEM methodology is always supported by the fast development of computational technology. The development of FEM methodology was made possible by the precise type of computer based tools such as CAD, CAE and CAM.

For the development of the structural design of this work, the diagram in figure 5.1 is used.

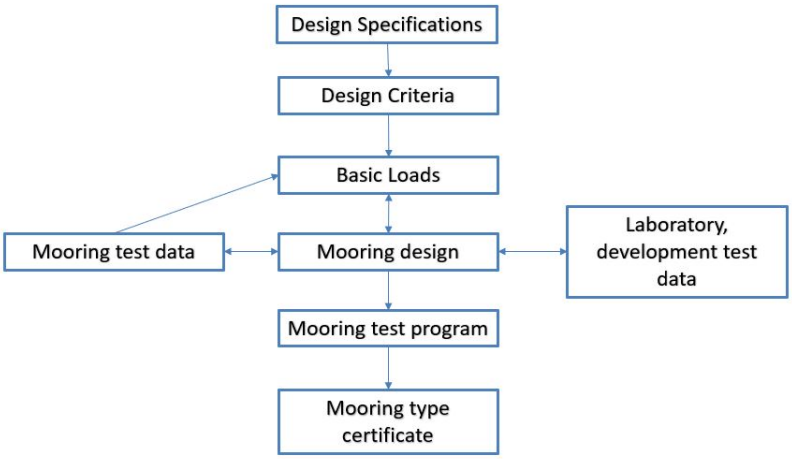


Figure 5.1: Diagram of mooring design for certification

As it can be seen in figure 5.1, the design specification from DNV will be analyzed building the foundations for the definition of the requirements. Then the basic loads from chapter 4 will be used, analyzed and compared to mooring test data, either from simulations or laboratory tests. Both test program and mooring type certification process will not be performed due to the costs involved in the certification process.

### 5.1.1 Design specifications

The design specifications in this chapter will be based on the norms of chapter 2. Several considerations will be latter developed in the structural analysis section. The main specifications are the depth, the number of mooring lines and segments, vessel characteristics, environmental conditions and costs.

### 5.1.2 Design criteria

Structural design criteria defines the considerations such as waves, wind and currents which are to be considered in the structural design analysis. The design considers three limit states, each one of them regarding a critical importance:

- ULS - Ultimate limit state - To ensure each mooring line have adequate strength to withstand all loads;
- ALS - Accidental limit state - To ensure that the system has the capacity to withstand the failure of one mooring line;
- FLS - Fatigue limit state - To ensure that each mooring line can withstand cyclic loading.

Using the method for structural reliability analysis, the safety margins can be taken. The design procedure shall be able to be adapted to any other geographical location either the environmental conditions are more or less severe. Fatigue limit state is mainly used for metallic (steel) components, specially when fatigue endurance cause by cyclic loads may be limiting the design. In the development of this work only steel components will be analyzed. Using this methodology a design curve for rupture under constant tension will be established in contrast to fatigue under cyclic tension [125].

A typical curve is presented in figure 5.2:

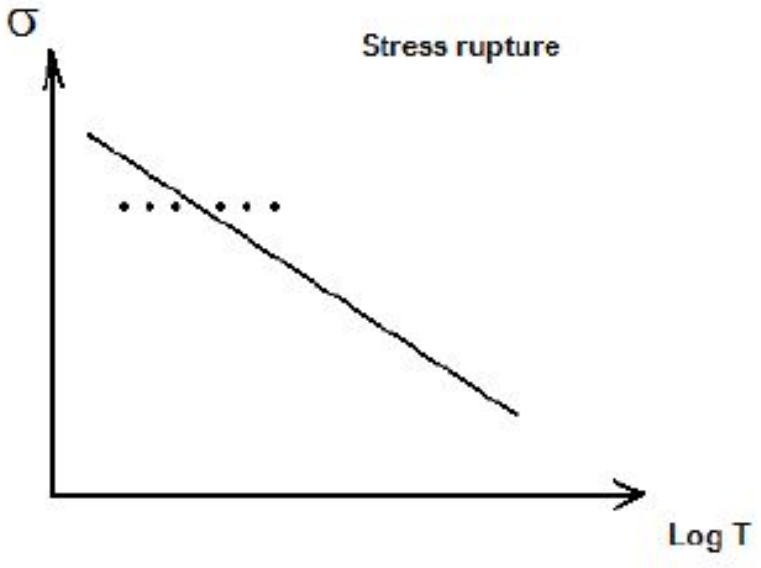


Figure 5.2: Typical stress rupture curve

the typical curve correlates the tension per number of cycles. There are two known classes for ULS and ACS. They are defined as:

- Class 1 Failing of the mooring system will not lead to unacceptable consequences such as collision with other platform or even loss of life, sinking or uncontrolled outflow of oil and gas;
- Class 2 Failing of the mooring system will lead to unacceptable consequences such as referred in class 1.

Adapting to the mooring system development of this work, only class 1 type will be considered since worst case conditions are used for this case. It is of a major importance to understand

major concepts such as strength, rigidity, displacements and others. Nowadays the structural design is performed for:

- Static ultimate and limit (yield) strength;
- Fatigue life.

The main objective is to achieve the best safety margin per lowest cost per lowest weight ratio. It is important to adapt project needs with suppliers products in order to have a standard design instead of having everything personalized, this point is known as design for manufacturing.

#### 5.1.2.1 Limit and ultimate loads

Both limit and ultimate loads predicts mooring system service life. The mooring system must be capable of supporting the limit loads without suffering detrimental permanent deformation [126]. In all limit loads, the deformation of the structure shall not interfere with safe operations while ultimate loads (or design loads) are the limit loads multiplied by a factor of safety.

$$Ultimate \quad load = Limit \quad loads * Factor \quad of \quad safety \quad (5.1)$$

According to DNV rules, the ultimate factor of safety is 1.5. In general the mooring line elements are not supposed to undergo higher loads than the limit loads, however an amount of reserve strength against complete structural failure is necessary due to several factors:

- The approximations involved in wave theory and structural analysis theory;
- Variation of the physical properties of the materials;
- Variation in mooring production and inspection standards.

### 5.1.3 Loads

FPSO loads are those forces and loadings caused by environmental conditions and passed to the mooring line system. It will establish the strength level of the full elements. The design loads are provided by Orcaflex analysis either for first mooring system and later optimization.

In the development of the design and structural analysis, the vessel is assumed to weathervane without any other propulsion means. The objective is to understand the loads in order to update the FEM models according to them. Any other maneuvers will not be considered in this study. The structural design is load dependent.

For the development of structural design, the considered loads are those achieved in the end of chapter 4. As it can be seen, the mooring line 7 in the bundle 2 withstands the maximum load of all the mooring lines in any point of the mooring line with an effective tension of 1649.0 kN. According to DNV rules and standards for position moorings [31] the chain elements must assure a minimum breaking factor of 2, multiplying the acquire loads per load factor the effective tension reaches 3298.0 kN.

In the structural analysis section an effective tension of 3300.0 kN will be considered for the calculation process. This value will be used in every interface between wire and chain. Assuming the same value for each of the segments connection, a conservative approach is being used.

### 5.1.4 Mooring design

As mentioned before the design of the mooring system consists in the development and analysis of the chain element links. In this context it is important to verify the location of the transitions points, the involved loads (like referred in the previous section) and chain links design. Hence, if each mooring line has 1880 meters and if all segments are withstanding the loads since they are connected one link to the next, the lengths are the same as in chapter 4, so we can consider that the segments have the following range lengths.

- Segment 1 - 0-50 meters;
- Segment 2 - 50-490 meters;
- Segment 3 - 490-1462 meters;
- Segment 4 - 1462-1870 meters;
- Semgnet 5 - 1870-1880 meters.

For the design and analysis of the mooring chain, only the transition from segment three to four, four to five and five to vessel will be performed. The only components to be analyzed will be the mooring links, the spiral strand wire cables will not be analyzed since the characteristics and properties are given by suppliers.

#### 5.1.4.1 Mooring chain links design

For the mooring chain links, 2 elements will be analyzed, studless and stud link elements. Although the optimization refers only the studless links, a study between the behavior of the two elements is also performed so the design for stud link is also given.

### 5.1.5 CAD - Dassault Catia V5

CATIA is an acronym for computer-aided three dimensional interactive application. It is a tool or a platform for CAD, CAE and CAM. It was developed by Dassault Systémes, a french company.

The company started the platform in 1977 by the french company aeronautical related AVIONS MARCEL DASSAULT. Initially it started in the aerospace and aeronautical field later adopted for naval, automotive, shipbuilding, railway, etc. In 1981 the name changed to CATIA after an agreement with IBM. Nowadays most of the CAD for the referred industries is performed through CATIA platform. Among some of the major users are Boeing, Airbus, Onera, Embraer, General dynamics etc. In the development of the mechanical design of this project all CADs were designed using CATIA.

In figure 5.3 the design of the full system in CATIA V5 is presented. All twenty mooring lines and all 24 risers can be seen. The design of both stud and stud less links are in figures 5.4 and

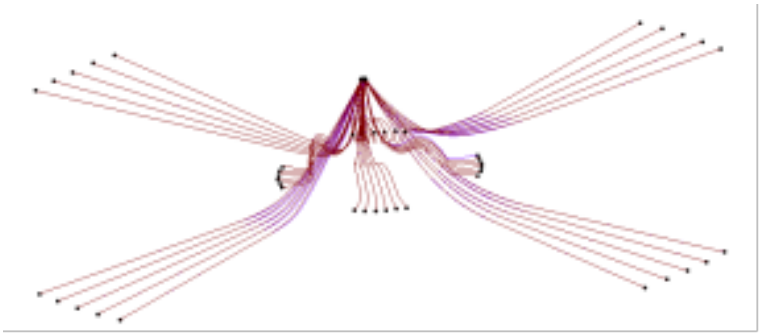

Figure 5.3: Design of the full system in CATIA V5

5.5

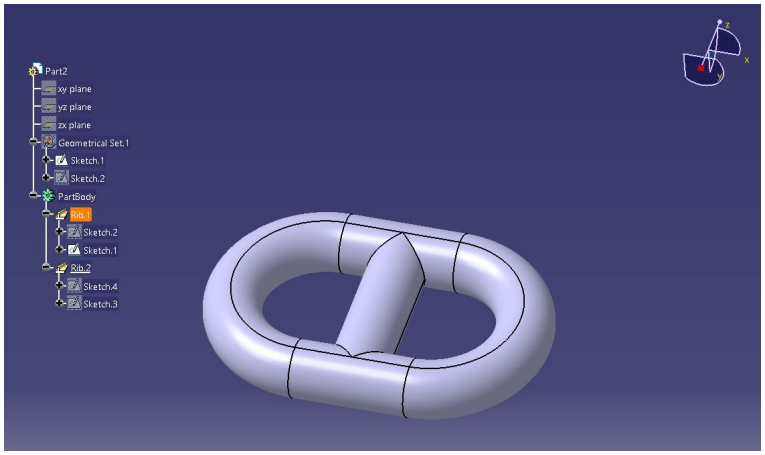


Figure 5.4: Stud link element

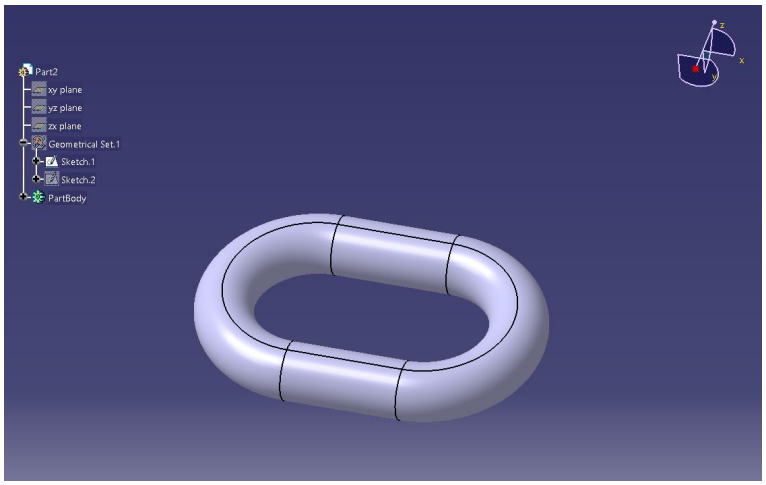


Figure 5.5: Stud less link element

## 5.2 Structural analysis - FEM

Like mentioned before, in the development of the mechanical design of any product, the last phase is the detailed design. The detailed design will assure that everything is checked according to plan without failure. However the detail design involves both design and structure analysis. In the development of the mooring system optimization the process is the same. It is of a major importance to guarantee that the optimized mooring system withstands the same loads as the former mooring system and it shall be valid for all mooring lines in the system.

In the second part of this chapter the structural analysis is performed through the use of three softwares, Altair's Hypermesh and Hyperview and MSC Nastran. The FEM process is detailed and the development is explained from meshing to validation.

In the development of this section it is important to understand all the process of FEM analysis from concepts to results, loads, constraints, materials, properties, margins of safety, FEM process itself, fatigue and involved theory. At the end of this subsection the results will be taken and the conclusions will be performed.

There are several methodologies for structural analysis furthermore designated as stress analysis. In figure 5.6 the main points are presented. It does not mean that any one is more important than other, all are important and shall be verified. Part of this scheme is referred before in this

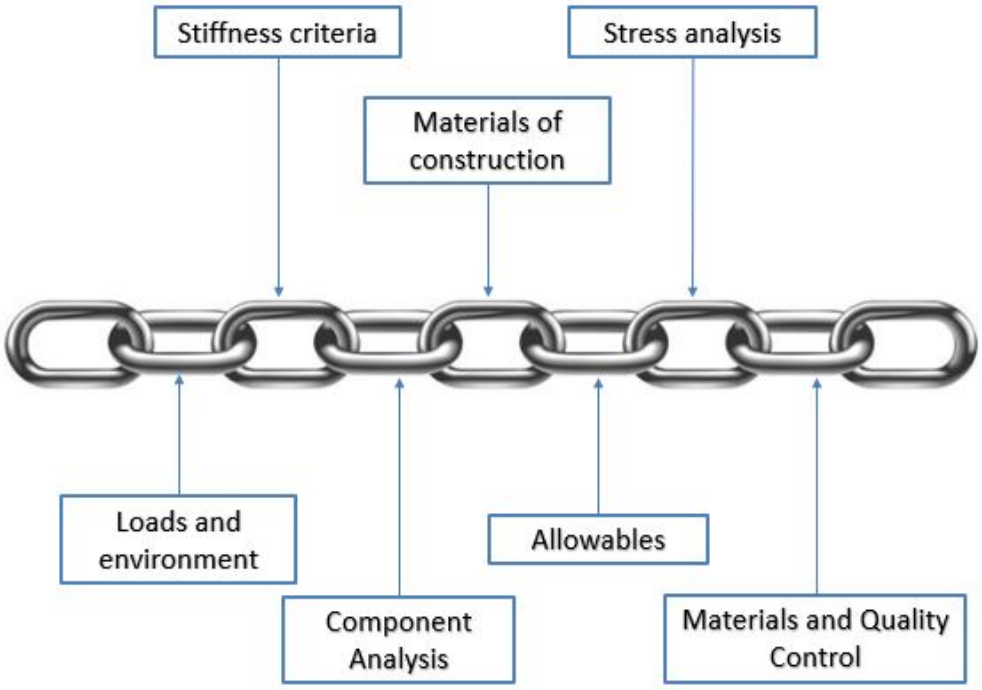


Figure 5.6: Main points for structural analysis

chapter in the design phase. From figure 5.6, the methodology consists in seven parameters, loads and environmental, stiffness criteria, component analysis, materials and construction, allowables, stress analysis and finally materials and quality control.

Loads and environment refers to the operational criteria of the mooring lines. As it was mentioned before has a static and a dynamic approach. For the development of this thesis, static analysis will be analyzed and dynamic will only be applied for fatigue analysis. It has the loads distribution, impact and deformations.

The stiffness criteria was mentioned before in the design sub section. For this analysis both limit and ultimate load conditions will be analyzed. Although thermal effects are important for the mooring system, it will not be considered for this work. Thermal effects may occur in specific locations in the oilfield due to underwater thermal vents.

Component analysis refers the system and subsystems analyzed. In the development of this chapter only studless and studlink chain elements will be verified. Although there are more components such as dee's and bow shackles, swivels, rings and other fittings, only chain element will be analyzed in FEM analysis.

The materials of construction are mainly to understand the stainless steel chain elements, the elements direction from mechanical construction as well as properties.

Allowables are the specific characteristics of the chain elements for specific conditions, shapes and dimensions. In order to verify the margins of safety it is important to know the allowable of the material. For the material's allowable, the main points are the yield stress, fatigue, deflections and stiffness.

The stress analysis is simple since the only analyzed components will be the chain links from the mechanical system. In a further phase experimental results should be performed, verified and compared.

Finally the materials and quality control. The main points are the ductility, the stress-stain curves and the specification conformance. Neither residual stress nor corrosion nor heat treat control will be analyzed in the development of this work.

### 5.2.1 FEM - Finite element method

For a precise analysis of the chain elements, computational aided engineering is needed like mentioned before. Hence it is important to understand the finite element method as well as how it works.

The finite element method is a numeric process for acquisition of approximate solutions of many problems in engineering, mainly when all study phenomena are driven by differential equations which analytical solutions are very hard or even impossible to obtain. It is then needed to made numerical technical solution approaches which allow the replacement of the exact analytical solutions for numerical approximate solutions [127]. Nowadays it finds application in most engineering areas, such as structural, heat transfer, fluid mechanics, electromagnetism, etc.

FEM was not developed by just one individual, however some references have referred M. J.

Turner as one of those who made it possible and applicable to general structural analysis over the period 1950-1962. There are some other names that have made some important contributions to the development of FEM such as B.M. Irons, R. J. Melosh and E.L. Wilson [127].

FEM was later popularized by academicians and the finite element therm has first used by Clough in 1960. Most commercial FEM softwares are from or where developed in the early 1970 and they are Abaqus, Adina Ansys, Nastran, etc. In engineering analysis there are two types of methods for calculation, the classic methods (finite differences) and the numerical analysis (finite elements). The classic method has the exact and approximate solutions while the numerical methods uses the methods of energy, boundary elements, finite differences and finite elements.

There are two mathematical methods for boundary problems (most known methods), they can be classified in Rayleigh-Ritz method and residual formulation of Galerkin.

### 5.2.2 Finite element method - Steps and theory

There are three steps in the method of finite elements, pre-processing, processing and post-processing. Pre-processing is the model is prepared and understood, the definition of the problem and the domain, the discretization or division of the domain in elements, numbering of the nodes and elements, and to generate the geometrical properties. The processing is the phase for running the analysis, where the elements equations can be obtained, where the differential equations are solved with the increment of the boundary conditions and where the definition of a linear or non-linear system is defined. Post-processing is the final step in the determination of the second variables as well as the visualization of final results.

In the discretization phase the division of the domain of the solution in finite elements is performed either in one, two or three dimensions. The interaction points are known as nodes and the sides are called lines or nodal planes. As for the elements equations in order to approximate the solution of each element a two step phase is performed. First a right function is chosen with unknown coefficients which will be used to approximate the solution, then the coefficients are evaluated for the objective to approximate the solution in an optimum way.

The approximate functions are chosen since they are easy to manipulate, polynomials are used normally for this type of situations. For the uni-dimensional case a polynomial of first order, or a straight line. The equation can be seen below

$$u_x = a_0 + a_1 x \quad (5.2)$$

u(x) is the dependent variable and $a_0$ and $a_1$ are the constants, x is the independent variable. The function must pass through the values u(x) in the final points of the elements $x_1$ and $x_2$. So we can write

$$u_1 = a_0 + a_1 x_1 \quad (5.3)$$

$$u_2 = a_0 + a_1 x_2 \quad (5.4)$$

Where $u_1 = u(x_1)$ and $u_2 = u(x_2)$. Those equations can be solved using the Cramer rule, where:

$$a_0 = \frac{u_1 x_2 - u_2 x_1}{x_2 - x_1} \quad (5.5)$$

$$a_1 = \frac{u_2 - u_1}{x_2 - x_1} \quad (5.6)$$

This result can be used in the previous equation where after changing the therms we can write:

$$u = N1u_1 + N2u_2 \quad (5.7)$$

Where

$$N_1 = \frac{x_2 - x}{x_2 - x_1} \quad (5.8)$$

$$N_2 = \frac{x - x_1}{x_2 - x_1} \quad (5.9)$$

The former equations are called approximation function while N1 and N2 are called interpolation functions. It can be seen in equation 5.3 that the polynomial is a first Lagrange one. It allows to estimate the intermediate values between the values $u_1$ and $u_2$ by nodes. Linear equations helps the manipulation of differentiation and integration. The differential equation of 5.3 is:

$$\frac{du}{dx} = \frac{dN_1}{dx}u_1 + \frac{d_N 2}{dx}u_2 \quad (5.10)$$

According to equations 5.8, the derivatives of $N_1$ and $N_2$ can be obtained as:

$$\frac{dN_1}{dx} = -\frac{1}{x_2 - x_1} \quad (5.11)$$

$$\frac{dN_2}{dx} = \frac{1}{x_2 - x_1} \quad (5.12)$$

So the derivative of u is:

$$\frac{du}{dx} = \frac{1}{x_2 - x_1}(-u_1 + u_2) \quad (5.13)$$

Rewriting the equation, we get the divided difference. The full integral can be written as:

$$\int_{x_1}^{x_2} u dx = \int_{x_1}^{x_2} (N_1 u_1 + N_2 u_2)\, dx \quad (5.14)$$

Each them on the right side is the integral of a right angle triangle with a $x_2 - x_1$ base, it means

$$\int_{x_1}^{x_2} u dx = \frac{1}{2}(x_2 - x_1)\, u \quad (5.15)$$

The full integral is:

$$\int_{x_1}^{x_2} u dx = \frac{u_1 + u_2}{2}(x_2 - x_1) \quad (5.16)$$

This theory is known as the trapezoidal rule. In the processing phase, the equations result will consist in a group of linear algebraic equations, which can be expressed in the matrix form as:

$$[k]\,(u) = [F] \quad (5.17)$$

[k] is the rigidity matrix of the element, (u) is the column vector of the unknown values of the nodes. For this case the displacements vector while [F] is the column vector which reflects the effect of any external influences applied to the nodes, it is the forces vector. With this matrix form it is possible to solve most engineering problems of linear stress analysis. This type is used as the stiffness criteria like referred in figure 5.6.

The post processing is where the results are verified after running the analysis using the matrix with all the properties, mesh, boundary conditions loads etc. In this specific case the mooring system is a primary structure and shall no fail. It is a stainless steel structure connected each link to the next link from production. In the mooring system each mooring line has a singular load path being attached to a swivel or to a shackle.

### 5.2.3 Stiffness criteria

There will be performed both limit and ultimate analysis like referred before in linear static analysis or solution 101 of Nastran. The failure criteria are displacements, Von Mises stress equivalent and strain on metallic parts. The Von Mises stress equivalent on metallic parts is computed as:

$$\sigma_\nu = \left[\frac{1}{2}\left[(\sigma_x - \sigma_y)^2 + (\sigma_y - \sigma_z)^2 + (\sigma_z - \sigma_x)^2\right] + 3\tau_{xy}^2\right]^{\frac{1}{2}} \quad (5.18)$$

Von Mises strain is obtained thought the equation:

$$\varepsilon_\nu = \left[\frac{4}{9} * \left(\varepsilon_x^2 + \varepsilon_y^2 - \varepsilon_x\varepsilon_y\right) + \frac{1}{3}\gamma_{xy}^2\right]^{\frac{1}{2}} \quad (5.19)$$

The margin of safety for ultimate load is given by equation 5.20

$$M.S. = \frac{FTu}{Load} - 1 \quad (5.20)$$

And the margin of safety for limit load is given by equation 5.21

$$M.S. = \frac{FTy}{Load} - 1 \quad (5.21)$$

As long as the margin of safety for tension yield (ALS) is above 1.35, the result is acceptable. The margin of safety for tension ultimate (ULS) is acceptable above 2.50 [125].

### 5.2.4 Load sign convention and reference systems

This section presents the reference system as well as the conventions adopted for the structural analysis of the mooring lines.

- X - Is the axial direction of the load;
- Y - Is the perpendicular direction of the load in the horizontal plane;
- Z - Is the perpendicular direction of the load in the vertical plane;

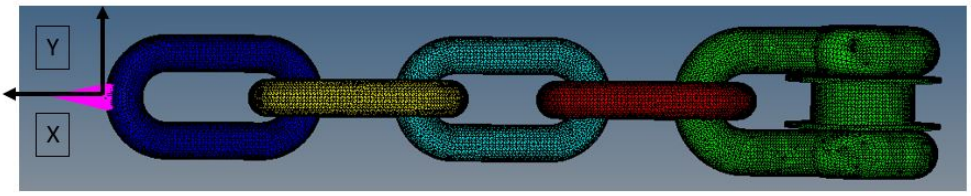


Figure 5.7: View 1 of load reference system

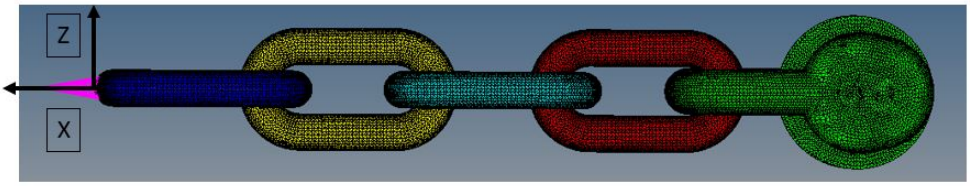


Figure 5.8: View 2 of load reference system

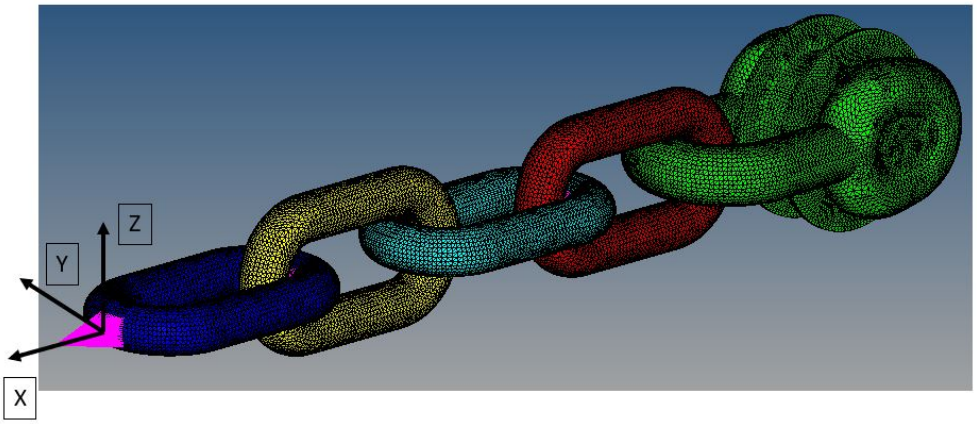


Figure 5.9: View 3 of load reference system

The load sign convention and the reference system can be seen in figures 5.7, 5.8 and 5.9.

### 5.2.5 Materials

The material of the mooring line links either studless or studlink are made of stainless steel. The used properties (from supplier) can be verified in table 5.1 and from table 3.3.

### 5.2.6 Software - Nastran & Altair

For the processing phase, Nastran is used. Nastran is a finite element analysis software initially developed for and by NASA for the United States aerospace industry. NASTRAN stands for Nasa Structural Analysis and the MacNeal-Schwendler Corporation was the main and active developers of the Nastran code. The first Nastran code was developed between 1960 and 1968 and several versions were released later and since 1990 a new updated version is developed and released every year. Nastran is the most used software in the aerospace industry according to some

Table 5.1: Material and properties (image from ref. [128])

| | | |
|---|---|---|
| Young Modulus | 200000.00 | MPa |
| Shear Modulus | 7700.00 | MPa |
| Poisson coefficient | 0.30 | N/A |
| Density | 7850.00 | $kg/m^3$ |
| R3 [Mpa] | Ftu | 690.00 |
| | Fty | 410.00 |
| R3S [Mpa] | Ftu | 770.00 |
| | Fty | 490.00 |
| R4 [Mpa] | Ftu | 860.00 |
| | Fty | 580.00 |
| R4S [Mpa] | Ftu | 960.00 |
| | Fty | 700.00 |

specialists, mainly for linear static and dynamic analysis.

On the other hand it is important to have a pre and a post processing software also known as a mesher. For the development of this thesis Altair software is going to be used. Altair was initially established in 1990 and the first product was Hypermesh. Later other important softwares were added to the Altair's package like FEKO, Hypermesh Acusolve etc.

### 5.2.7 FEM model description

After the design in CATIA V5 the model is opened in Hypermesh for treating the geometry, it is important to create the mesh to join all parts with same kind of material in the same collector. In the development of this work a 3D element analysis is performed due to its shape. The used elements are tetra10. Tetra10 elements are 3D elements of second order with 10 nodes. These type of elements are used when brick type elements can't be used. For studless link elements, bricks could be used, however for stud links these elements could not be used due to irregularities. For a matter of consistence both analysis have tetra10 elements. In figure 5.10 a tetra element of second order is show.

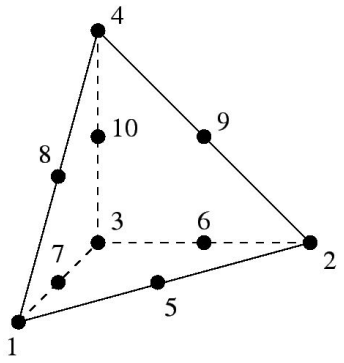


Figure 5.10: Tetra element of second order (image from ref. [128])

In the development of this study, there are six elements with the same property, there are four element links, a shackle and a swivel. The connection between nodes was made using node equivalence. In order to have an accurate result is it important to have a mesh convergence

of the FEM model. The six elements can be seen in 5.7. In order to have the best results the model is according to Hypermesh's standards and consideration, which means that the quality index is below 0.7 as it can be seen in figure 5.11.

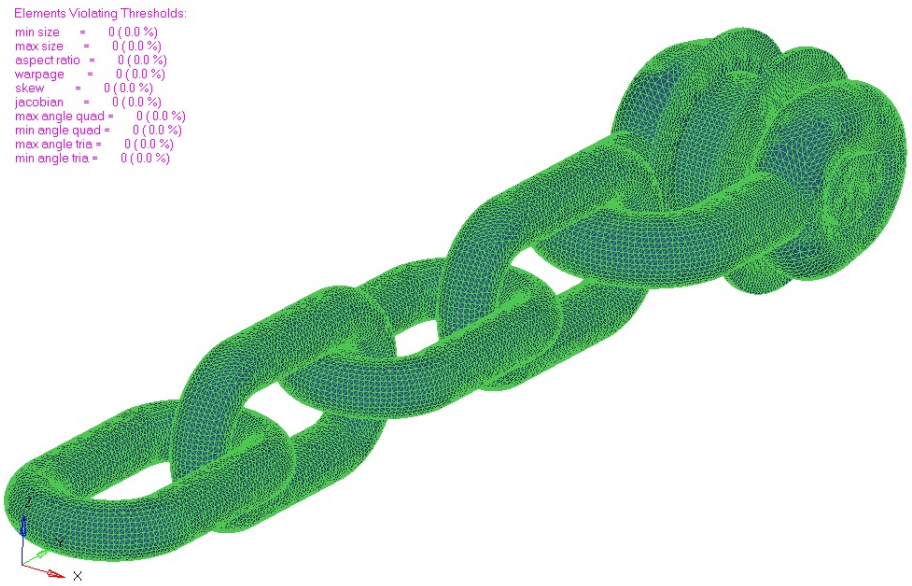


Figure 5.11: Quality index of the second order 3D elements

### 5.2.8 FEM Mesh convergence

In order to have a better precision in the results, the mesh convergence must be performed. There must be demonstrated that simulation converges to an accurate solution independent of the size of the mesh. Also two terms must be considered, convergence (number the elements per running time) and precision (in this case the tension is the convergence parameter).

For the convergence of the FEM model, it is necessary to determine the necessary number of elements independent of the size of the mesh assuring that the stress response (deformation, Von Mises, etc.) will converge. The element type is an agreement between the geometry size and shape, versus the time allotted for project. In the development of this work the process can be seen in table 5.2.

Table 5.2: FEM - Mesh Convergence

| FEM - Convergence and Mesh Independence | | | | | | | |
|---|---|---|---|---|---|---|---|
| FEA mesh | Case<br>N. of elements | 1<br>81437 | 2<br>98264 | 3<br>98844 | 4<br>118744 | 5<br>228278 | 6<br>660203 |
| FEA Results | Error offset<br>Solve time [s] | 4.99e-1<br>183 | 3.76e-1<br>300 | 1.10e-1<br>756 | 2.73e-3<br>1823 | 2.27e-5<br>2813 | 0.1e-7<br>4305 |

Through the use of the previous table, it can be decided the convergence per solved time ratio according to stress in the components. The mesh convergence can be seen in figure 5.12.

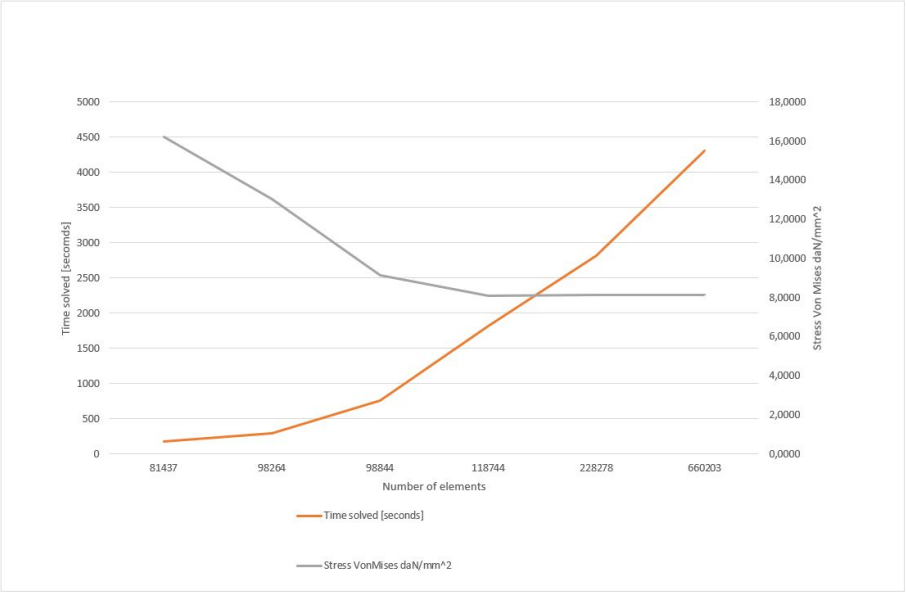


Figure 5.12: Mesh convergence Vs solved time (FEM)

From figure 5.12, for the specific case of the mesh convergence the best ratio of precision in the results per processing time is by using elements between 10 and 15 millimeters. Hence for all analysis this ratio will be used.

### 5.2.9 Connections, constraints and forces

The connection between the chain elements is performed through a rigid element, a RBE2 element. Each link is connected to another link through two rigid elements. These elements allow the connection between elements passing all loads equally distributed to the next one. It is however important not to consider the nodes and elements in which the rigid elements are connected since the stresses will be much higher due to the physical limitation of the rigid elements. The rigid elements are not dictated by stiffness, mass or forces, they have a linear relationship with non elastic displacements. Either stiffness, mass or loads at dependent degree of freedom transferred to independent degree of freedom.

In order to run the model in the linear solution, the model has to have all degrees of freedom constrained so to be possible to verify the displacements and stress in the proper component without major modulation errors. These constraints are known in Nastran as SPC or single point constraints. In this work since the main objective is the verification and analysis of the link elements, the constraints will be applied to the shackle, or/and in the mooring rope.

On the other hand the loads are used in this work through a card named force, which has its own axis system with direction and value according to the loads presented in the previous chapter. In figures 5.13 and 5.14 the rigid elements can be seen. In figure 5.15 the single point constraint can be verified while in figure 5.16 and 5.17 the force element can be checked.

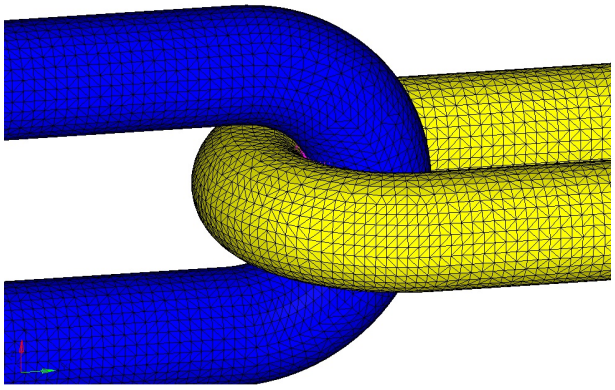

Figure 5.13: Rigid element between chain links

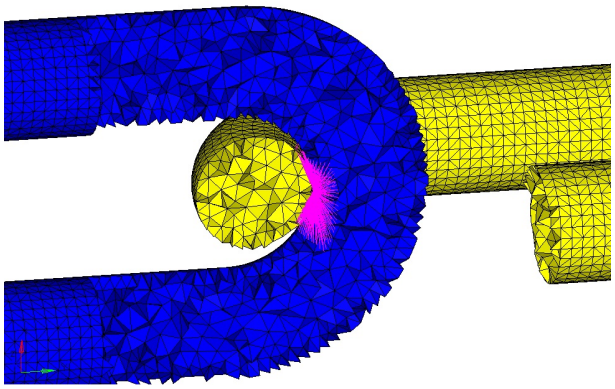

Figure 5.14: Detail of rigid element between chain links

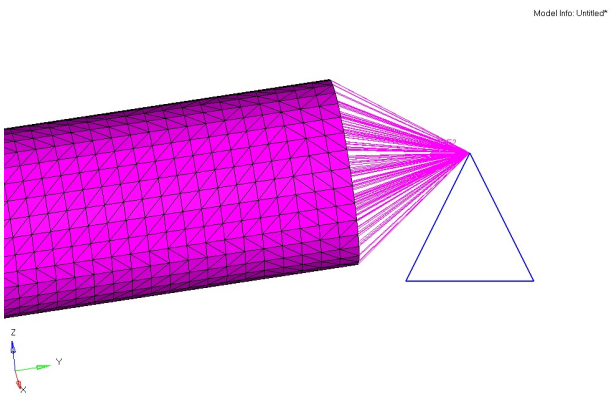


Figure 5.15: Detail of single point constraint

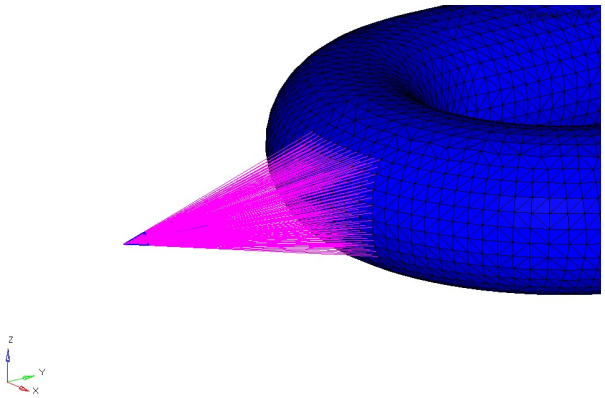

Figure 5.16: Force applied in the model

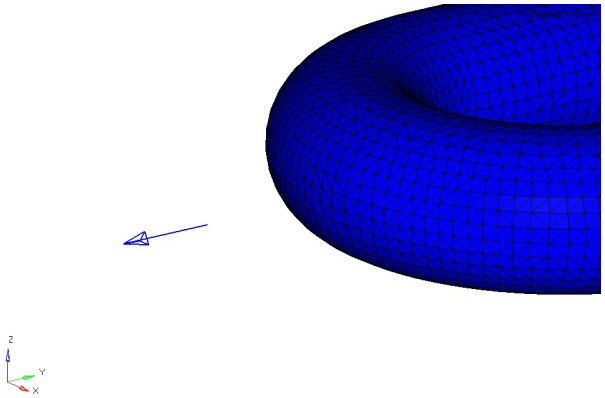

Figure 5.17: Detail of the force applied in the model

### 5.2.10 Results

The results are visualized with Hyperview software (Altair). The most important parameter is to verify if the chain can withstand the loads or not either for former mooring chain and for updated mooring chain. In order to be conservative, in all analysis the maximum load value in table 4.6 will be used.

Besides the normal stress applied in an element link it is also important to verify the points of interest in each link. So to understand how the load path on an element link is developed, three specific sections will be analyzed in detail. These sections are the most common sections in which the chain elements are known to break [70]. These three sections are known as straight, bend and crown section and they as can be seen in figure 5.18. These sections show the regions where there are the higher principal stresses results, as well as the potential fatigue life crack propagation direction.

Like mentioned before in this chapter only certain sections will be analyzed, the analyzed segments will be those which can withstand the most loads in the full length of the chain. Both former and optimized chains have 157 mm in segment 5 and the segment 4 has 152 mm for former chain and 137 mm for optimized chain, the analysis presented in this chapter will only

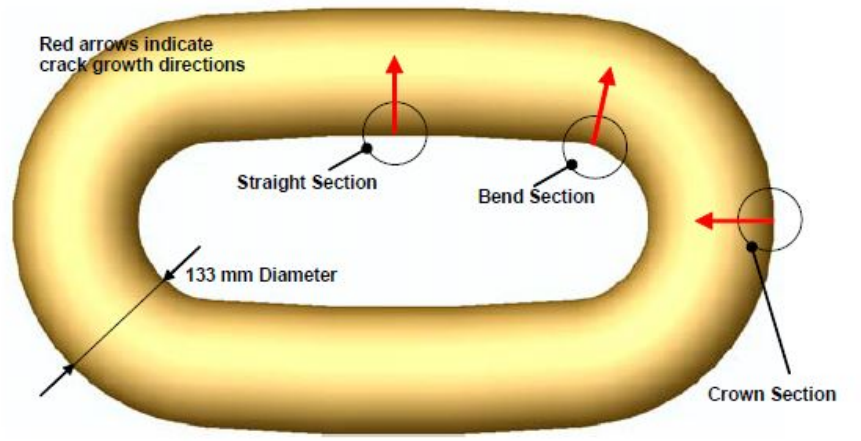


Figure 5.18: Hot spot stress locations (image from ref. [70]

analyze these three diameter chain size elements.

#### 5.2.10.1 Studless chain elements

The displacement of the 157 mm diameter studless chain can be seen in figure 5.19. As it can be seen it has a maximum displacement of 4.95 mm for operational load (limit load).

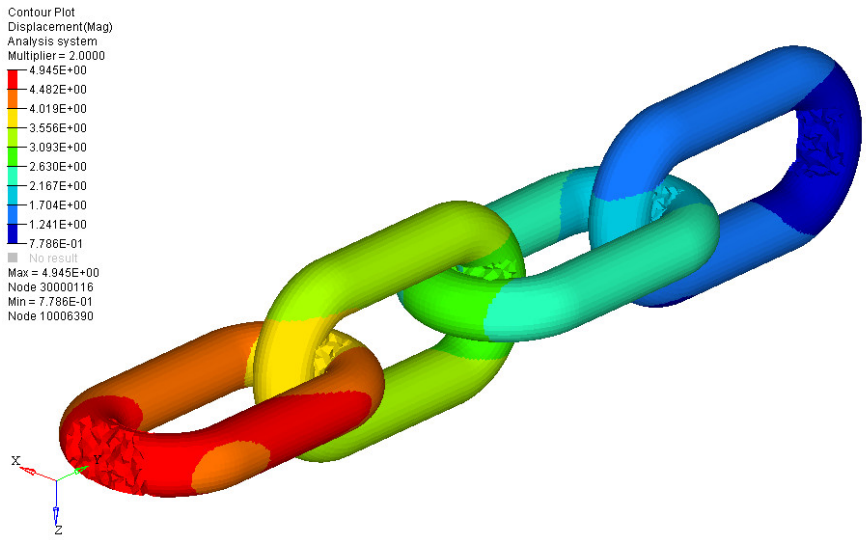


Figure 5.19: 157mm studless chain element link displacement

On the other hand the Von Mises stress approach on those elements have a limit load value of 281.80 MPa as presented in figure 5.20. Since the material is isotropic the analysis for ultimate condition is commutative. Considering that the chain is R4 and both ultimate and Yield allowables are according to table 5.1, we have a margin of safety for Yield of 1.05, while we have a margin of safety for ultimate of 1.03. As it can be seen the worst condition is for ultimate load stress. This analysis can be used for both former and updated mooring chain.

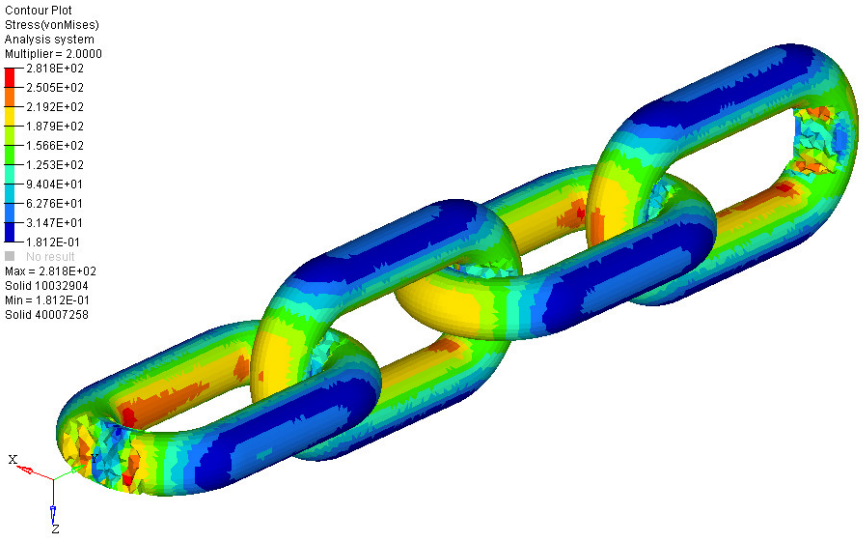


Figure 5.20: 157mm studless chain element link stress

For the displacement of the 152mm diameter studless chain elements (former chain), a total of 5.47mm was verified from figure 5.21 (for limit load). Once again it is important to understand that it already has a factor of two both in limit and ultimate analysis recommended by DNV.

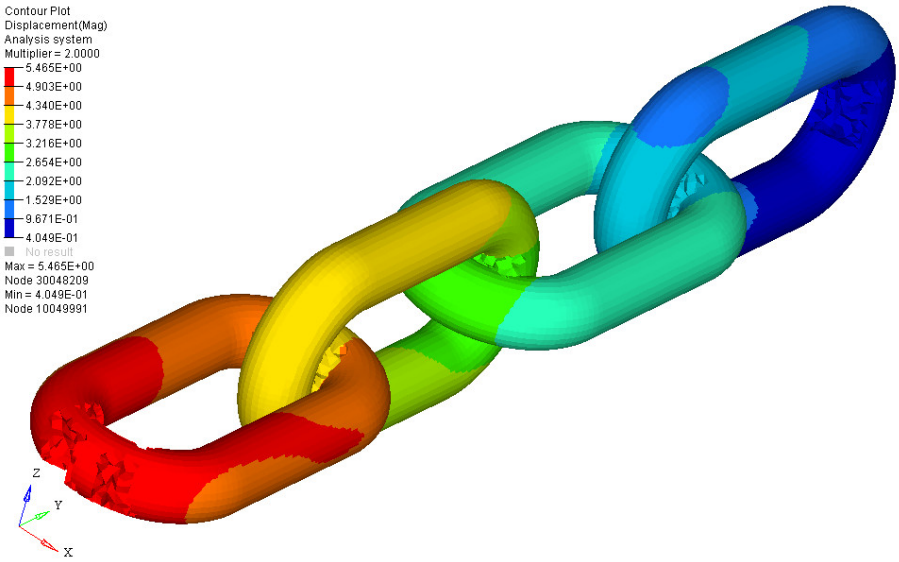


Figure 5.21: 152mm studless chain element link displacement

The stress for limit load of 152mm studless link chain elements have a value of 352.00 MPa. Assuming the same conditions as before, we have a Yield margin of safety of 0.65 while for Ultimate load we have a margin of safety of 0.63 as from figure 5.22.

The new studless chain for the updated mooring chain with 137mm of diameter has a displacement of 5.56mm as shown in figure 5.23.

Hence the updated mooring line with 137mm of link diameter has a margin of safety for limit state of 0.33 while for ultimate load it has a margin of safety of 0.31 (figure 5.24).

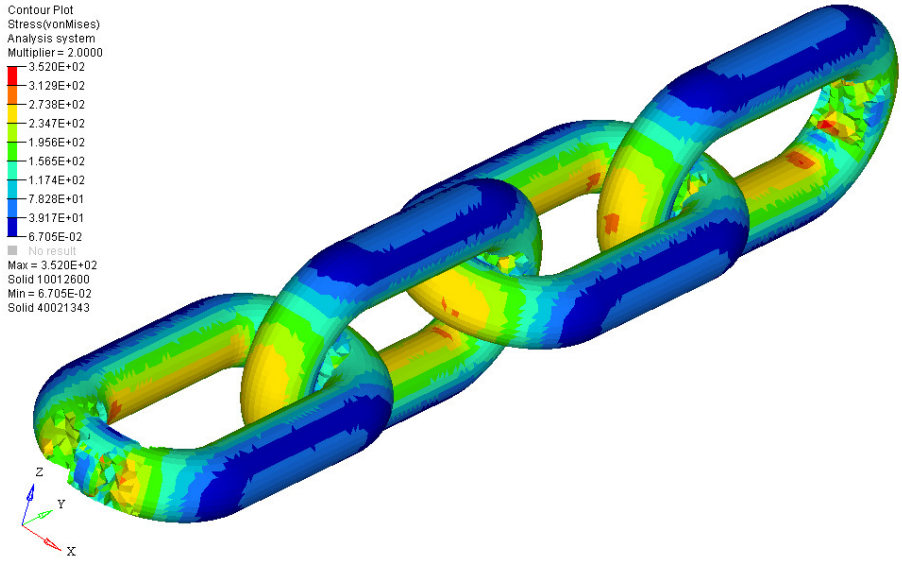


Figure 5.22: 152mm studless chain element link stress

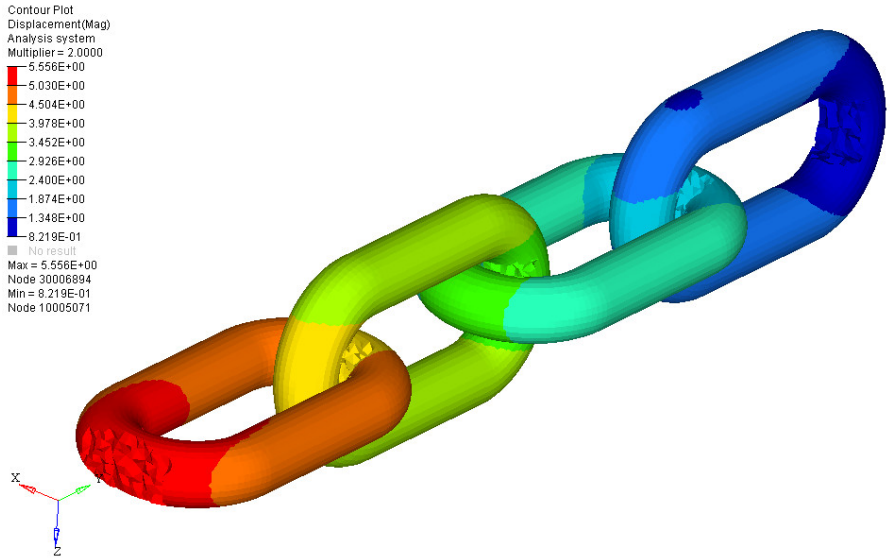


Figure 5.23: 137mm studless chain element link displacement

From the analysis, the chain can be changed for a new configuration with new sized mooring line links. Some elements were in contact with RBE2 type elements, these elements are rigid and they pass some nonexistent forces in the chain links.

#### 5.2.10.2 Stud link chain elements

One important study is to understand what would happens if the chain links were stud link elements instead of studless links. For this study the displacements are less important since the study is specific to analyze the margins of safety and how they vary with the same load as well as the load path itself. Since the final segment (157 mm) shall be the same, the comparison between studless and stud link elements was only performed for 152 mm and 137 mm.

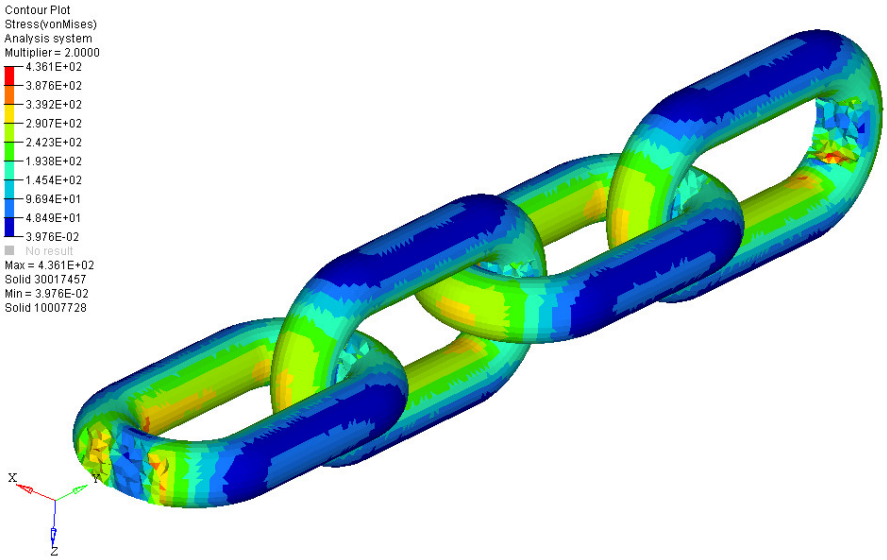


Figure 5.24: 137mm studless chain element link stress

The margin of safety for stud link element chain of 152 has a value of 298.30 MPa which means that for limit load the margin of safety if 0.94 while for ultimate load it has a value of 0.92. In figure 5.25 the stud link chain limit stress can be observed.

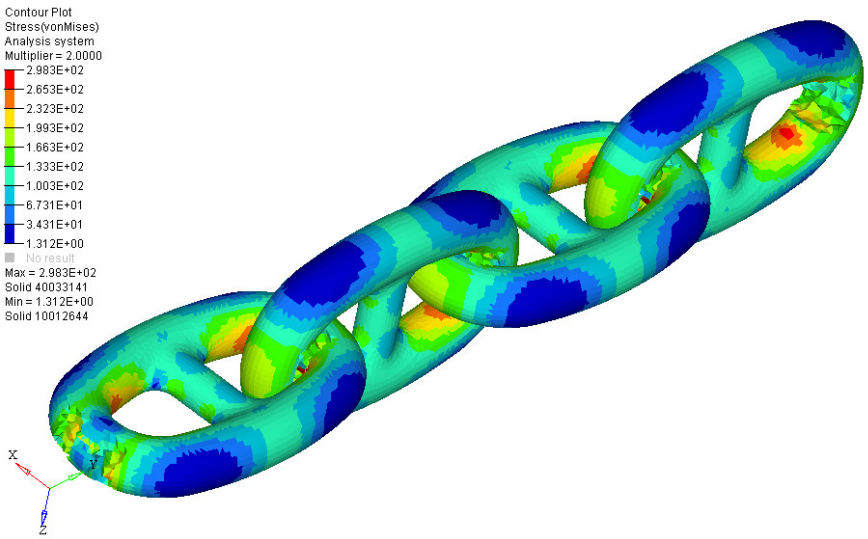


Figure 5.25: 152mm stud link chain element link stress

For the last stud link chain the margin of safety for limit load is 0.62 while for ultimate load it is 0.61. In figure 5.26 Von Mises stess for stud link chain type can be verified.

Hence we can verify that the margins of safety are very close for both chain as it can be seen in table 5.3

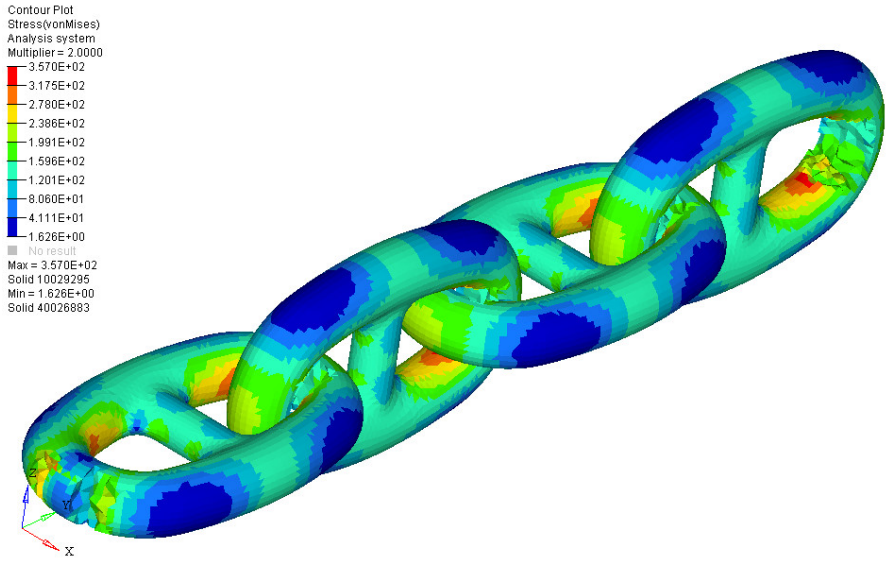


Figure 5.26: 137mm stud link chain element link stress

Table 5.3: Margins of safety - Studless Vs Stud link

| Diameter [mm] | L.L. studless | L.L. Stud link | U.L. studless | U.L. studlink |
|---|---|---|---|---|
| 137 | 0.33 | 0.62 | 0.31 | 0.61 |
| 152 | 0.65 | 0.94 | 0.63 | 0.92 |
| 157 | 1.06 | N/A | 1.03 | N/A |

### 5.2.10.3 Hot spot stress location

Like mentioned before, it is important to understand how the stress is influenced from the geometry of the element links. Within this context the center element link was analyzed in detail. These sections are important mainly for fatigue life estimation, in mooring chain the stress state in the chain dictates the fatigue performance due to the design tensions. In figure 5.27 the load path for a studless link can be verified.

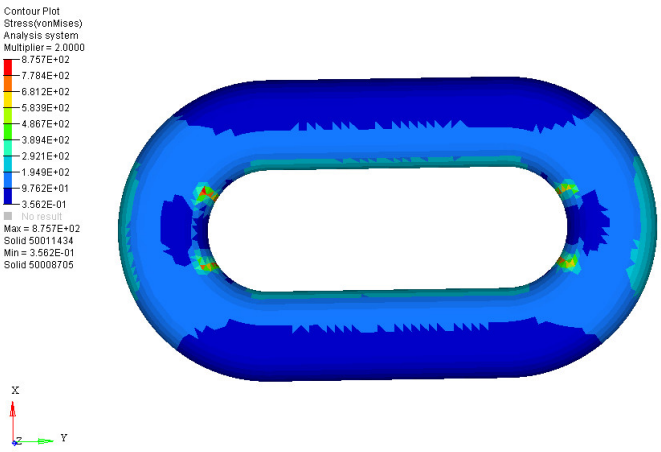


Figure 5.27: Central studless element link general load path

Here it is possible to conclude that if the force increases the element will tend to stretch and

the parallel bars will tend to join since they will both be heading to the center. However for stud link element the path will tend to a different direction as can be seen in figure 5.28. It is important to refer that the stress shall not be taken into consideration since the rigid elements are not considered for the analysis. This point is applicable to all load path analysis.

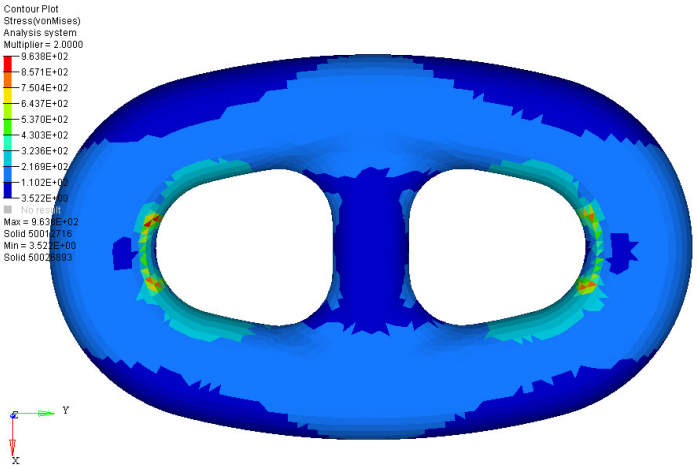


Figure 5.28: Central stud link element link general load path

Hence the load path is very different from the studless link. Since the stud is in the middle of the chain element, the bars will not tend to join between them, however there is a higher stress in the inner sections.

For the straight section it is o a major importance to understand the referred points discussed earlier. In figure 5.29 it is possible to verify that the inner section of the chain element link has a higher value of 203.14 MPa then the outer section with a lower stress value of approximately 40.00 MPa. Both top and bottom sections should be similar, however since the model is performed with 3D elements there are always same differences since the elements are not completely symmetric.

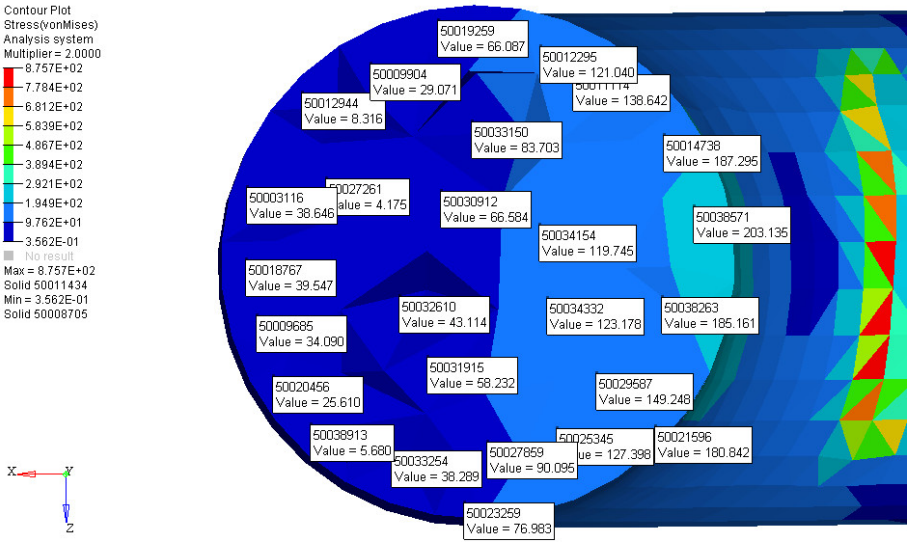


Figure 5.29: Straight section of a studless link element load path

The straight section of the studlink is a little different due to the stud link. As can be seen in figure 5.30, the inner section of the chain element has a much lower stress value, however the outer section is withstanding more load then the studless link chain element. Once again the model was expected to have the same stress level on both upper and lower section.

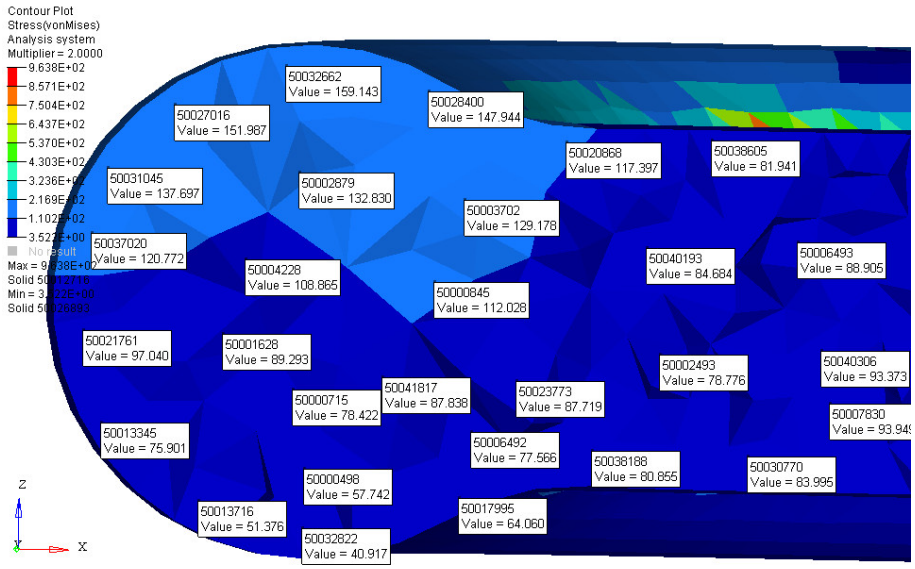


Figure 5.30: Straight section of a stud link element load path

On one hand the bend section, has a different condition. Both in figure 5.31 and in figure 5.32 the load paths can be verified.

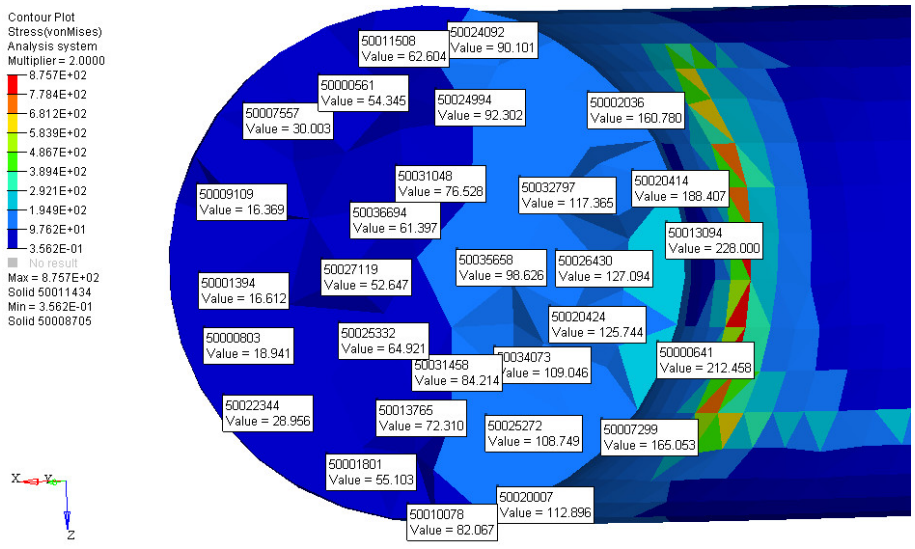


Figure 5.31: Bend section of a studless link element load path

The studless link has a central stress of 228.00 MPa at the inner section lower then stud link chain element 245.00 MPa, the same is valid for the outer section (16.61 MPa in the studless link and 43.72 MPa in the stud link element chain). Although the stud link has the central stud, the stress in the bend section is higher. This point is the critical point for stud link chains.

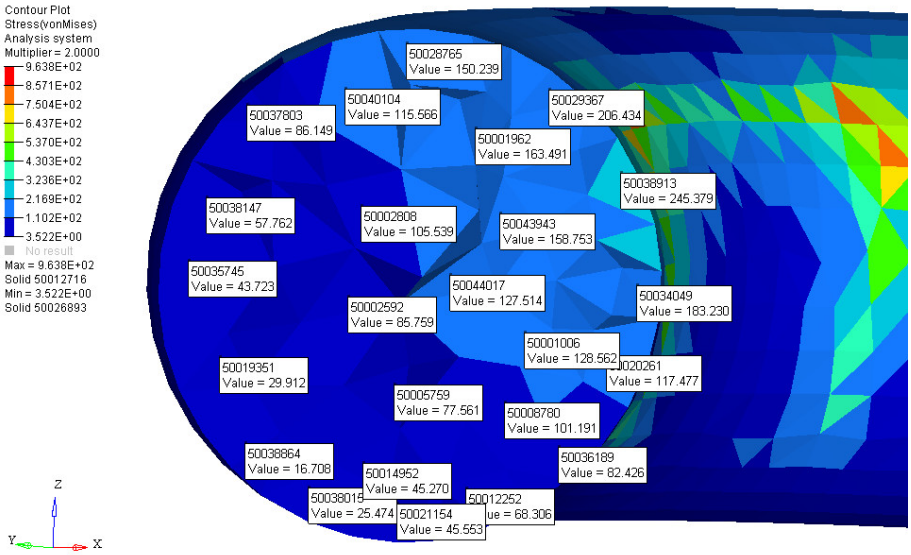


Figure 5.32: Bend section of a stud link link element load path

Finally the crown section is one of the main breaking sections where crack propagation occurs. The load path of the studless link can be seen in figure 5.33 while the load path for stud link can be seen in figure 5.34.

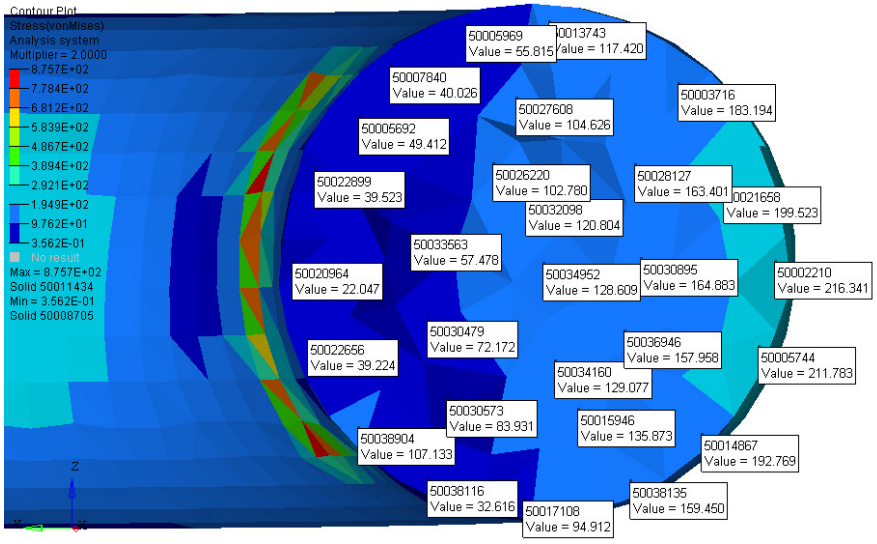


Figure 5.33: Crown section of a studless link element load path

The inner section of the studless chain element link has a lower value 22.05 MPa while for the stud link chain element the stress has a value of 80.68 MPa. The outer section of the studless link has a much higher load 216.34 MPa while the stud link reaches a maximum value of 171.43 MPa.

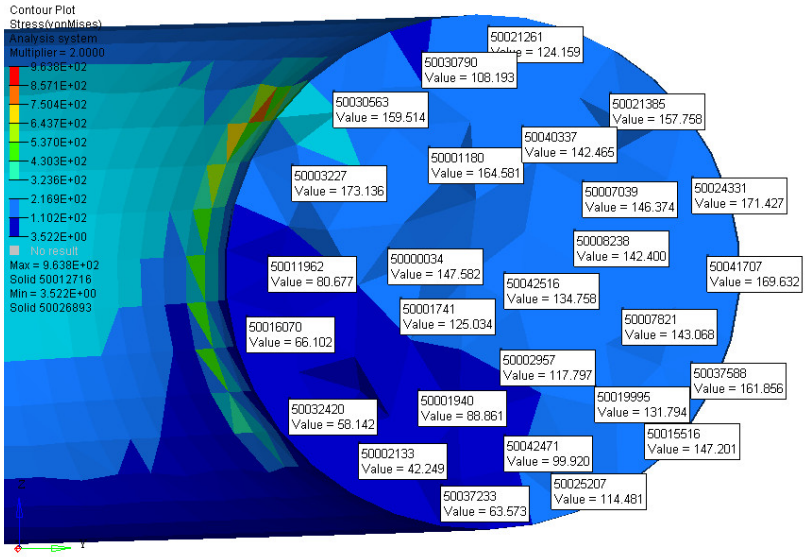


Figure 5.34: Crown section of a stud link link element load path

### 5.2.11 Fatigue life

For the design of fatigue life, it is important to understand how many cycles will the chain have before maintenance operations. Hence it has a major importance to refer that this analysis where performed for the worst case condition of the FPSO. The environmental conditions where the most harsh possible, this means that this condition can happen once in a 50 years period. For the fatigue life an expected value of 30% [41] lower then the worst case condition is assumed (this value was verified by comparing same authors, and DNV rules examples).

The fatigue analysis is based on S-N data. The design based on S-N curves are obtained from fatigue tests. The S-N curves are based on DNV-RP-C203 [129]. The curves are based on the mean value minus 2 times the standard deviation of experimental data. They assumed a probability of 97.7% that failure will not occur.

The typical SN curve is given by:

$$\log(N_t) = \log(\bar{a}) - m\log(\Delta\sigma) \quad \textbf{(5.22)}$$

Where $N_t$ is the number of cycles to failure stress range $\Delta\sigma$, m is the inverse negative slope of the S-N curve design and $\bar{a}$ intercepts the design curve with the logarithmic (N) axis. The stress range (nominal) applied to a chain link is equal to the external force (load) divided by the cross area of the chain element link.

The fatigue life shall be considered according to figure 5.35.

For the calculation of the fatigue life of the mooring chain elements the stress loads are in table 5.4.

The studless chain will have between 30000 and 100000 cycles, while the stud link chain will

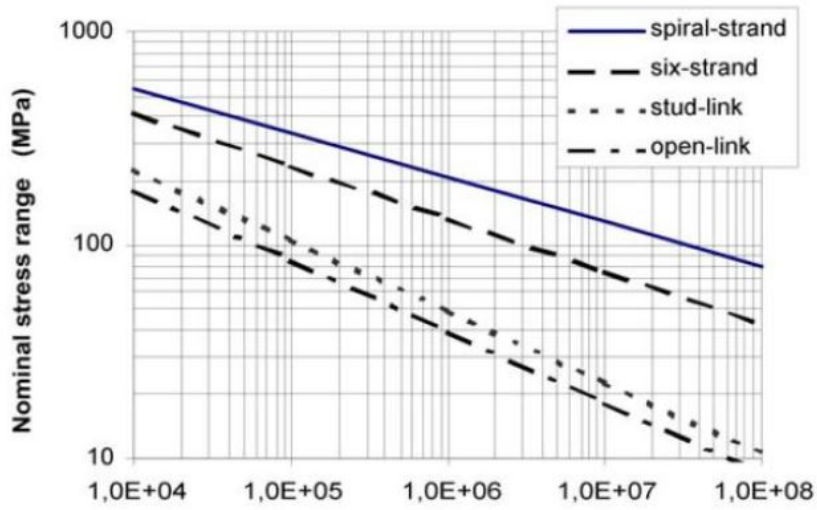


Figure 5.35: Cycles to failure (image from ref. [31])

Table 5.4: Fatigue life - Loads

| Diameter [mm] | S.less Stress[MPa] | S.Less 30% Stress[MPa] | S.link Stress[MPa] | S.Link 30% Stress[MPa] |
|---|---|---|---|---|
| 137 | 436.10 | 130.83 | 357.00 | 107.10 |
| 152 | 352.00 | 105.60 | 298.30 | 49.49 |
| 157 | 281.80 | 84.54 | N/A | N/A |

have between 80000 and 150000, which means that none of the chains will have infinite life (above 1000000 cycles).

## 5.3 Conclusions

The main objective of this chapter was to verify if the new configuration of the updated mooring lines could withstand all the loads. In this context the design and structure analysis were performed.

In the structural design phase, the design considerations were verified as well as the typical criteria for the FEM analysis. The critical elements were understood and the element links were designed according both to DNV and standard aeronautical best practices. For the structural analysis the FEM process was detailed and the theory was explained.

At the end of the chapter both displacements and Von Mises criteria stress were obtained for the updated studless chain. However a detailed comparison between studless and stud link element chain was performed. This study allowed to understand if the load path was critical for studless chain elements since these type of elements is lighter then stud link chain elements.

Since most chain elements breaks in one of the three main sections, a detailed analysis on those sections were performed as well. At the end of the chapter it was possible to understand that the studless link are lighter and cheaper then stud link mooring lines and can withstand the loads for the analyzed case. It is important also to mention that smaller margin of safety will

occur for the smaller diameter as expected. The results shown that the stud link has a higher margin of safety then the studless chain.

At the end of the chapter the results were verified and conclusions were taken. In the next chapter a full conclusion of the thesis itself will be performed and both difficulties and next work will be detailed.

# Chapter 6

# Conclusions & Final remarks

In the previous chapter both design and stress analysis were performed in critical segments so to verify if the new updated chain could withstand all the loads from the new system. So, the last chapter consisted in applying the design rules in the elements as well as all the theory beneath the structural finite element method simulating the chain itself.

After all critical points were analyzed, results were observed and margins of safety were taken. Conclusions regarding the comparison between studless and stud link were achieved and the implementation of the new mooring system was considered to be necessary for a further optimization of FPSO's. Hence this new chapter intends to perform the final conclusions, the recommendations for future work, the difficulties verified along the work and finally the publications performed during the dissertation time.

## 6.1 Conclusions

This subsection presents the main points of this dissertation, focusing on the contribution of performing a validation and optimization process in the design of a FPSO vessel mooring lines. Since the main objective was to have an efficient and continuous systems less expensive then the former one.

During the development of this thesis, summarized information was referred alongside the dissertation with partially conclusions performed at the end of each chapter.

### 6.1.1 Summary of the thesis

On the first chapter is was presented the main basis of the theme alongside with the importance of understanding the complete sequence of events, requirements and components involved in the oil and gas industry, focusing on the mooring system. The motivation beneath this theme was explained with main head set with the European commission objectives for the next years. It was verified the need to explore the sea industry in order to have a competitive, modern and updated role in the European blue economy.

The objectives were explained and understood either for the specific case of the Schiehallion field or for the Portuguese sea business development. Opportunities were explained and at the end of the chapter an outline of the thesis was performed.

In chapter two, a macro description of the problem was detailed together with the latest developments of this field of expertise. The evolution of the energy consumption was explained and the old but normal dependence of oil and gas was verified. The general concepts of the

oil and gas industry was detailed and the main components for oil and gas extraction were detailed. The oilfield was mentioned for a better comprehension of the main causes for the need to replace the old FPSO for the new one from the oilfield recent discoveries to FPSO storage capacity.

Then the mooring system was explained and environmental conditions were detailed. The constraints of the in situ location lead to the mooring line individual components such as chain or wire ropes. The calculation process for waves, wind and current was understood and then the state of the art for mooring systems was detailed with the latest developments in this field.

Chapter three started with the mooring analysis. Initially, the vessel characteristics were understood and the loads in the structure were obtained. The statics of a mooring line was explained and maximum structural design conditions were detailed. Then two concepts were presented, the quasi-static both in frequency and in time domain, with this information it was possible to understand the loads in the structure.

The theory behind the catenary equation was detailed either for inelastic and elastic mooring systems. Hereafter a system with five segments was detailed and equations were developed. For the dynamic of the mooring lines, the equations of motion were detailed again for frequency and time domain. At the end of the chapter the analysis in Orcaflex was performed taken into consideration the initial limitations and assumptions, boundary conditions, constraints and loads. An explanation of the model in the software Orcaflex was performed alongside with elements types and before obtaining the results, a mesh convergence was performed in order to reduce computational time regarding results accuracy. Then conclusions were taken.

In the fourth chapter the optimization of the mooring line was developed. Initially the mooring costs were detailed in order to justify the need for this subject. The requirements and opportunities were identified and the optimization took place. Both methodology and Matlab software was detailed and assumptions were taken. At the end of the chapter, the results shown the optimization process and the difference in the expenses for former and updated mooring systems. Through this information a paper was published in conference.

In chapter five there was a need to check in detail, if the new mooring system would withstand all loads or not. Hence in this chapter the structural design was performed. Design specification, criteria and loads were identified and the specific location for the detailed analysis was identified. Then with software CATIA V5 the design phase took place.

Later in the chapter the structural analysis begun. Initially the main points for structural analysis were verified and the finite element method was explained. The steps for FEM were analyzed and the theory was considered. The FEM model was performed and the simulation was explained from load sign convention, materials, conditions, properties to the detailed description of the model.

Later, the results were detailed either for studless or stud link elements and after the identification of the hot spot for stress locations the results were compared. Fatigue life for the new components was obtained as well as margins of safety.

### 6.1.2 Effective conclusions

The main objective of this thesis was to developed a mooring line optimization for the FPSO Glen Lyon in the Schiehallion field. It was of a major importance to implement a methodology to reduce the costs in the development of a new an updated mooring system. It was a major importance to apply new studies for further development in areas in which the European commission considers to be of a major priority for the development of Europe sea business known as blue economy. It was as well an objective to to be able to pass this knowledge to further projects in other industries other then oil and gas.

Within this context, this study proved to be an efficient study for further implementation in oil and gas industry in the Schiehallion field and for FPSO Glen Lyon. It was possible to verify that the objectives of this study were achieved since the proposed mooring system would be less expensive than the previous one, having both margins of safety and vessel offset next to the actual mooring system fulfilling the norms and standards of the industry.

As it could be verified the real offset is 61.2 meters while the equivalence in Orcaflex software (first analysis) was 58.4 meters. The optimized mooring system has an offset of 59.7 meters which validates the optimization from the offset point of view.

In terms of mooring chains, it could be verified that even for a safety factor of 2 applied at the mooring line that withstood the most harsh loads, it had a margin of safety of 0.33. It could be also verified that bend section is the section most likely to break. At the end of the optimization it can be verified that the new mooring system is 14.8 million euros less expensive than the previous mooring system which validated the purpose of this dissertation.

It was verified also that the most probable breaking criteria would be due to fatigue life. Since the loads were high the fatigue would be faster. If the chain element diameters were higher, the model mooring system would be able to withstand more cycles.

This study can be implemented in the Glen Lyon mooring line, however since the actual mooring system is already installed it does not make sense to implement it, except for new mooring lines. The mooring lines are known to break every 8 to 10 years. This study is valid for any FPSO but it shall be performed before the installation. Nowadays, the mooring system engineering plan intends to be the most conservative one, however the costs implemented are higher and the industry is known to have very high incomes, so the conservative approach is used.

Since the European commission identified the Europe's new opportunities and job-creation potential in the blue economy, this study can be applied to four of the five major value chains sectors, blue energy aquaculture, marine coastal and cruise tourism and finally marine resources. This study can be used in all of this sectors since for all of them requires the use of complex mooring systems. This study can be used for further developments of the Portuguese industry. It is important to realize that with the extension of the Portuguese platform shelf, more and more jobs and incomes can come from the Portuguese sea activities. In a country with more then 90% of national territory in the sea it is of a major importance to develop it.

Portuguese companies like CEIIA, Ocean Scan, Abyssal OS, institute of system and robotics etc., can benefit from this study implementing their products and studies in the ocean saving costs

in the development of new surface platforms and facilities. Summarizing, the new optimized mooring system was developed, the chain elements path loads were identified and the industry norms were fulfilled. At the end of this work all objectives were achieved.

Both steps and methodology involved in the design of this work, can be used for further mooring developments saving capital expenditures.

### 6.1.3 Difficulties and limitations

There were several limitations during the development of this thesis. First and furthermore the first identified limitation was the acquisition of precise information. This industry is very strict in releasing information out of the industry level, this lead to older information and difficulty to validate the study.

Although there is a lot of information about the subsea industry, the mooring system is always performed in the same form. This mean that for the segmented mooring line, the calculus process was very difficult to implement since almost all information regarding a mooring line with several segments was not able to be obtained.

Other difficulty found during this work was the data from the vessel, for a most accurate analysis of the vessel, it would be necessary to use one other software and analysis to obtain with better precision the vessels RAO's since they were calculated by mathematical models. For a accurate analysis this result could be given by an hydrodynamic software, e.g. Ansys Fluent.

The script in Matlab was difficult to implement since the equations were all for a unique line instead of a set of segments. This study have some limitations too, since it worked with several variables, one of them was the full length of the mooring line. With less variables the result could be preciser in terms of final capital expenditures, a study to verify this situation would be needed beforehand.

In the structural analysis chapter, one of the limitation was the connection between one link to the other. Hence it was used a rigid element, however one other type of contact would be preferable instead of an RBE2. This rigid elements passed forces to the structure and it does not allowed a proper connection between the elements, however since the main objective was to developed a full system it took less importance. It would be of major importance to try a new software that took in consideration the friction between elements. It would be beneficial to have a more simplified connection element. Nastran does not have this type of element as far as the author knows.

The main difficulty in the development of this work is the validation part. For a proper validation it would be necessary to have physic tests, however due to the involved costs this validation does have been performed. It would be necessary to have a tank with capacity to have an FPSO connected to twenty mooring lines and connected to twenty four risers besides the environmental conditions. Even for a very small model, the test would not allow a proper comparison with the actual system due to some considerations mentioned in DNV norms.

### 6.1.4 Future work

This thesis was characterized to study and implement a new updated mooring system for the FPSO Glen Lyon in the Schiehallion field. For future work the author would suggest the following objectives:

- Perform a study just for the FPSO response amplitude operators. This study would be very important since it would allow to minimize the errors, this type of study would help to understand if there were any other factors involved in the model that would affect the turret in the FPSO. A study for the turret itself would be important to understand how much load the vessel will eventually pass to the mooring system.
- To perform a bench test for validation. This test would have a complex system, however the involved costs would be very high. These tests would only be possible with the collaboration of oil and gas related companies.
- It would be of a major importance to apply this methodology for other projects different then oil and gas related projects. For example in the development of this work the author worked in a project to Portuguese fish farm and the methodology was applied. Since this project was required by a contractor it cannot be released to an academic level. It would be of a major importance to have a study of this type for fish farms for salmons, meagre, seabass, tuna, etc.
- A FEM study regarding a new updated version for the contacts of the link elements would be very important since it would have some very important factors there are not performed yet so far, at least found by the author. It would be necessary to try new software for this connection type, maybe Radioss, LS Dyna, Abaqus or Optistruct.
- It would very important to perform a FEM study regarding the whip effect in the mooring line when the elements touch the seabed. Due to waves and currents the mooring system is always being pushed in this harsh cycle. Most of the mooring lines breaks in those precise elements. It would be important to understand this factor and how it can be avoided.
- This study was only used for a single worst case conditions, it would be important to perform the study for the standard in situ normal conditions, this is believed to rise the margins of safety of the elements.
- The chain elements are only used for tension, hence it would be important to study the effects of the tension with bending moment. Since the mooring line acts as a catenary it means that it has tension plus bending effects from cable reel.
- It would be very important to perform this study for aquaculture in two locations in Portugal, near the cost of Aveiro and at Madeira island.

## 6.2 Publications during this work

During the four years of the development of this work some papers were published either for this specific theme either for other themes. Some of them as main author, others as secondary author.

### 6.2.1 Publications dissertation related

- P. Figueiredo, F. Brójo, ”Optimization of FPSO Glen Lyon mooring lines from vessel positioning to detailed stress analysis”, International meeting on marine research, IMMR2018;
- P.Figueiredo, F.Brójo, ”Parametric study of multi-component mooring lines at catenary form in terms of anchoring cost”, $4^{th}$ International conference on energy and environmental research, ICEER2017;

### 6.2.2 Publications dissertation non related

- P. Ferreira, P. Figueiredo, A. João, A. Guerman, F. Dias,”Project and Validation of a Magnetic Field Generator for MECSE CubeSat under Controlled Environment” , III Latin American cubesat, LACW2018
- A. Azevedo, J. Monteiro, P. Figueiredo, T. Rebelo, A. João, A. Guerman, F. Dias, ”MECSE: Cubesat Mission Aiming to Measure and Manipulate the Ionospheric Plasma Layer”, $4^{th}$ IAA Conference On University satellite missions and cubesat workshop, IAA2017;
- A. Azevedo, J. Monteiro, P. Figueiredo, T. Rebelo, A. João, A. Guerman, F. Dias, ”Mission Analysis and Conceptual Design of MECSE Nanosatellite”, $10^{th}$ Pico and nano satellite workshop, IAA2017;
- P. Figueiredo, F. Brojo, ”Theoretical analysis of ammonium-perchlorate based composite propellants containing small size particles of boron”, $4^{th}$ International conference on energy environment research, ICEER2017;
- D.Brandão, P. Figueiredo, T. Rebelo, ”CFD Analysis of Axisymmetric Nose and Tail Configurations of an Autonomous Underwater Vehicle”, $11^{th}$ European fluid mechanics conference, EFCM11;

# Bibliography

[1] Y. Bai and Q. Bai, *Subsea engineering handbook*, G. P. Publishing, Ed. Gulf Professional Publishing, 2012. 1, 7, 9, 10, 13, 28

[2] T. E. E. COMMUNICATION FROM THE COMMISSION TO THE EUROPEAN PARLIAMENT, THE COUNCIL, S. COMMITTEE, and T. C. O. T. REGIONS, "Blue growth - opportunities for marine and maritime sustainable growth," EUROPEAN COMMISSION, Tech. Rep., 2012. 2, 3, 4

[3] C. Europeia, "Plano de ação para uma estratégia marítima na região atlântica para um crescimento inteligente, sustentável e inclusivo," Comissão Europeia, Tech. Rep., 2013. 2

[4] BP, "Schiehallion and loyal decommissioning programme phase i environmental and socio-economic impact assessment," BP Exploration Operating Company Limited, Tech. Rep., 2012. 4, 14, 15, 16

[5] Statistica, "Statistic - global crude oil demand," Internet, June 2006. [Online]. Available: https://www.statista.com/statistics/271823/daily-global-crude-oil-demand-since-2006/ 8

[6] H. Devold, *Oil and gas production handbook: an introduction to oil and gas production*. Lulu. com, 2013. 9, 11

[7] BP, "Schiehallion and loyal decommissioning programmes phase i," BP Exploration Operating Company Limited, Tech. Rep., 2013. 14, 15, 16, 82

[8] T. P. Ha, "Frequency and time domain motion and mooring analyses for a fpso operating in deep water," Ph.D. dissertation, Newcastle University, 2011. 14, 16, 18, 19, 44, 49, 59

[9] BP, "Schiehallion and loyal decommissioning programme phase i decommissioning comparative assessment," BP Exploration Operating Company Limited, Tech. Rep., 2012. 15, 17

[10] ——, "Schiehallion and loyal decommissioning programme phase i - decc inventory list," BP Exploration Operating Company Limited, Tech. Rep., 2013. 15, 20

[11] ——, "Quad 204 project - environmental stateman," BP Exploration Operating Company Limited, Tech. Rep., 2010. 18, 19

[12] [Online]. Available: https://www.offshore-technology.com/projects/schiehallion/ 18

[13] BP. (2017) 19

[14] [Online]. Available: https://www.offshore-mag.com/articles/print/volume-77/issue-8/european-update/bp-advancesbrownfield-technologywith-quad-204-start-up.html 20

[15] KBR, "Glen lyon fpso," BP Exploration Operating Company Limited, Tech. Rep., 2015. 19

[16] BP, "Scope of work for 'proof of concept' mooring design," BP Exploration Operating Company Limited, Tech. Rep., 2008. 20, 23, 24, 27, 28, 31, 32, 35, 36, 37, 68, 70, 143, 144, 145

[17] N. Barltrop, *Floating structures: a guide for design and analysis. vols. 1 and 2*. Oilfield Publications Ltd, 1998. 21, 37

[18] M. Isaacson and O. Nwogu, "Wave loads and motions of long structures in directional seas," *Journal of Offshore Mechanics and Arctic Engineering*, vol. 109, no. 2, pp. 126–132, 1987. 21

[19] P. Ruol and L. Martinelli, "Wave flume investigation on different mooring systems for floating breakwaters," in *Coastal Structures 2007: (In 2 Volumes)*. World Scientific, 2009, pp. 327–338. 21

[20] [Online]. Available: https://www.offshore-mag.com/articles/print/volume-70/issue12/top-5-projects/petrobras-cascadechinook-inaugurate-fpso-production-in-gom.html 22

[21] [Online]. Available: http://www.dyna-mac.com/about-us/corporate-milestones/ 22

[22] K. A. Ansari, *Mooring Dynamics of Offshore Vessels*, S. of Engineering, Ed. Gonzanga University, 2008. 24

[23] E. Bjørnsen, "Chains in mooring systems," Master's thesis, Institutt for konstruksjonsteknikk, 2014. 25, 46

[24] B. Zanuttigh, L. Martinelli, and M. Castagnetti, "Screening of suitable mooring systems," Alma Mater Studiorum Universita Di Bologna, Tech. Rep., 2012. 25, 27, 29

[25] API, "Design and analysis of station keeping systems for floating structures," API - American Petroleum Institute, Tech. Rep., 2005. 25, 26, 29, 52

[26] CENTEC, "Mooring and anchoring systems mooring line dynamics," centre for Marine Technology and Ocean Engineering. 26

[27] W. J. Harris R.E., Johanning L., "Mooring systems for wave energy converters: A review of design issues and choices," *Heriot-Watt University, Edinburgh,*, 2004. 28, 41

[28] Y.-H. Kuo, "Suction pile installation applications utilizing predicted and real-time monitores suction pressures," 2015 Science, Engineering & Technology Seminar, June 2015. 28

[29] CENTEC, "Mooring and anchoring systems mooring failures," centre for Marine Technology and Ocean Engineering. 28

[30] [Online]. Available: https://intermoor.com/information-center-23/press-releases24/intermoorwins-designfabrication-installationand-hookup-contract 29

[31] D. N. Veritas, "Position mooring;," DET NORSKE VERITAS, Tech. Rep., 2009. 29, 42, 52, 53, 87, 88, 104, 127

[32] ——, "Offshore mooring chains," DET NORSKE VERITAS, Tech. Rep., 2009. 29

[33] ——, "Offshore mooring fibre ropes," DET NORSKE VERITAS, Tech. Rep., 2010. 29

[34] ——, "Offshore mooring steel wire ropes," DET NORSKE VERITAS, Tech. Rep., 2009. 29

[35] B. Veritas, "Fatigue of top chain of mooring lines due to in-plane and out-of-plane bendings," Bureau Veritas, Tech. Rep., 2014. 29

[36] API, "Recommended practice and design offshore mooring," American Petroleum Institute, Tech. Rep., 2001. 29

[37] I. S. Organization, "Petroleum and natural gas industries — specific requirements for offshore structures - part 7 - stationkeeping systems for floating offshore structures and mobile offshore units," International Standard Organization, Tech. Rep., 2013. 30, 53

[38] ——, "Ships and marine technology — stud-link anchor chains," International Standard Organization, Tech. Rep., 2008. 30

[39] S. Norsok, "Materials selection," Standard Norsok, Tech. Rep., 2004. 30

[40] ——, "Structural design," Standard Norsok, Tech. Rep., 2004. 30

[41] ——, "Collection of metocean data," Standard Norsok, Tech. Rep., 1997. 30, 35, 44, 126

[42] ——, "Design of steel structures," Standard Norsok, Tech. Rep., 1998. 30

[43] Y. Bai, *Marine structural design*. Elsevier, 2003. 31, 91, 101

[44] D. C. Grant, "Advances in metocean design criteria from the 1970s to the present day," CSci, Tech. Rep., 2014. 33

[45] C. L. Bretschneider, "Wave variability and wave spectra for wind-generated gravity waves," CORPS OF ENGINEERS WASHINGTON DC BEACH EROSION BOARD, Tech. Rep., 1959. 32

[46] W. J. Pierson and L. Moskowitz, "A proposed spectral form for fully developed wind seas based on the similarity theory of sa kitaigorodskii," *Journal of geophysical research*, vol. 69, no. 24, pp. 5181–5190, 1964. 32

[47] K. Hasselmann, T. Barnett, E. Bouws, H. Carlson, D. Cartwright, K. Enke, J. Ewing, H. Gienapp, D. Hasselmann, P. Kruseman *et al.*, "Measurements of wind-wave growth and swell decay during the joint north sea wave project (jonswap)," *Ergänzungsheft 8-12*, 1973. 32

[48] J. A. Ewing, "Wave prediction: Progress and applications," *6th International Ship Structures Congress, Boston*, 1976. 32

[49] S. K. Chakrabarti, *Hydrodynamics of offshore structures*. WIT press, 1987. 32, 37

[50] M. Longuet-Higgins, "On the statistical distribution of the heights of sea waves," *Journal of Marine Research*, 1952. 34

[51] G. Lloyd, "Rules for the certification and construction - structural design," GL, Tech. Rep., 2016. 37, 39

[52] [Online]. Available: http://portal.emodnet-bathymetry.eu/ 37

[53] K. Ansari, "Mooring with multi-component cable systems," *ASME J. Energy Resour. Technol*, vol. 102, pp. 62–69, 1980. 39

[54] T. Nakajima, S. Motora, M. Fujino *et al.*, "On the dynamic analysis of multi-component mooring lines," in *Offshore Technology Conference*. Offshore Technology Conference, 1982. 39

[55] H. Van den Boom, "Dynamic behavior of mooring lines," *BOSS'85 Behavior of Offshore Structures*, pp. 359–368, 1985. 39

[56] N. U. Khan and K. A. Ansari, "On the dynamics of a multicomponent mooring line," *Computers and Structures*, 1986. 39

[57] R. Singh and J. Verma, "Evaluation of force-displacement relationship for multicomponent mooring cable by fem," *Computers & structures*, vol. 30, no. 5, pp. 1079–1089, 1988. 40

[58] K. A. Ansari, "On the design of multi-component cable systems for moored offshore vessels," *Energy Conversion and Management*, vol. 31, no. 3, pp. 295–307, 1991. 40

[59] A. Dercksen, L. Hoppe *et al.*, "On the analysis of mooring systems using synthetic ropes," in *Offshore Technology Conference*. Offshore Technology Conference, 1994. 40

[60] W. C. Webster, "Mooring-induced damping," *Ocean Engineering*, vol. 22, no. 6, pp. 571–591, 1995. 40

[61] S. Mavrakos, V. Papazoglou, M. Triantafyllou, and J. Hatjigeorgiou, "Deep water mooring dynamics," *Marine structures*, vol. 9, no. 2, pp. 181–209, 1996. 40

[62] R. Balzola, "Mooring line damping in very large water depths," Master's thesis, Massachusetts Institute of Technology, 1999. 40

[63] M. H. Vaz, M. A. & Patel, "Lateral buckling of bundled pipe systems," *Marine Structures*, 1999. 40

[64] C. Macfarlane, "Statics of a three component mooring line," *Ocean Engineering*, 2001. 41

[65] J. I. Gobat and M. A. Grosenbaugh, "A simple model for heave-induced dynamic tension in catenary moorings," *Applied Ocean Research*, vol. 23, no. 3, pp. 159–174, 2001. 41

[66] P. Pacheco, P. P. Kenedi, and J. C. F. Jorge, "Elastoplastic analysis of the residual stress in chain links," in *OMAE'2002-21st International Conference on Offshore Mechanics and Arctic Engineering*, 2002. 41

[67] E. Kreuzer and U. Wilke, "Mooring systems–a multibody dynamic approach," *Multibody System Dynamics*, vol. 8, no. 3, pp. 279–296, 2002. 41

[68] P. P. A. Ong and S. Pellegrino, "Modelling of seabed interaction in frequency domain analysis of mooring cables." *Structural Engineer*, vol. 81, no. 20, pp. 13–14, 2003. 41

[69] P. Pacheco, P. P. Kenedi, J. C. F. Jorge, H. Gama, M. A. Savi, and A. Paiva, "Modeling residual stresses in offshore chain links using finite element method," in *COBEM-2003, 17th International Congress of Mechanical Engineering, São Paulo*, 2003. 41

[70] P. M. Vargas, T.-M. Hsu, and W. K. Lee, "Stress concentration factors for stud-less mooring chain links in fairleads," in *Proceedings of OMAE*, 2004. 41, 117, 118

[71] R. Hobbs and I. L Ridge, "Torque in mooring chain. part 1: background and theory," *The Journal of Strain Analysis for Engineering Design*, vol. 40, no. 7, pp. 703–713, 2005. 42

[72] P. Jean, K. Goessens, D. L'Hostis *et al.*, "Failure of chains by bending on deepwater mooring systems," in *Offshore Technology Conference*. Offshore Technology Conference, 2005. 42

[73] T. LACERDA, "Análise de sistemas de ancoragem de plataformas flutuantes," Master's thesis, Universidade Federal do Rio de Janeiro, 2005. 42

[74] I. Ridge, R. Hobbs, J. Fernandez *et al.*, "Predicting the torsional response of large mooring chains," in *Offshore Technology Conference*. Offshore Technology Conference, 2006. 42

[75] W. S. Yang, "Hydrodynamic analysis of mooring lines based on optical tracking experiments," Ph.D. dissertation, Texas A&M University, 2007. 42

[76] K. Wingerei, "Dynamics and damping in mooring lines," Master's thesis, University of Oslo, 2008. 42

[77] I. E. Udoh, "Development of design tool for statically equivalent deepwater mooring systems," Master's thesis, Texas A&M University, 2008. 42

[78] T. Lassen, E. Storvoll, and A. Bech, "Fatigue life prediction of mooring chains subjected to tension and out of plane bending," in *28th International Conference on Offshore Mechanics and Arctic Engineering, Honululu*, 2009. 43

[79] F. I. A. Samad *et al.*, "Performance of catenary mooring system," Master's thesis, Universiti Teknologi Malaysia, 2009. 43

[80] L. B. Neto, R. D. Machado, and M. B. Hecke, "Finite element analysis of buried pipelines subjected to buckling," *International journal of Modeling and Simulation for the Petroleum industry*, vol. 3, no. 1, 2009. 43

[81] C. Y. Song, J. Lee, and J. M. Choung, "Reliability-based design optimization of an fpso riser support using moving least squares response surface meta-models," *Ocean Engineering*, vol. 38, no. 2, pp. 304–318, 2011. 43

[82] M. Yassir, V. Kurian, I. Harahap, and A. Nabilah, "Parametric study on multi-component catenary mooring lines for offshore floating structures," in *The Asia-Pacific Offshore Conference*, 2010. 43, 52

[83] I. Ridge, P. Smedley, and R. Hobbs, "Effects of twist on chain strength and fatigue performance: small scale test results," in *ASME 2011 30th International Conference on Ocean, Offshore and Arctic Engineering*. American Society of Mechanical Engineers, 2011, pp. 183–189. 43

[84] P. C. Vicente, A. Falcão, and P. Justino, "Slack-chain mooring configuration analysis of a floating wave energy converter," in *26th International workshop on water waves and floating bodies, Athens, Greece*, 2011. 43

[85] S. Wales, P. L. Sincock, M. Santosa *et al.*, "Impact of catenary embedment on the mooring performance of a deep water floating production unit," in *The Twenty-first International Offshore and Polar Engineering Conference*. International Society of Offshore and Polar Engineers, 2011. 44

[86] V. Kurian, M. Yassir, C. Ng, and I. Harahap, "Nonlinear dynamic analysis of multi-component mooring lines incorporating line-seabed interaction," *Journal of Applied Sciences, Engineering and Technology*, 2013. 44

[87] U. M. Ba, "Analysis of mooring and steel catenary risers system in ultra deepwater," Ph.D. dissertation, Newcastle University, 2012. 44

[88] A. F. Kiecke, "Simulated fatigue damage index on mooring lines of a gulf of mexico truss spar determined from recorded field data," Master's thesis, Texas A&M University, 2012. 44

[89] T. Elsayed, M. Fahmy, and R. Samir, "A finite element model for subsea pipeline stability and free span screening," *Canadian Journal on Mechanical Sciences and Engineering*, vol. 3, no. 1, p. 13, 2012. 44

[90] Z. Wang, "An evolutionary optimisation study on offshore mooring system design," Ph.D. dissertation, University of Wollongong, 2012. 45

[91] L. Castro-Santos, S. F. González, V. Díaz-Casas, J. Ángel, and F. Formoso, "Position keeping costs of floating offshore platforms for marine renewable energies," in *Conferencias del XXIII Congreso Panamericano de Ingeniería Naval, Costa Afuera e Ingeniería Portuaria COPINAVAL*, 2013. 45

[92] P. Bastid and S. D. Smith, "Numerical analysis of contact stresses between mooring chain links and potential consequences for fatigue damage," in *ASME 2013 32nd International Conference on Ocean, Offshore and Arctic Engineering*. American Society of Mechanical Engineers, 2013, pp. V02BT02A037–V02BT02A037. 45

[93] J. A. M. Farfan, "Modal analysis of deepwater mooring lines based on a variational formulation," Master's thesis, Texas A&M University, 2013. 45

[94] L. Castro-Santos, S. Ferreño González, and V. Diaz-Casas, "Methodology to calculate mooring and anchoring costs of floating offshore wind devices," in *International Conference on Renewable Energies and Power Quality (ICREPQ)*, vol. 1, 2013. 45

[95] M. O. Chrolenko, "Dynamic analysis and design of mooring lines," Master's thesis, Norwegian University of Science and Technology, 2013. 45

[96] V. M. P. Bico, "Amarração de plataformas offshore flutuantes com cabos de poliéster," Master's thesis, Instituto Superior de Engenharia de Lisboa, 2013. 45

[97] A. R. C. Girón, F. N. Corrêa, A. O. V. Hernández, and B. P. Jacob, "An integrated methodology for the design of mooring systems and risers," *Marine Structures*, vol. 39, pp. 395–423, 2014. 46

[98] M. Vineesh.M.V, Nithin V Sabu, "Finite element analysis of mooring cable," *International Journal of Engineering Research and Applications*, 2014. 46, 91

[99] Y. Wang, C. Zou, F. Ding, X. Dou, Y. Ma, and Y. Liu, "Structural reliability based dynamic positioning of turret-moored fpsos in extreme seas," *Mathematical Problems in Engineering*, vol. 2014, 2014. 46

[100] M. O. Ahmed, A. Yenduri, and V. Kurian, "Behaviour of mooring systems for different line pretensions," *Applied Mechanics and Materials*, vol. 567, p. 204, 2014. 46

[101] T. Fan, D. Qiao, and J. Ou, "Innovative approach to design truncated mooring system based on static and damping equivalent," *Ships and Offshore Structures*, vol. 9, no. 6, pp. 557–568, 2014. 46

[102] H. Zaroudi, K. Rezanejad, and C. G. Soares, "Assessment of mooring configurations on the performance of a floating oscillating water column energy convertor," *Renewable Energies Offshore*, pp. 24–26, 2014. 46

[103] H. Y. C. L. Siow, J. Koto and A. Matsuda, "Strength analysis of fpso's mooring lines," in *The 1st Conference on Ocean Mechanical and Aerospace*, 2014. 47

[104] J. Rosen, G. Farrow, A. Potts, C. Galtry, W. Swedosh, D. Washington, A. Tovar *et al.*, "Chain fears jip: Finite element analysis of residual strength of degraded chains," in *OTC Brasil*. Offshore Technology Conference, 2015. 47

[105] X. Gang, S. Liping, and C. Chuanyun, "Deepwater mooring system equivalent truncated intelligent optimization design," *International Journal of Innovation Sciences and Research*, 2015. 47

[106] L. C. Stendal, "Analysis methods for mooring systems with focus on accidental limit state," Master's thesis, NTNU, 2015. 47

[107] Y. Du, W. Wu, D. Tang, Q. Yue, F. Li, and R. Xie, "A novel underwater measurement method for mooring system using self-contained technique," *Advances in Mechanical Engineering*, vol. 7, no. 5, p. 1687814015585973, 2015. 47

[108] M. A. Bhinder, M. Karimirad, S. Weller, Y. Debruyne, M. Guérinel, and W. Sheng, "Modelling mooring line non-linearities (material and geometric effects) for a wave energy converter using aqwa, sima and orcaflex," in *Proceedings of the 11th European Wave and Tidal Energy Conference, Nantes, France*, 2015, pp. 6–11. 47

[109] A. F. Camarão, M. V. Pereira, F. A. Darwish, and S. H. Motta, "Structural mechanics applied to mooring components design," in *ECF15, Stockolm 2004*, 2013. 47

[110] L. Crudu, D. Obreja, and O. Marcu, "Moored offshore structures-evaluation of forces in elastic mooring lines," in *IOP Conference Series: Materials Science and Engineering*, vol. 147, no. 1. IOP Publishing, 2016, p. 012096. 48

[111] D. Qiao, J. Yan, and J. Ou, "Fatigue analysis of deepwater hybrid mooring line under corrosion effect," *Polish Maritime Research*, vol. 21, no. 3, pp. 68–76, 2014. 48

[112] O. DeAndrade and A. Duggal, "Analysis, design and installation of polyester rope mooring systems in deep water," in *Offshore Technology Conference, Houston, Paper OTC*, vol. 20833, 2010. 48

[113] A. Potts, G. Farrow, A. Kilner *et al.*, "Investigations into break strength of offshore mooring chains," in *Offshore Technology Conference*. Offshore Technology Conference, 2017. 48

[114] C. A. Bartholomew, B. Marsh, and R. Hooper, *US Navy Salvage Engineer's Handbook*, N. S. S. C. Direction of Commander, Ed. Direction of Commander, Naval Sea Systems Command, 1992. 51

[115] O. C. I. M. Forum, "Effective mooring," Witherby & Co. Lto, 32/36 Ayesbury street, London EX1EOET, England, 1989. 52

[116] J. N. Newman, "The drift force and moment on ships in waves," *Journal of Ship Research*, 1967. 55

[117] O. Faltinsen, *Sea loads on ships and offshore structures*. Cambridge university press, 1993, vol. 1. 56

[118] CENTECCen, "Mooring and anchoring systems mooring line statics," centre for Marine Technology and Ocean Engineering. 60

[119] O. Ltd., *Orcaflex Manual*, D. U. C. L. . . AJ, Ed. Orcina Ltd, 2017. 67, 71, 72, 73

[120] *An introduction to Orcaflex*. 68

[121] BP, "Technical note - preliminary hull form qd-bp-mr-tec-0003," BP, Tech. Rep., 2013. 68, 146, 147, 148

[122] ——, "Qd-bp-mr-spe-0002qd-bp-mr-spe-0002," BP Exploration Operationg Company Limited, Tech. Rep., 2009. 68, 69

[123] R. de Morais Amaral, "Métodos computacionais em engenharia mecânica," Master's thesis, Faculdade de ciências e tecnologia - Universidade nova de Lisboa, 2008. 89

[124] J. H. Tsuruta, "Um estudo sobre algoritmos genÉticos," Ministério da agricultura e do abastecimento, Tech. Rep., 2008. 89

[125] D. N. Veritas, "Position mooring," DET NORSKE VERITAS, Tech. Rep., 2008. 103, 111

[126] M. C.-Y. Niu, *Airframe structural design*. Conmilit Press Hong Kong, 1988. 104

[127] P. C. Francisco Mercês de Mello, *Elementos finitos - Formulação residual de Galerkin*, M. Robalo, Ed. Edições Silabo, 2010. 108, 109

[128] W. H. FAA, *Metallic Materials Properties Development and Standardization (MMPDS)*, F. A. Administration, Ed. Federam Aviation Administration, 2011. 113

[129] D. N. Veritas, "Dnv-rp-c203," Det Norske Veritas, Tech. Rep., 2011. 126

# Appendix A

# Annexes

## A.1 Riser analysis assumptions

The production riser properties are presented in figure A.1.

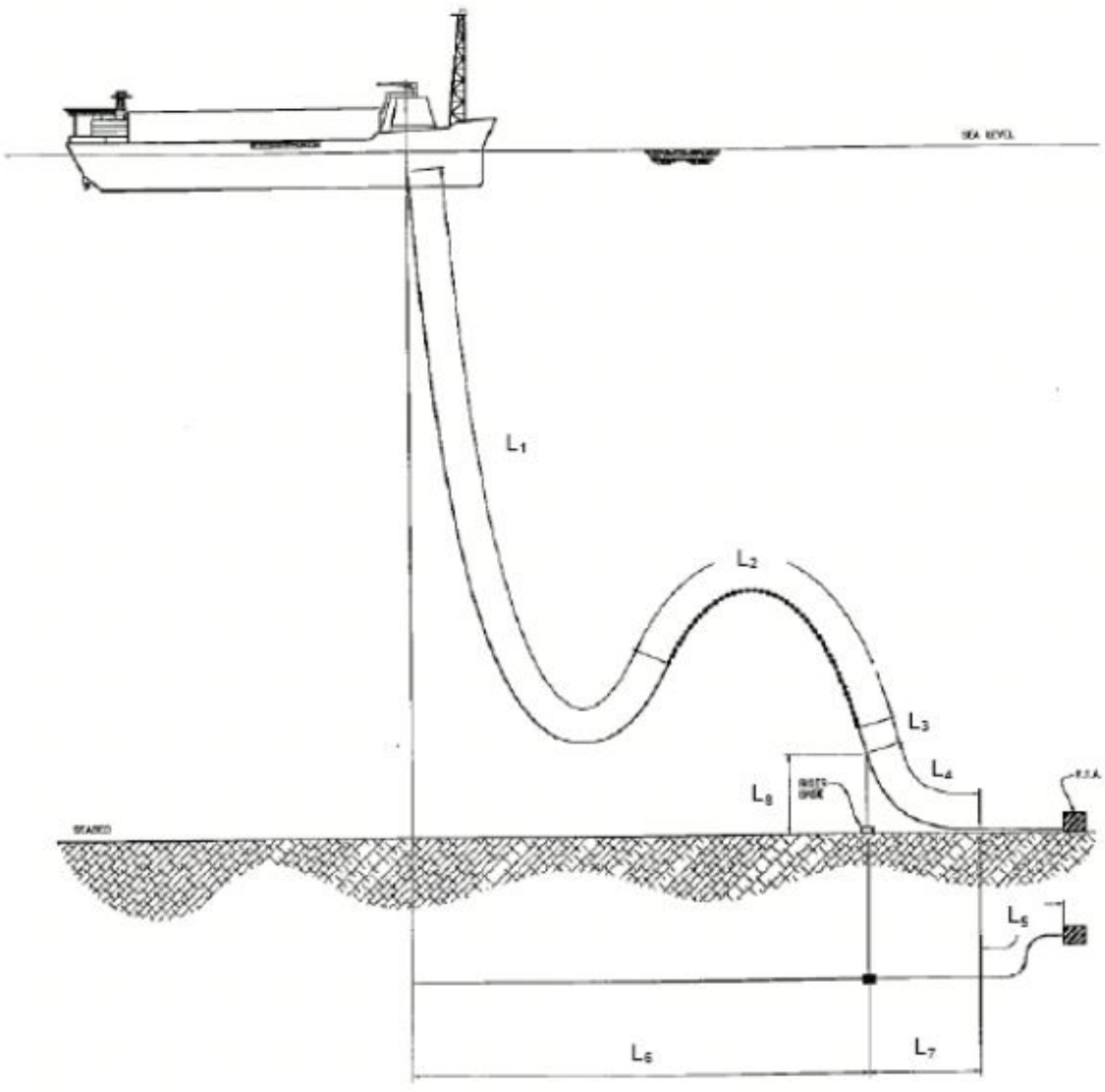


Figure A.1: Schematic of Production Riser (image from ref. [16])

Table A.1: Riser configuration parameters [16])

| Parameter | Symbol | Value |
|---|---|---|
| Heading from FPSO (degree clockwise from north) | | 128.5 |
| Length between hang-off bending stiffener flange and buoyant section [m] | $L_1$ | 4.0 |
| length of byoyancy section [m] | $L_2$ | 175.0 |
| Length between buoyancy section and hold-down clamp [m] | $L_3$ | 15.0 |
| Length between hold-down and hold-back clamps [m] | $L_4$ | 29.0 |
| Total length of riser in analysis [m] | $L_1$+$L_2$+$L_3$+$L_4$ | 629.0 |
| Nominal horizontal distance from riser hang-off to riser base [m] | $L_6$ | 270.0 |
| Nominal horizontal distance from riser base to hold-back clamp [m] | $L_7$ | 20.0 |
| Hold-down tether length including elevation from riser base [m] | $L_8$ | 12.5 |

Table A.2: Riser properties (image from ref. [16])

| Parameter | Value |
|---|---|
| Outer diameter [m] | 0.373 |
| Internal Volume [l/m] | 48.180 |
| Density of internal fluid $[kg/m^3]$ | 300.000 |
| Mass of internal fluid [kg/m] | 14.750 |
| Mass (in air) empty [kg/m] | 254.040 |
| Total mass [kg/m] | 268.790 |
| Bending stiffness $[Nm^2]$ | 64.820E3 |
| Torsional stiffness $[Nm^2/rad]$ | 0.170E8 |
| Axial stiffness [N] | 1.110E9 |
| Operating pressure [bar] | 20.000 |

Table A.3: Hydrodynamic coefficients (image from ref. [16])

| Parameter | Normal drag | Normal Inertia | Tangential Drag | Tangential Inertia |
|---|---|---|---|---|
| Riser down to 40m below water level | 1.05 | 1.80 | 0.00 | 0.00 |
| Riser down to 40m and 70m below water level | 0.80 | 1.80 | 0.00 | 0.00 |
| Riser down to 70m and 150m below water level | 0.70 | 1.80 | 0.00 | 0.00 |
| Riser down to 40m and 70m below water level | 0.90 | 1.80 | 0.00 | 0.00 |
| Riser from 300m to buoyancy section | 0.90 | 1.80 | 0.00 | 0.00 |
| buoyancy section | 0.90 | 1.80 | 0.50 | 0.50 |
| Riser below buoyancy level | 1.20 | 1.80 | 0.00 | 0.00 |

Table A.4: Mass of buoyancy section including riser (image from ref. [16])

| Parameter | Value |
|---|---|
| Mass of buoyancy section, in air, full of seawater (kg/m) | 526.30 |
| Mass of buoyancy section, in air, empty (kg/m) | 475.90 |
| Mass of internal fluid (kg/m) | 14.75 |
| Mass of buoyancy section, in air, full of fluid (kg/m) | 490.65 |

Table A.5: Marine growth profile (image from ref. [16])

| Water depth [m] | thickness [mm] | Density $[kg/m^3]$ |
|---|---|---|
| 0.00 - 40.00 | 50.00 | 1300.00 |
| 40.00 - 70.00 | 20.00 | 1100 |
| >70.00 | 0.00 | 0.00 |

Table A.6: Weight and outer diameter of riser including marine growth (image from ref. [16])

| Water depth [m] | OD [mm] | Mass of marine growth [kg/m] | Total mass (kg/m) |
|---|---|---|---|
| 0.00 - 40.00 | 0.473 | 86.40 | 355.20 |
| 40.00 - 70.00 | 0.413 | 26.70 | 296.00 |

Table A.7: Riser combined properties (image from ref. [16])

| Description | Depth below MSL [m] | OD [m] | Mass (kg/m) | Bending stiffness |
|---|---|---|---|---|
| Riser+Uraduct+heavy MG | 17.80 to 40.00 | 0.5453 | 421.74 | 77.90E3 |
| Riser+Uraduct+light MG | 40.00 to 70.00 | 0.4850 | 352.76 | 77.90E3 |
| Riser+Uraduct | -70.00 to 77.80 and sag bend | 0.4453 | 320.60 | 77.90E3 |

## A.2 Hull Considerations

The hull form has the following dimensions:

- Length 270 m
- Breadth 52 m
- Depth 30 m

The FPSO will have 3 operating draughts,these parameters will be of a major importance to hydrostatic analysis.

- Full Load Draught 20.0 m approx.253 000 tonnes
- Export Draught 16.1 m approx.201 000 tonnes
- Export Draught 12.2 m approx.150 000 tonnes

For the development of this work only full load draught will be taken in consideration. The full load draught is based on a 98 % oil storage, about 1 million bbls. Figure A.2 show the turret detail on the FPSO.

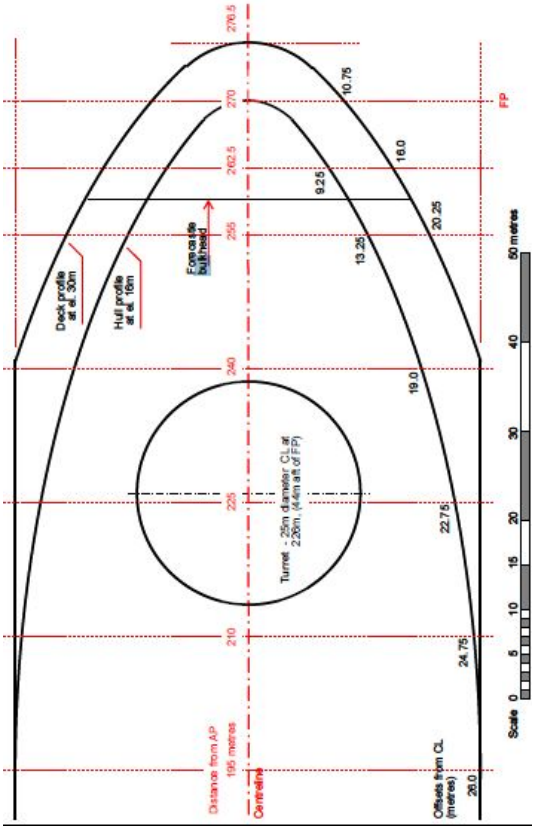


Figure A.2: Forward hull plan (image from ref. [121])

Figure A.3 shows the main dimensions of the FPSO Glen Lyon. Figure A.4 shows the freeboard profile.

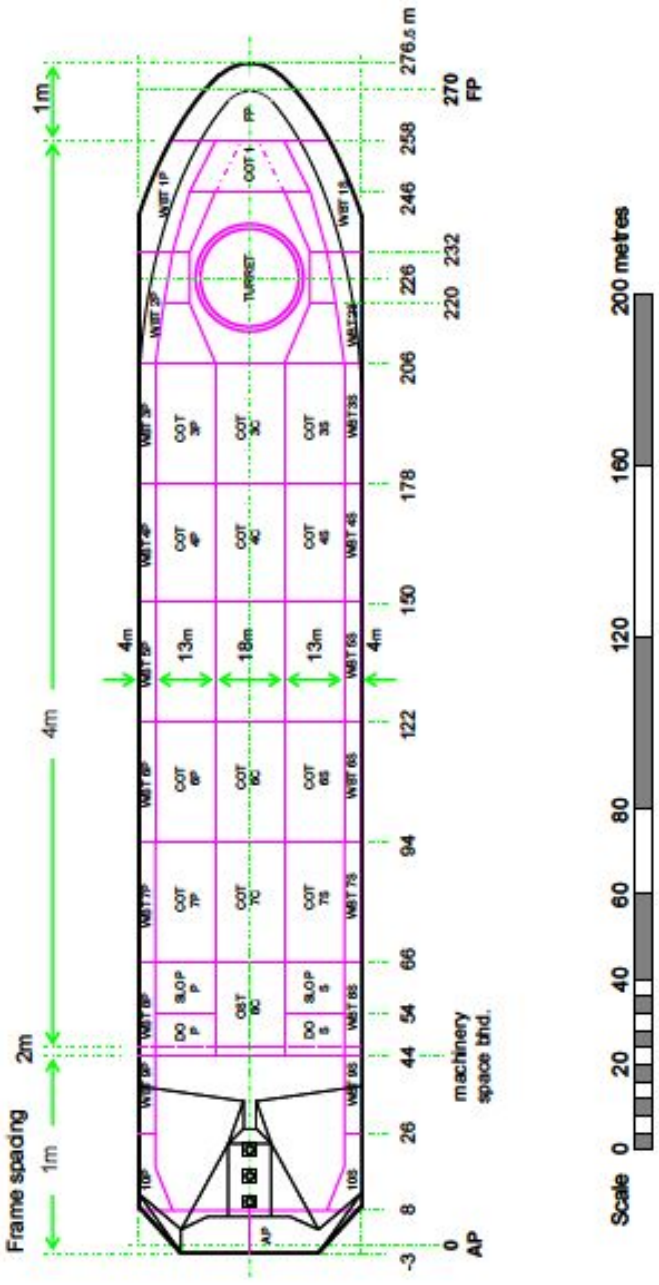


Figure A.3: Hull design of Glen Lyon (image from ref. [121])

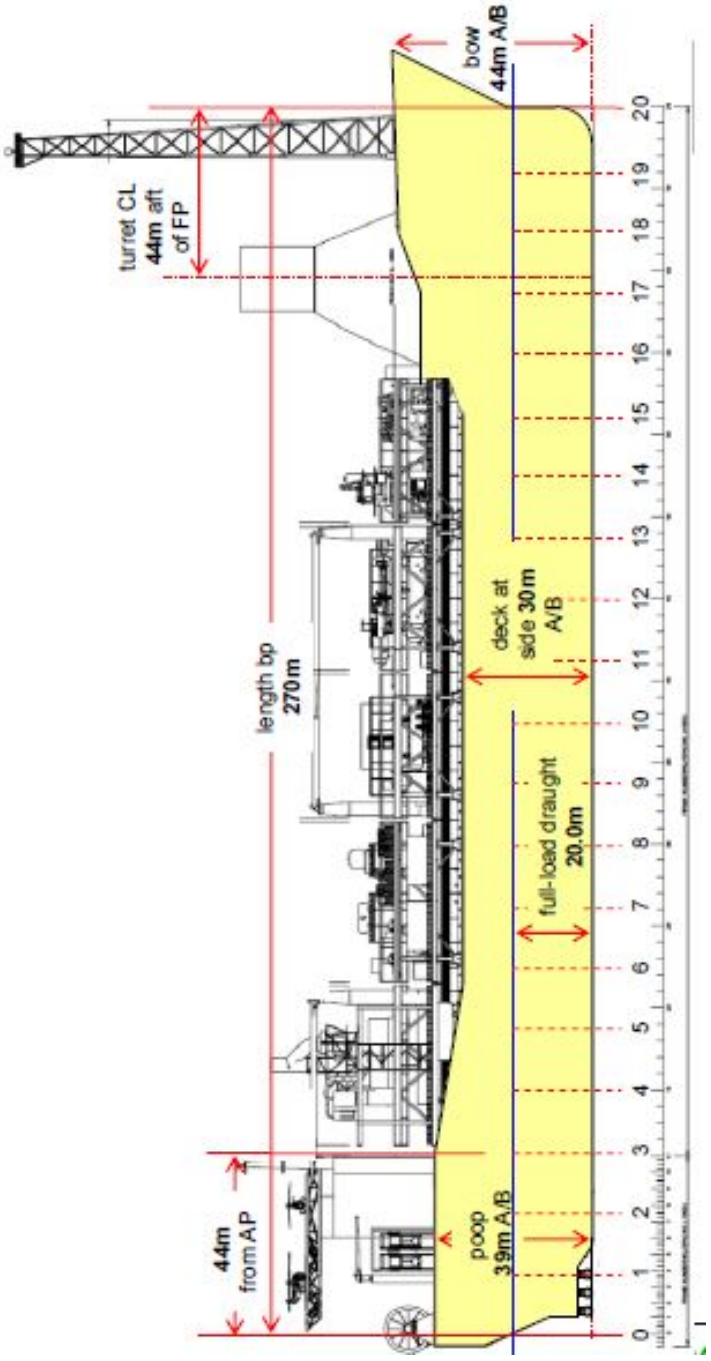


Figure A.4: Freeboard Profile (image from ref. [121])